



DISSERTATION

Titel der Dissertation

Toward the total synthesis of euphosalicin

verfasst von

Mag. Christian Aichinger

angestrebter akademischer Grad

Doktor der Naturwissenschaften (Dr.rer.nat.)

Wien, 2015

Studienrichtung (lt. Studienblatt): A 091 419 Chemie

Dissertationsgebiet lt. Studienblatt: Chemie

Betreut von: Univ.-Prof. Dr. Johann Mulzer

Zunächst möchte ich mich bei meinen Eltern bedanken. Euer bedingungsloser Rückhalt und euer Vertrauen ermöglichten es mir, einen eigenständigen Weg durch das Studium und das Leben zu finden.

Simone Bächler danke ich für die gemeinsame Zeit, den grenzenlosen Rückhalt und die unerschöpfliche Unterstützung, gerade auch in schwierigen Zeiten. Ohne Dich hätte ich diese Herausforderung nicht meistern können.

Ein großes Dankeschön richte ich auch an Jakob und Verena Anger für eure Freundschaft und euren Beistand in schwierigen Zeiten.

Ich danke Mag. Adolf Weilguny dafür, mich zu Schulzeiten für Chemie zu begeistern. Ohne Dein Engagement hätte ich mich nicht für ein dieses Studium entschieden können.

Mein besonderer Dank gilt Prof. Michael Widhalm für die Betreuung meiner Diplomarbeit, bei der ich erste Erfahrungen in organischer Synthesechemie sammeln durfte. Unzählige interessante Gespräche und Diskussionen mit Dir machten mich zu einem besseren Chemiker.

Für das spannende Thema, die Betreuung der Doktorarbeit bedanke ich mich bei Dr. Uwe Rinner. Ohne Deine stete Unterstützung wäre diese Arbeit nicht möglich gewesen. Ich möchte mich auch bei Prof. Johann Mulzer bedanken für Ihren ungebrochenen Enthusiasmus für Chemie, Ihre exzellenten Vorlesungen und Ihre Unterstützung während der Dissertation. Der gesamten Arbeitsgruppe danke ich für die stete Unterstützung und das angenehme Arbeitsklima. Im speziellen danke ich Christoph Lentsch, Rita Fürst, Maria Kauderer und Christian Dank für die schöne Zeit. Ein großes Dankeschön richte ich auch an Tina Nowikow und Christoph Schmölzer für die gemeinsam erlebte Zeit, innerhalb und außerhalb der Universität.

Besonderen Dank möchte ich auch Prof. Hanspeter Kählig richten, für Deine Hilfestellung bei allen Fragen hinsichtlich NMR Spektroskopie sowie für die Unterstützung im Rahmen des Praktikums für Biologen und Ernährungswissenschaftler.

I. Table of Contents

I.	Table of Contents	i
II.	Abbreviations	iii
1.	Introduction	1
1.1.	Biological origins and related diterpenes	1
1.2.	Biosynthetic considerations	4
1.3.	Biological activity	5
1.4.	Cancer causes and carcinogenesis	5
2.	Previously published syntheses	13
2.1.	(±)-16-Normethyljatrophone (Smith III, 1981)	13
2.2.	(+)-Hydroxyjatrophone A and B (Smith III, 1989)	16
2.3.	(±)- <i>epi</i> -Jatrophone and (±)-jatrophone (Hegedus, 1990)	18
2.4.	(+)-Jatrophone (Wiemer, 1992)	21
2.5.	(-)-15-O-Acetyl-3-propionyl-17-O-norcharaciol (Hiersemann, 2006)	23
2.6.	(-)-15-O-Acetyl-3-O-propionylcharaciol (Hiersemann, 2009)	26
2.7.	Other approaches toward jatrophane derivatives	28
3.	Results and discussion	31
3.1.	Retrosynthetic analysis of euphosalicin	31
3.2.	The first-generation approach	37
3.3.	Second-generation approach: retrosynthetic analysis	45
3.5.	Third-generation approach: retrosynthetic analysis	49
4.	Conclusion	67
5.	Experimental procedures	69
6.	Spectral data	88
7.	Appendix	96
7.1.	Copyright of figures and schemes	96
7.2.	References	96

7.3.	Abstract in English	103
7.4.	Abstract in German.....	104
7.5.	List of publications.....	105
7.6.	Curriculum vitae.....	107

II. Abbreviations

abs.	Absolute (water-free) solvent
Ac	Acetyl-
ADP	Adenosine diphosphate
ATP	Adenosine triphosphate
9-BBN	9-Borabicyclo[3.3.1]nonane
Bn	Benzyl-
b.r.s.m.	Based on recovered starting material
Bu	Butyl-
Cp	Cyclopentadienyl anion or ligand
DDQ	2,3-Dichloro-5,6-dicyano-1,4-benzoquinone
DIAD	Diisopropyl azodicarboxylate
DIBAL	Diisobutylaluminium hydride
DIC	<i>N,N'</i> -Diisopropylcarbodiimide
DIPA	Diisopropylamine
DIPEA	Diisopropylethylamine
DMAP	4-Dimethylaminopyridine
DMAPP	Dimethylallyl pyrophosphate
DMSO	Dimethylsulfoxide
dppf	1,1'-Bis(diphenylphosphino)ferrocene
d.r.	Diastereomeric ratio
EDC	1-Ethyl-3-(3-dimethylaminopropyl)carbodiimide
EI	Electron ionization (for mass spectrometry)
e.r.	Enantiomeric ratio
ESI	Electrospray ionization (for mass spectrometry)
Et	Ethyl-
HMPA	Hexamethylphosphoramide
HPLC	High-performance liquid chromatography
HRMS	High resolution mass spectrometry
HWE	Horner-Wadsworth-Emmons reaction
HYTRA	2-Hydroxy-1,2,2-triphenylethyl acetate
IBX	2-Iodoxybenzoic acid

Ipc	Isopinocampheyl-
IPP	Isopentenyl pyrophosphate
IR	Infrared spectroscopy
KHMDS	Potassium bis(trimethylsilyl)amide
LDA	Lithium diisopropyl amide
LHMDS	Lithium bis(trimethylsilyl)amide
LLB	$\text{LaLi}_3(\text{binaphthoxide})_3$
MDR	Multi-drug resistance
Me	Methyl-
MOM	Methoxymethyl-
MRP1	Multidrug resistance-associated protein 1
MS	Mass spectrometry
NCS	<i>N</i> -Chlorosuccinimide
Nic	Nicotinoyl-, or 3-pyridinecarbonyl-
NMO	<i>N</i> -Methylmorpholine <i>N</i> -oxide
NMR	Nuclear magnetic resonance
NOE	Nuclear Overhauser effect
PE	Petroleum ether
PGP	P-glycoprotein
PMB	4-Methoxybenzyl-
PMP	4-Methoxyphenyl-
PPTS	Pyridinium <i>p</i> -toluenesulfonate
py	Pyridine
RCM	Ring closing metathesis
R_f	Retardation factor in the context of chromatography
rt	Room temperature
SAR	Structure activity relationship
TBAF	Tetrabutyl ammonium fluoride
TBS	Tert-butyl dimethylsilyl-
TES	Triethylsilyl-
THF	Tetrahydrofuran
TLC	Thin layer chromatography
TMEDA	Tetramethylethylenediamine

TMS	Trimethylsilyl-
Tf	Trifluoromethanesulfonyl-
Ts	Tosyl-, or 4-toluenesulfonyl-
UV	Ultraviolet light

1. Introduction

Euphosalicin (Figure 1, **1**) is a diterpene, isolated in 2001 by the Hohmann group.¹ It is highly oxygenated and contains nine stereogenic centers, five of which are contiguous. So far, it is the only known natural product featuring a [11.3.0] bicyclic carbon skeleton.² All hydroxy groups are esterified: five carry acetyl groups and two hold nicotinoyl (Nic, 3-pyridinecarbonyl-) groups.

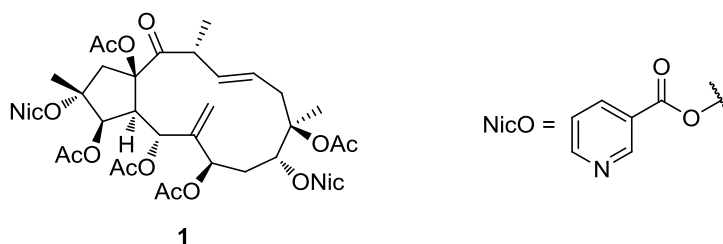


Figure 1: Euphosalicin

1.1. *Biological origins and related diterpenes*

Euphosalicin was isolated from the plant *Euphorbia salicifolia*, which is shown in Figure 2. The genus *Euphorbia* encompasses more than 2000 species which are endemic in all parts of the world.³ Commonly, members of the genus are called spurges (“Wolfsmilch” in German). They have been used in folk medicine for a long time, as their names attest: *Euphorbus* was the name of the 1st century physician who discovered therapeutic properties of the plants⁴ while the name “spurges” derives from *expurgare*,⁵ meaning “to purge”. Applications include the treatment of cancers and various skin conditions, such as sores, warts and papillomas.⁶



Figure 2: *Euphorbia salicifolia*

During the 20th century, these plants attracted the attention of natural product isolation groups due to their therapeutic potential. A large variety of related terpenes have been

discovered, such as the lathyranes, daphnanes, tiglanes and jatrophanes.³ Many of them show a wide range of biological activity, ranging from potent tumor promotion to anti-viral activity.

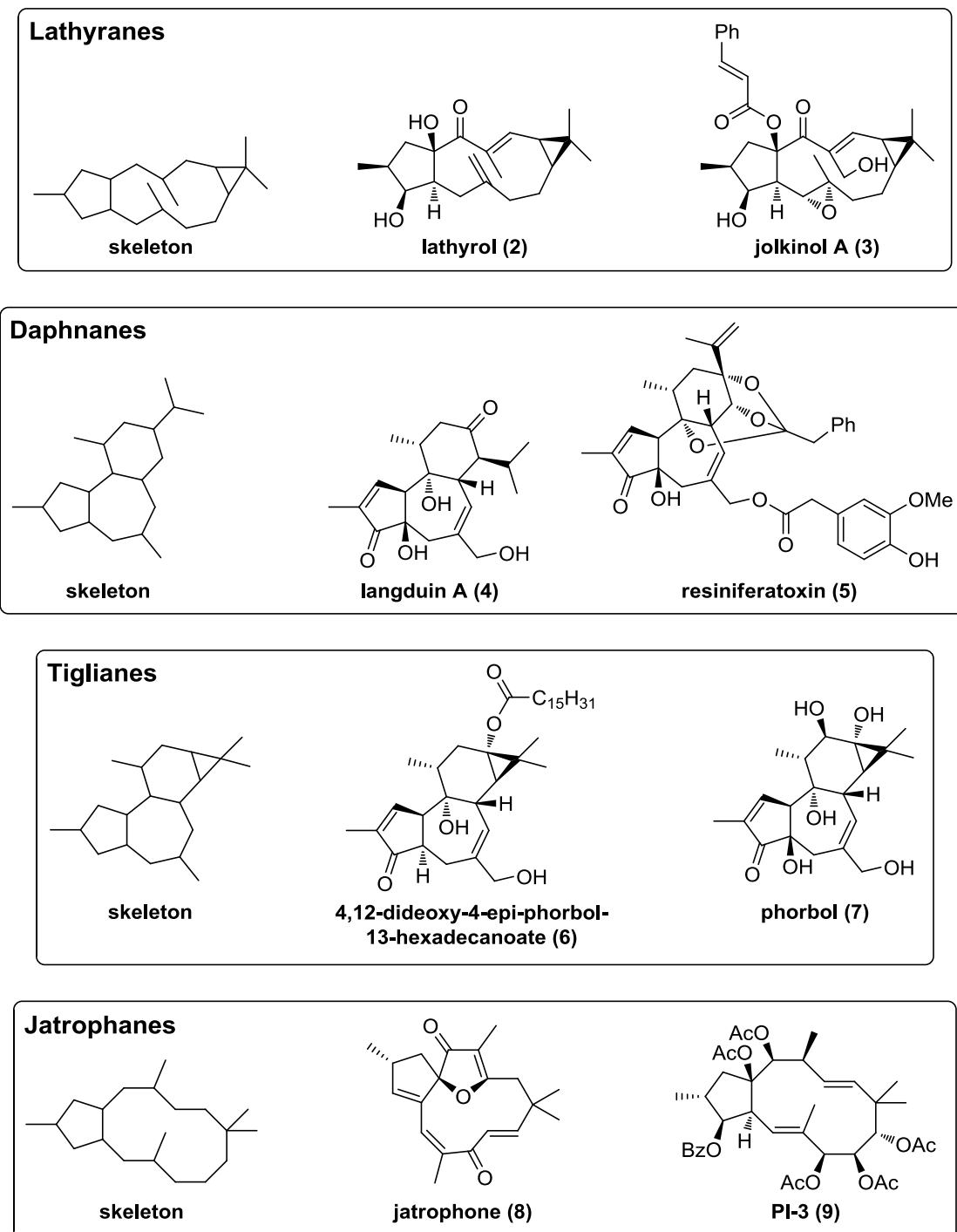


Figure 3: Classes of diterpenes found in *Euphorbia* plants, along with specific examples

Figure 3 shows the carbon skeleton along with concrete examples (2–9) for the above mentioned categories. The compounds within one group can vary considerably, mostly

in the oxygenation pattern or the sidechains. In langduin A (**4**), for example, the isopropyl unit is shifted compared to all other daphnanes, most likely through a pinacol-type rearrangement.

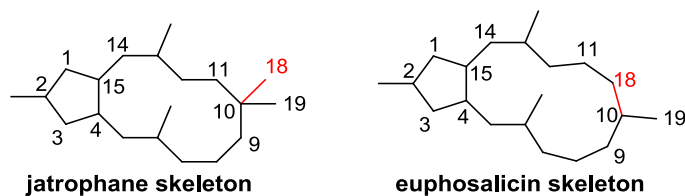


Figure 4: Formal incorporation of the jatrophane C18 methyl group leads to euphosalicin

Euphosalicin (**1**) is closely related to the jatrophanes; however, instead of having a 12-membered ring, it features a 13-membered ring. Formally, the C18 methyl group is incorporated into the macrocycle under ring expansion (Figure 4). This fact is also mirrored in the proposed atom numbering scheme for euphosalicin. The numbering system shown is used for all jatrophane derivatives in this thesis.

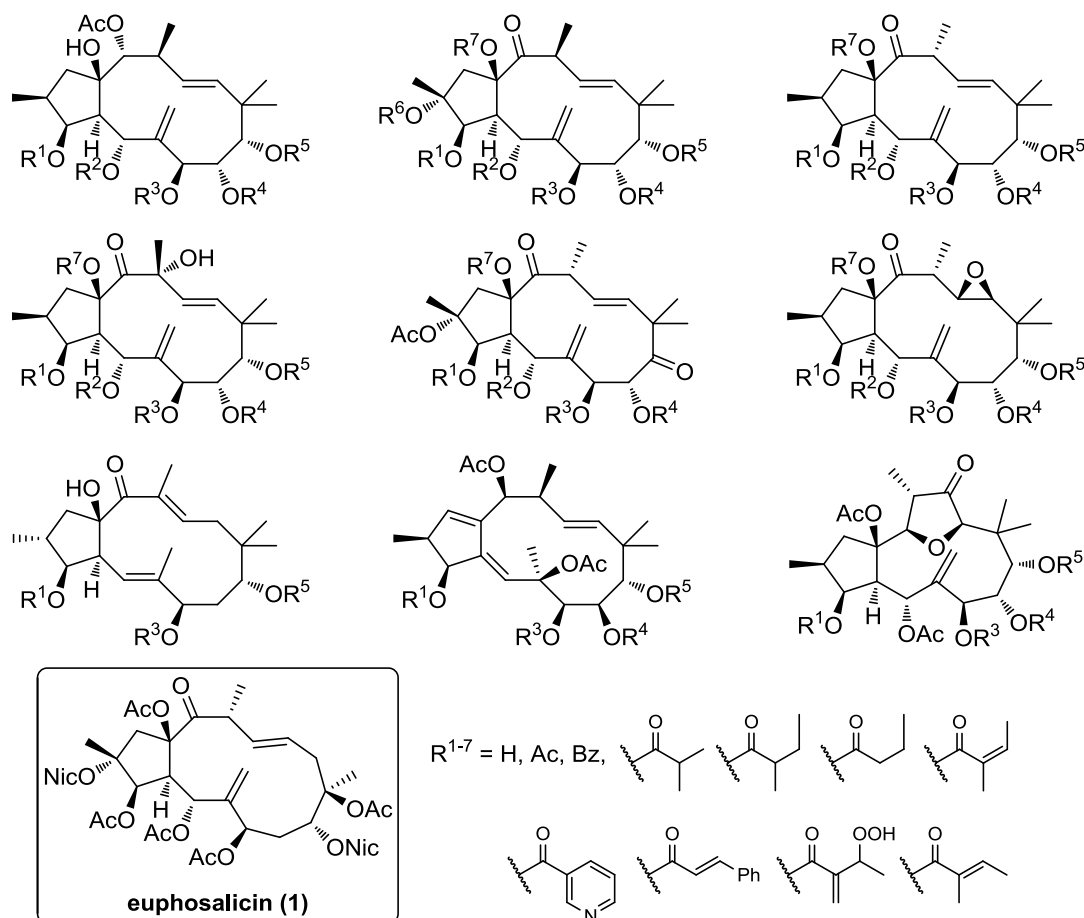


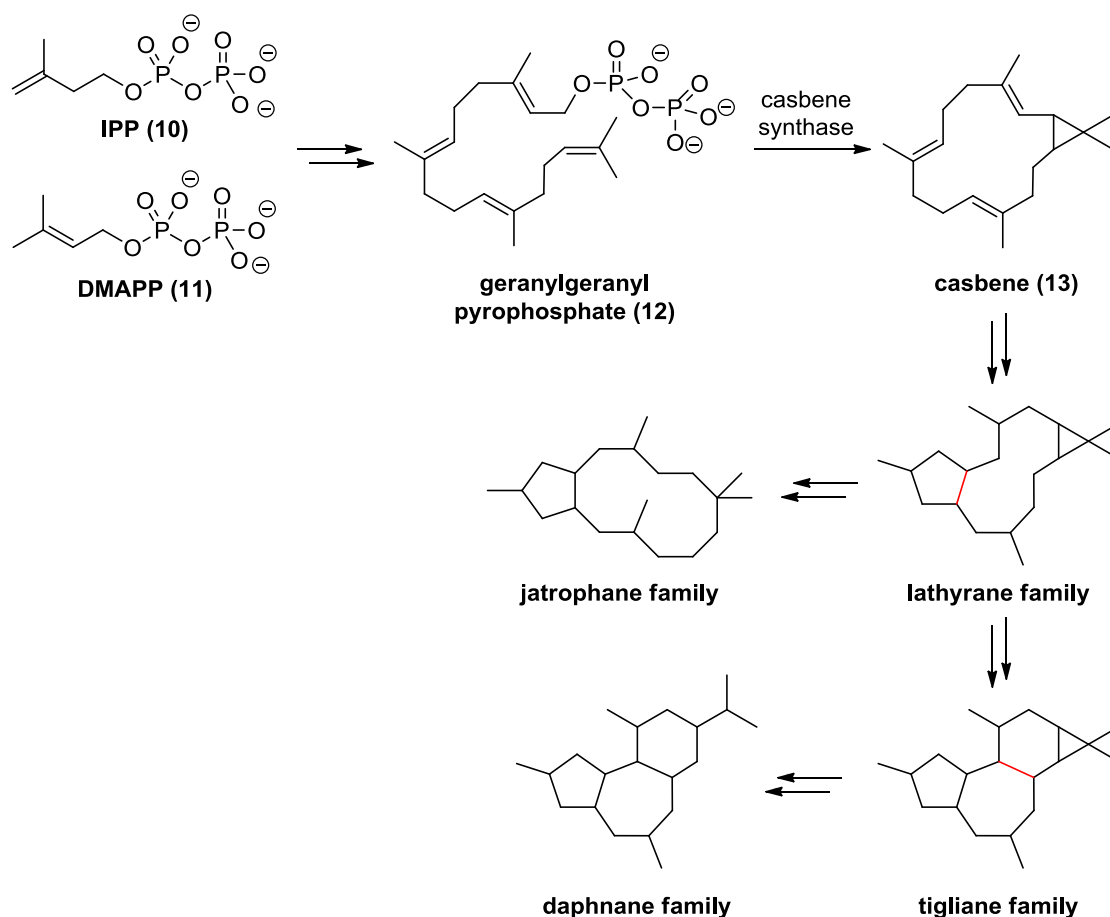
Figure 5: Examples for the variety of jatrophanes; euphosalicin for comparison

A closer look at the class of the jatrophanes reveals a large variety of compounds differing in their oxidation patterns, ester side-chains and unsaturation pattern. Figure 5 gives an overview of the jatrophanes, including euphosalicin (**1**) for comparison.

Clearly, euphosalicin's substitution pattern matches very well with that found in the jatrophanes, further attesting to the close relationship.

1.2. Biosynthetic considerations

It is interesting to note that all the terpenes shown above have a methyl-substituted five-membered ring on one end, and a dimethyl substitution pattern on the opposite end of the molecule. This can be explained by the fact that they all share geranylgeranyl pyrophosphate, the precursor to the diterpenes, as their common ancestor. To investigate this relationship further, it is informative to examine the biosynthetic routes leading to these natural product families.



Scheme 1: Biosynthetic pathways leading to diterpenes isolated from *Euphorbia* species

As with all terpenes, the biosynthesis (shown in Scheme 1) starts with the production of the two isoprene equivalents, isopentenyl pyrophosphate (IPP, **10**) and dimethylallyl

pyrophosphate (DMAPP, **11**).⁷ These two are then oligomerized to geranylgeranyl pyrophosphate (**12**), which already contains all the carbon atoms found in the skeleton of the diterpenes. In the next step, a cationic cyclization catalyzed by casbene synthase⁸ leads to the simplest member of the casbane family, casbene (**13**).⁹ Intramolecular formation of the 5-membered ring then leads to the lathyranes. From here, the jatrophanes are formed *via* cyclopropane opening, while the tiglianes are generated by a further cyclization steps. Finally, the daphnanes are then derived from tiglane precursors by a ring opening.^{10,11}

The exact synthetic pathways leading to the individual members of the different diterpene families are not fully understood, yet. Similarly, the biosynthetic precursor of euphosalicin (**1**) has not been elucidated so far. Given its similarity to other jatrophanes, it could be produced from a member of that family, but the mechanism for the crucial ring expansion giving the [11.3.0] framework is still unclear.

1.3. Biological activity

Many of the diterpenes shown above are biologically active. Resiniferatoxin (**5**), for example, tastes 1000 times as hot as capsaicin, the main bioactive constituent of hot peppers.¹² Meanwhile, the esters of phorbol (**7**) are potent tumor promoters,¹³ and jatrophone inhibits tumor growth.¹⁴

Euphosalicin (**1**) has been shown to suppress the activity of *Herpes simplex* virus (HSV) type 2, with an IC₅₀ value of 4.0 µg/mL = 4.8 µM.¹⁵ Herpes simplex affects 60-95% of all adults worldwide.¹⁶ Type 1 primarily infects the face area, especially around the mouth, as well as the central nervous system. In contrast, type 2 infections are mainly found around anus and genitalia. Euphosalicin's activity may become important in case resistances against the currently used more potent drugs, such as acyclovir, develop.

The second major biological target of euphosalicin is the inhibition of P-glycoprotein (PGP), a membrane transporter responsible for multi-drug resistance during cancer chemotherapy.^{1,17} Significant signs of inhibition are apparent at a concentration of 40 µg/mL = 48 µM.

1.4. Cancer causes and carcinogenesis

Cancer is the second most common cause of death in Austria, with about 25% of the population dying of cancerous diseases.¹⁸

Several risk factors can directly cause the development of cancer, such as smoking, infections and genetic predisposition, while others are associated with increased cancer incidence, like poor diet and life style choices.^{19,20} As an example, Figure 6 shows the correlation between smoking and lung cancer.²¹

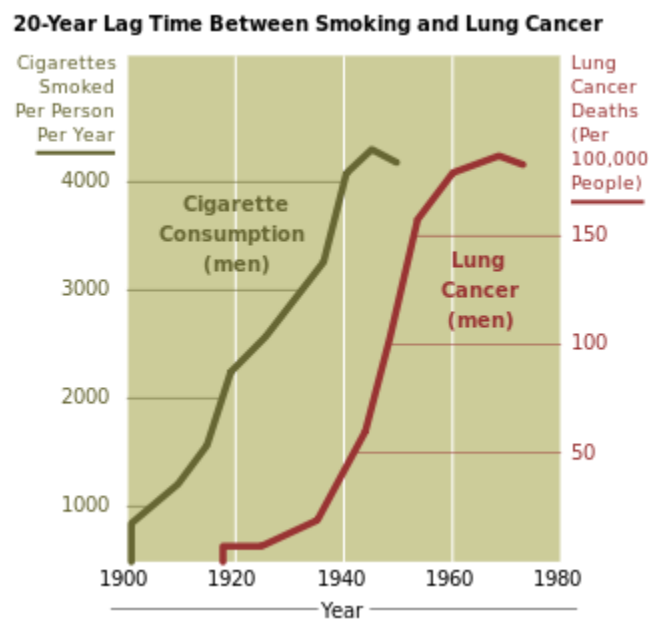
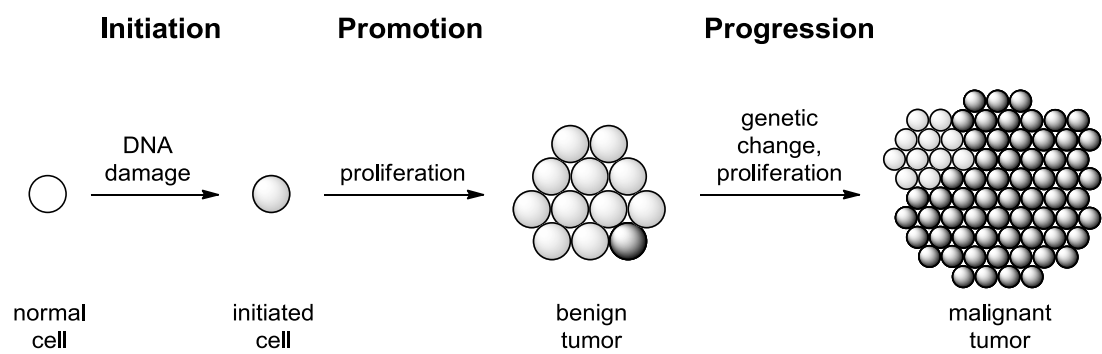


Figure 6: Correlation between smoking and lung cancer

Carcinogenesis is a multi-step process encompassing the transformation of normal cells into cancer cells due to biochemical and genetic alterations. Three stages are commonly distinguished: initiation, promotion and progression (Scheme 2).



Scheme 2: Multistage carcinogenesis

The main hallmark of tumor initiation is the manifestation of irreversible genetic damage, caused by insufficient DNA-repair or apoptosis (programmed cell death) failure after DNA damage. The resulting mutations may cause sustained proliferative signaling, complete loss of apoptosis or inactivation of tumor suppressor genes. During

promotion, initiated cells are multiplied leading to several clones inheriting the identical genomic mutations. Tumor promoting agents are not necessarily mutagenic and are not carcinogenic alone; rather, they decrease the latency between initiation and tumor development. The progression stage is characterized by the acquisition of more aggressive traits, resulting in increased invasion, angiogenesis and ultimately metastasis. To enable further growth, solid tumors can induce the formation of new blood vessels through the secretion of growth hormones, in a process called angiogenesis. This is crucial for providing sufficient oxygen and nutrients for the rapidly proliferating cells. Further, angiogenesis offers the possibility for individual tumor cells to enter the blood stream allowing transport throughout the body and invasion into previously healthy tissue.²²⁻²⁵

1.5. Cancer therapy and multi-drug resistance

Common treatment options for cancer include surgery, radiation therapy and chemotherapy. Recently, immunotherapy and combined therapies are gaining more importance. However, all of these treatment strategies have their drawbacks and limitations. Surgery offers the possibility to completely cure the cancer by physically removing the tumor. This option is limited to tumors which have not invaded nearby tissue and are in an accessible location, though. Radiation therapy can only be used to treat solid tumors (as opposed to, for example, cancers affecting the blood) destroying cancer cells by damaging their DNA using high-energy radiation.²⁶ Since normal cells are also damaged during irradiation, treatments need to be carefully planned to minimize side effects. Cancer immunology aims to use the immune system to fight cancer. These therapies either activate specific components of the immune system to detect and kill cancer cells or to counteract stimuli secreted by cancer cells leading to immunosuppression.^{27,28} Immunotherapy is a promising research area, but is currently not applicable to all types of cancer.²⁹

Despite many advanced therapeutic methods being developed over the past decades, chemotherapy is the most common treatment of different cancers. Classical chemotherapy uses cytotoxic agents to kill rapidly dividing cells. This affects tumors due to their growth speed, but it can harm healthy tissues with rapidly proliferating cells in the body, such as the digestive tract, hair follicles and bone marrow. The results are the well-known side effects of chemotherapeutics. Newer anticancer approaches aim to

target specifically mutated versions of proteins found in tumors, or proteins commonly over-expressed by cancer cells.³⁰

A major problem for chemotherapy is the development of resistances of the cancer cells against drugs. This might be due to mutations of the proteins targeted by the chemotherapeutics, which is facilitated by the inherent genomic instability of many cancer cells. Another reason for resistance against chemotherapeutics might be the up-regulation of proteins which quickly metabolize the drug, resulting in its inactivation, or shutdown of active transport systems transporting the agent into and out of the cell.³¹

All these resistance mechanisms are specific to individual drugs. In contrast, many tumor cells over-express active transporter proteins causing the efflux of all drug-like molecules. Once this happens, it effectively diminishes the usefulness of any type of chemotherapy. This efficient process is the predominant resistance mechanism found in many types of cancer and it's referred to as "multi-drug resistance" (MDR).^{32,33}

Several transporter proteins have been identified so far, with PGP being the most prominent. It belongs to the family of ATP-binding cassette transporters which possess trans-membrane domains. Using energy provided by ATP, PGP enables the active transfer of ions or molecules across the cell membrane. In healthy individuals, PGP shows high expression levels in the intestine, the liver and kidneys and is involved in the maintenance of the blood-brain barrier. Its normal purpose includes the protection of sensitive tissue against chemically-induced stress.³⁴

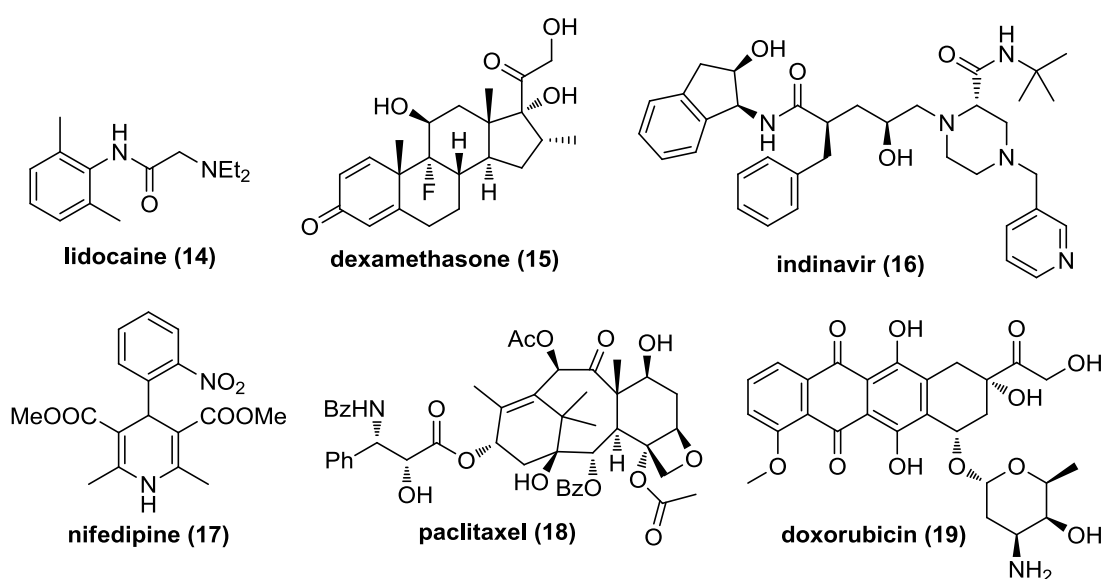


Figure 7: P-glycoprotein (PGP) substrates

To visualize the wide variety of substrates transported by PGP, Figure 7 depicts several examples.³⁵ As can be seen, PGP is able to transport a diverse array of compounds, starting from the small anesthetic lidocaine (**14**) and the antianginal nifedipine (**17**) over medium sized glucocorticoid dexamethasone (**15**) to the large antiretroviral indinavir (**16**) and the chemotherapeutics doxorubicin (**19**) and paclitaxel (**18**). Furthermore, there are no readily apparent structural motives common to those substrates.

In light of the high substrate specificities often found in enzymes, it is interesting to consider the origin of PGP's huge substrate scope. Figure 8 depicts a crystal structure of murine PGP, showing its several trans-membrane domains that are responsible for substrate binding. The energy for the active pumping process is derived from ATP, which binds to the two nucleotide-binding domains located on the cytoplasm-facing end of the protein.

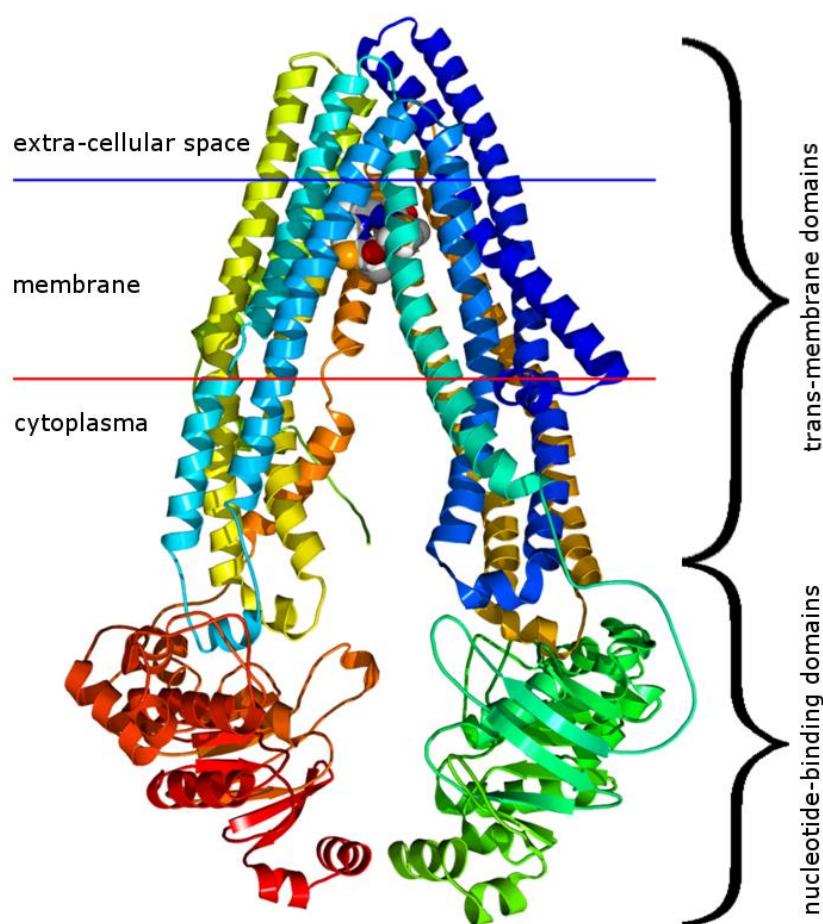


Figure 8: Crystal structure of mouse P-Glycoprotein,³⁶ showing the trans-membrane domains and the two nucleotide-binding domains

Figure 9 depicts the detailed operation of PGP. A substrate (magenta) migrates into PGP's internal drug-binding pocket from within the lipid bilayer. It is held until ATP

(yellow) binds to the nucleotide binding domains, whereupon the induced conformation change forces the substrate back out of the cell. Hydrolysis of ATP and release of ADP and phosphate then initiates a conformation change back to the initial state, so PGP is ready to bind the next substrate.³⁶

It is crucial that PGP does not actually pump substrates from the cytosol to the extracellular space. Instead, it takes its substrate from within the lipid bilayer of the membrane itself. Since most “drug-like” molecules are rather apolar,³⁷ their effective concentration in the nonpolar membrane is higher than in the aqueous mediums surrounding it (Figure 10). This concentration difference between polar solution and nonpolar membrane leads to a higher effective pumping speed for less polar compounds. It is likely that this mechanism already determines the substrate selectivity of PGP to a certain degree. Put another way, it is not only the inherent substrate preference of the transporter that is important, but also the enrichment effect obtained by the substrate uptake from the membrane lipid bilayer.³⁸

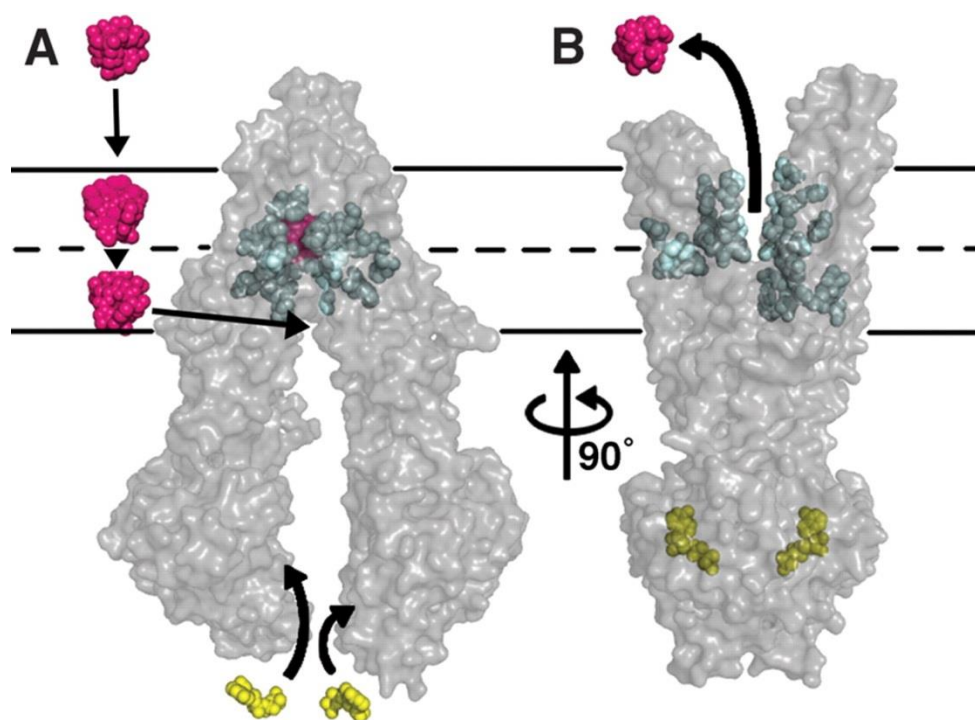


Figure 9: Operation of P-glycoprotein (PGP): (A) The substrate (magenta) migrates into PGP's substrate binding pocket *via* the lipid bilayer. (B) Upon binding of ATP (yellow), the substrate is expelled into the intercellular space. From Aller et al., *Science* **2009**, 323, 1718–1722. Reprinted with permission from AAAS.

A second factor determining the substrate scope is the large size of the binding pocket in PGP's trans-membrane domains.³⁶ This enables the transfer of large molecules, with examples up to 2300 Da being known.³⁹

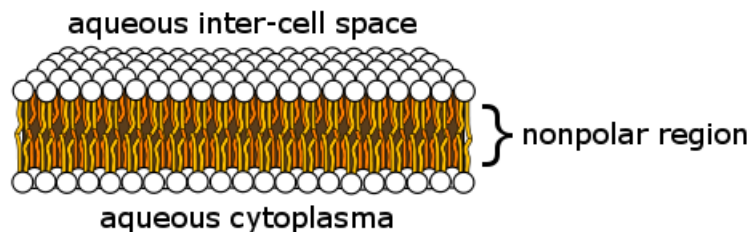


Figure 10: Lipid bilayer of the cell membrane. Lipophilic molecules are enriched in the nonpolar region

Thus, the overexpression of PGP and related proteins by tumor cells is a major obstacle to the success of modern chemotherapy. While it is possible to design drugs specifically for not being transported by PGP, this adds further complications to the drug discovery process. Additionally, large swaths of already known chemotherapeutics generally work well, and are only stymied by multi-drug resistance.

Accordingly, since the discovery of MDR, the search for agents that can block the PGP function has become a major research area. Many different MDR modulators have been identified, and several of those candidates progressed into advanced clinical trials. However, so far none of them have entered routine clinical use.^{40,41} Figure 11 shows three compounds (**20–22**) that were evaluated in clinical trials.

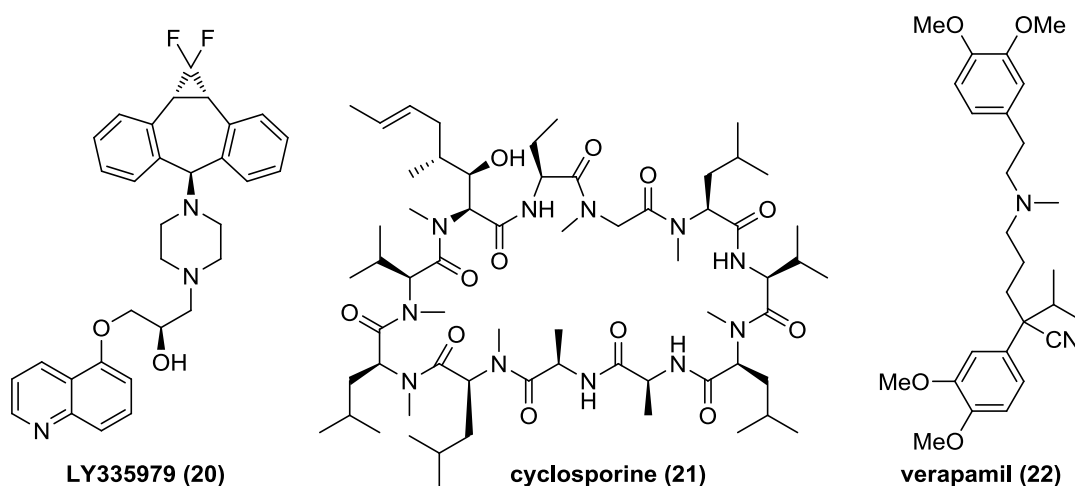


Figure 11: Three PGP inhibitors that progressed into clinical trials

The failure of all the compounds evaluated in clinical studies has several reasons. The most common are low selectivity and potency, high toxicity, and adverse interactions

with the chemotherapeutics they are intended to be used with.⁴¹ Hence, there is still need for new classes of PGP inhibitors as lead structures for drug discovery. The wide differences between the known MDR modulators makes formulation of a common binding hypothesis difficult, though, which presents a problem for rational drug design approaches.

Since euphosalicin (**1**) and many jatrophanes inhibit PGP, they became the subject of intensive research over the last few years. An especially active area is natural product isolation from *Euphorbia* species, where many new MDR modulators have been discovered over the last 10 years.^{42–47} The large number of isolated compounds also enables recognition of first structure activity relationship (SAR) trends.⁴⁸

What is noticeably missing, though, is a directed development effort to turn these promising results into actual drugs. The most likely reason for this gap is the chemical complexity of most jatrophanes, and the difficult synthetic access. To make this class of natural products more attractive for drug development teams, better synthetic approaches are needed. Further, simpler analogs of euphosalicin (**1**) and the related jatrophanes must be found that are easier to synthesize, while still retaining good inhibitory potency against PGP.

Accordingly, the goal of this thesis was to develop a synthetic route toward euphosalicin (**1**). Ideally, the route should also allow access to simplified analogs to make MDR modulators based on jatropane derivatives more approachable for the development of drugs.

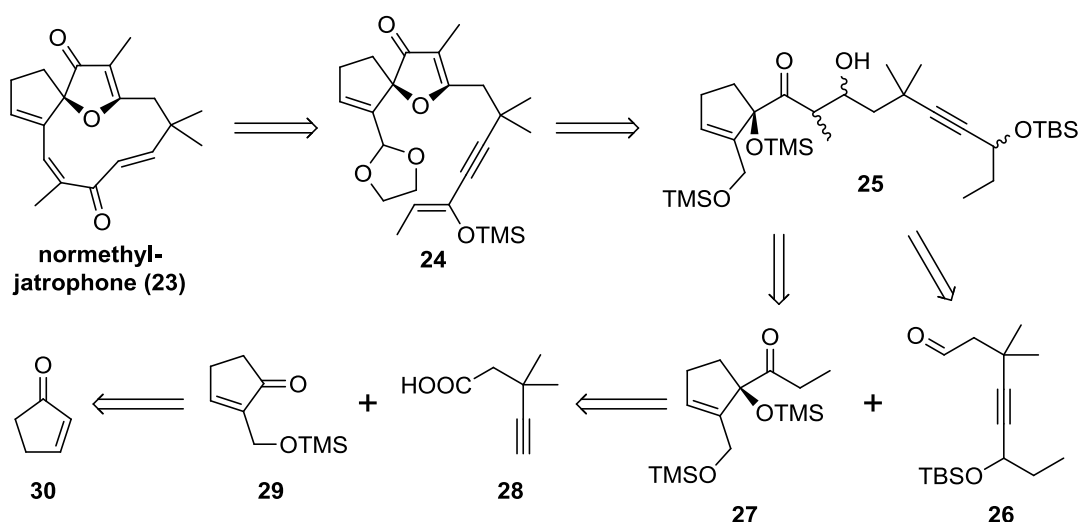
2. Previously published syntheses

Although the first member of the jatrophanes was discovered as far back as 1970,¹⁴ only few total syntheses of jatrophanes or their derivatives were published in the following 30 years. Synthetic interest in these compounds has been increasing since the early 2000's, when their MDR modulating properties were discovered.⁴² Currently, several research groups are working on the total syntheses of jatrophanes and related terpenes.

2.1. (\pm)-16-Normethyljatrophone (Smith III, 1981)

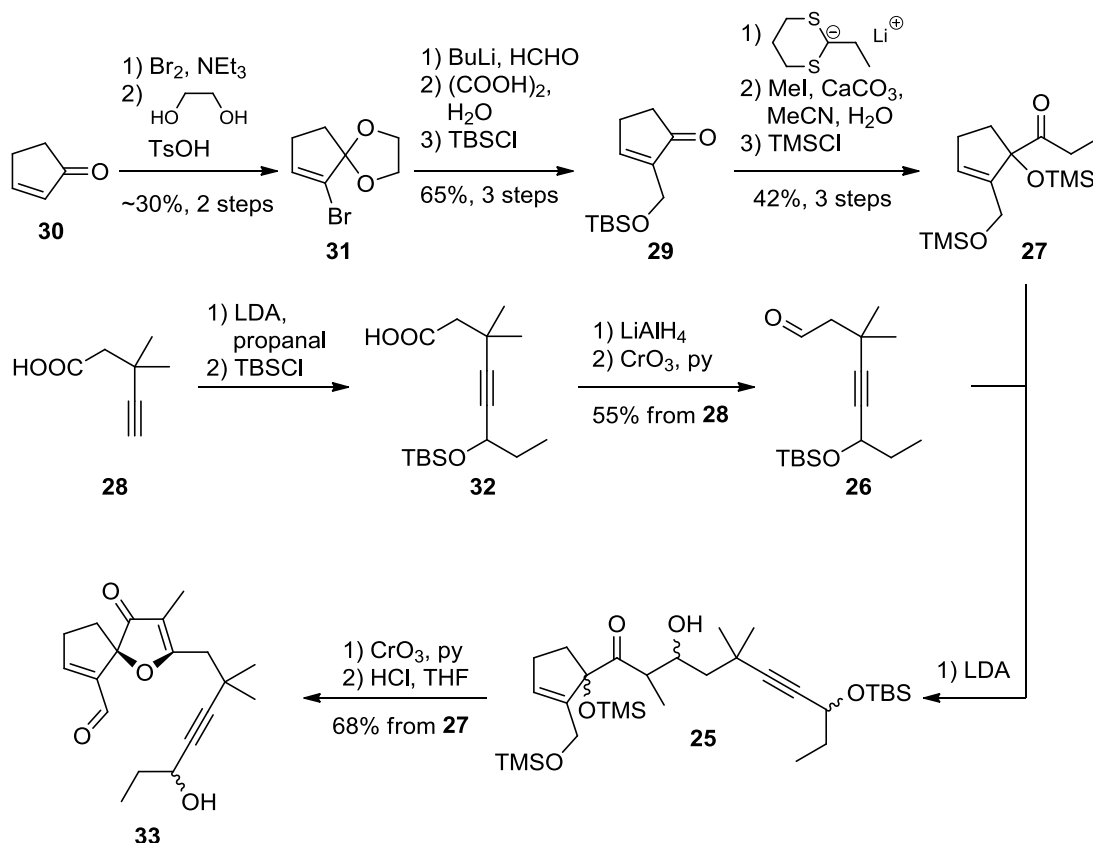
In 1981, A. B. Smith III published a synthesis of racemic 16-normethyljatrophone (**23**), a jatrophane derivative missing the methyl substituent on position 2 of the five-membered ring. In a note added in the proof, he commented that his group had also synthesized jatrophane itself *via* the same route in the meantime.⁴⁹

The main synthetic challenges are the closure of the macrocycle, and the construction of the spiro system. Smith elegantly solved both problems and derived a convergent retrosynthesis, which is shown in Scheme 3. He opted for a late stage ring closure of **24** under aldol conditions. The construction of the spiro-(2H)-furan-3-one (**25**) was planned to involve a new, acid-catalyzed protocol developed by his group. The cyclization precursor **25** should be accessible using an aldol coupling of two roughly equal-sized fragments **26** and **27**, which could be derived from **28** and **29**, respectively. Ketone **29** was obtained from cyclopentenone **30**, *via* a previously developed sequence.⁵⁰



Scheme 3: Smith's retrosynthetic analysis for normethyljatrophone **23**

The synthesis, shown in Scheme 4, starts off with the preparation of **29** from **30**. Cyclopentenone **30** is brominated and then converted to acetal **31**, which can undergo lithium halogen exchange with BuLi. Addition of formaldehyde to this solution, followed by hydrolysis of the dioxolane and TBS protection of the primary alcohol gives **29**. This is smoothly converted to ketone **27** through a three-step procedure: addition of lithio-2-ethyl-1,3-dithiane followed by deprotection of the dithiane with concomitant cleavage of the TBS ether, and finally TMS protection of both alcohols.



Scheme 4: Synthesis of the fragments and the subsequent fragment coupling

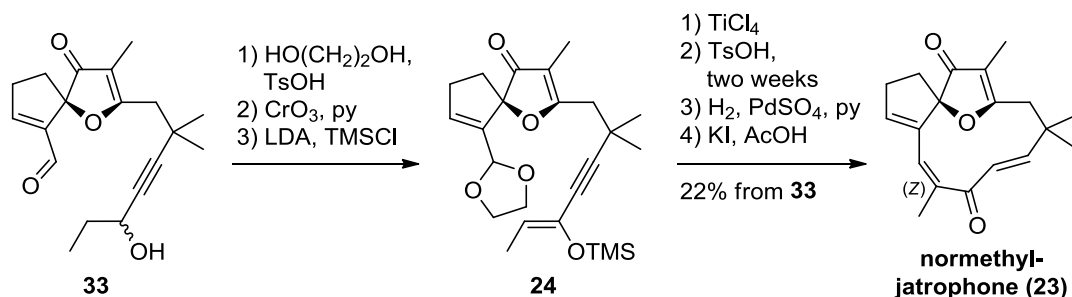
The synthesis of the second fragment, **26**, begins with alkyne **28**, which is deprotonated to the dianion before addition of propanal. TBS protection of the resulting alcohol then gives **32**, which is converted to aldehyde **26** through a reduction-oxidation sequence. Fragment coupling of **27** and **26** under conventional aldol conditions using LDA gives **25** as a mixture of 4 diastereomers. Since the target normethyljatrophone **23** contains only one chiral center, two of the three stereocenters will be removed over the next steps, rendering this issue inconsequential.

The next operation is the construction of the spirocyclic (2H)-furan-3-one **33**. This is smoothly effected by Collins oxidation⁵¹ and subsequent treatment with HCl in dry tetrahydrofuran (THF). Interestingly, the oxidation step also cleaves the primary OTMS ether under formation of the aldehyde, which does not interfere with the following acid-mediated cyclization.

At this stage, the Smith group begins examining the aldol-based ring closure. After the failure of their initial attempts, they reason that two parameters are crucial for successful cyclisation: a) selective generation of the ketone enolate, without deprotonation of the aldehyde and b) irreversible addition, without the possibility for retro-aldol reactions. The solution satisfying both requirements is the Mukaiyama aldol reaction,⁵² which utilizes a pre-formed silyl enol ether as nucleophile, and traps the resulting alkoxide in-situ as TMS ether.

Scheme 5 shows how the Smith group put these plans into practice. Following protection of the aldehyde in **33** as acetal, the requisite silyl enol ether is produced by oxidation of the secondary alcohol and enolization to give **24**. TiCl₄ effects the Mukaiyama aldol reaction, and subsequent exposure to toluenesulfonic acid triggers elimination of the ethylene glycol remnants. However, this elimination leads to the undesired (*E*) double bond, instead of the (*Z*) geometry found in jatrophone. This problem can be overcome by continued exposure to the elimination conditions for 2 weeks, whereupon the double bond is isomerized to the more stable (*Z*) configuration.

The final part of the synthesis concerns the reduction of the alkyne. After the failure of one-step reduction⁵³ using Cr²⁺, success is finally met *via* reduction over palladium(II) sulfate to give the (*Z*) double bond, followed by isomerization using potassium iodide and acetic acid.



Scheme 5: Completion of Smith's normethyljatrophone synthesis

In summary, normethyljatrophone **23** is produced in 18 steps from cyclopentenone **30**, in an overall yield of 1.2%.

This synthesis showcases Smith's approach to generating (2H)-furan-3-ones and demonstrates the capabilities of the Mukaiyama aldol reaction, being the only protocol working for this difficult closure of an 11-membered ring. However, no details are given for the synthesis of jatrophone itself, which presents a significantly greater challenge due to the second stereogenic center on the 5-membered ring. The extension of Smith's synthesis to jatrophone itself is not trivial, as Hegedus described (see below).

2.2. (+)-Hydroxyjatrophone A and B (Smith III, 1989)

Shortly after his publication of a normethyljatrophone synthesis, Smith III was involved in the isolation and characterization of several new jatrophanes.⁵⁴ Among them were hydroxyjatrophone A **33** and hydroxyjatrophone B **34**, which feature an OH group on C2 (shown in Figure 12).

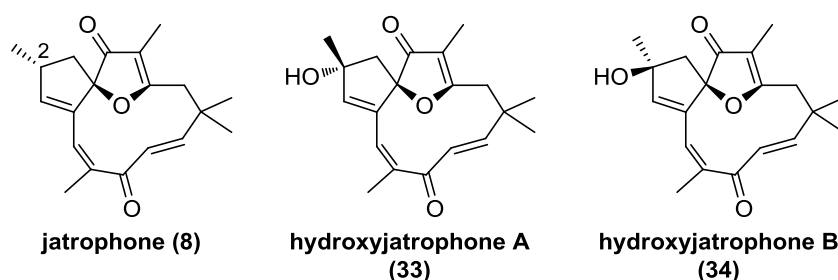
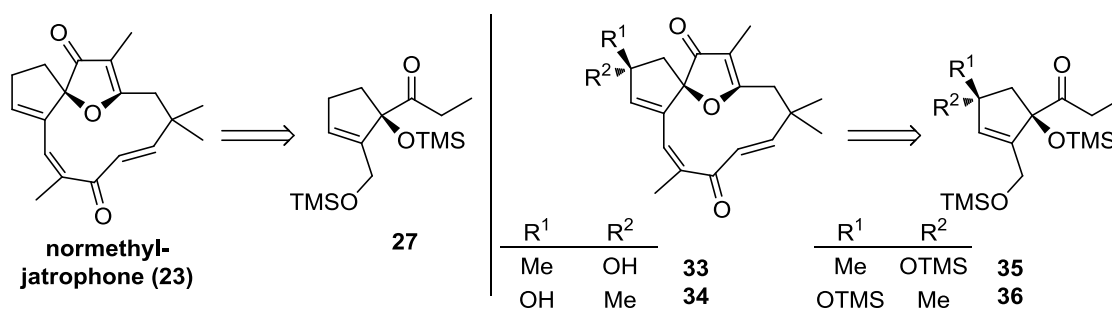


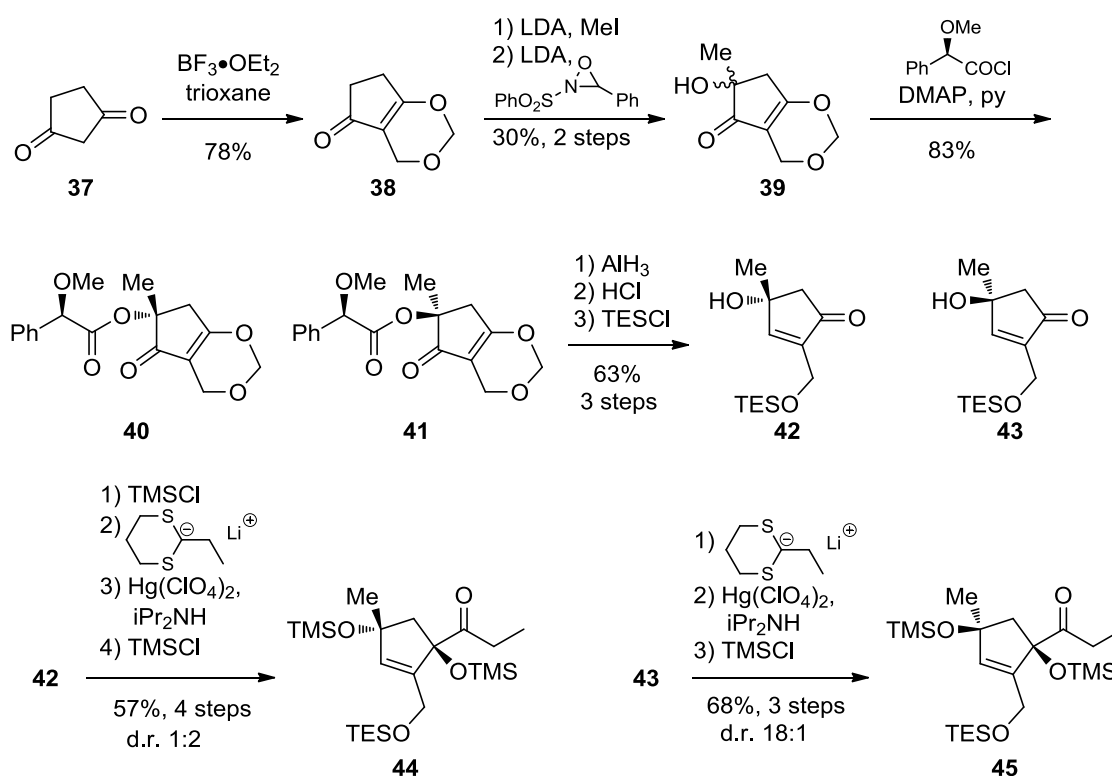
Figure 12: Jatrophone and hydroxyjatrophone A & B

Eight years after their isolation, Smith III published a total synthesis of these two compounds.⁵⁵ A careful analysis of his previous route to normethyljatrophone shows that slight modifications to the starting material might suffice to access **33** and **34** (Scheme 6). If **35** and **36** can be obtained instead of **27**, the hydroxyjatrophones would be formed without further modifications to the synthesis.

Scheme 7 describes the routes toward cyclopentenones **35** and **36**.⁵⁶ The synthesis starts with a transformation of cyclopentanedione **37** to vinylogous ester **38**, with trioxolane acting as formaldehyde source. Methylation of the ketone and subsequent α -hydroxylation using Davis' oxaziridine^{57–59} provides **39**. At this point, the racemate is resolved by esterification with *O*-methyl-mandeloyl chloride and separation of the diastereomers by chromatography to give **40** and **41**.



Scheme 6: Slight modification to an early intermediate leads to several related jatrophanes



Scheme 7: Route to the 5-membered ring building blocks

Exposure of each of these compounds to aluminium hydride leads to reductive removal of the mandelate and reduction of the ketone. Upon exposure of the resulting intermediate to HCl, the secondary alcohol is eliminated and the desired enone is generated *via* cleavage of the dioxolane. Subsequent triethylsilyl ether (TES) protection of the primary alcohol delivers compounds **42** and **43** from **40** and **41**, respectively. Here, the paths to the two different hydroxyjatrophones diverge briefly. While **43** is directly exposed to lithioethylthiane to give an impressive 18:1 diastereomeric ratio toward the desired isomer (Scheme 7, bottom right), **42** is TMS protected first. Despite the bulky TMS group, addition of the lithium organyl still occurs predominantly from

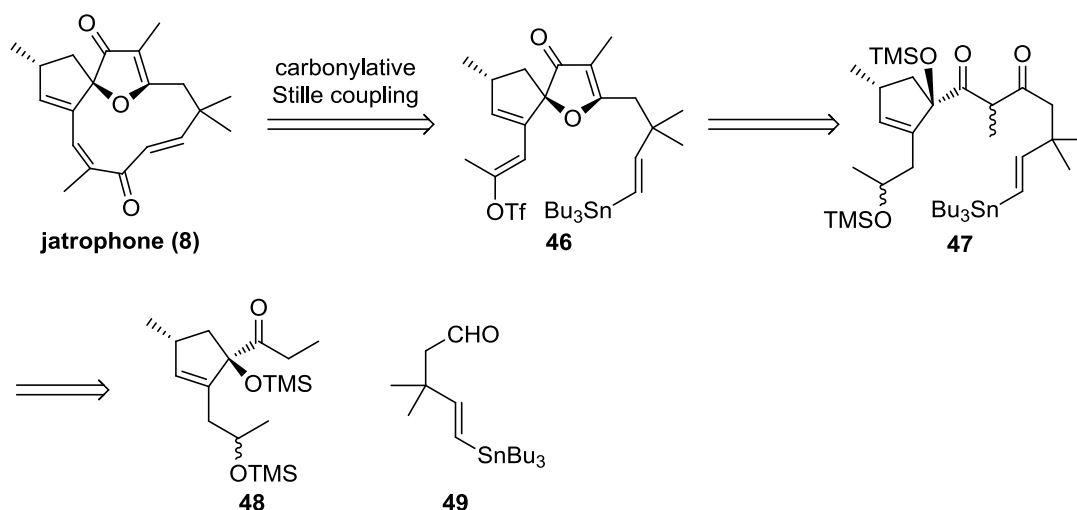
the undesired face of the molecule. Moving on nonetheless, the dithiane is cleaved and the remaining molecule is subjected to global TMS protection to obtain **44** and **45**.

The further steps to hydroxyjatrophone A and B closely track the previously published route to normethyljatrophone. The total yields were 0.2% and 0.6% over 21 and 20 steps, for hydroxyjatrophone A and B, respectively.

While this achievement demonstrates the flexibility of Smith's route toward jatrophone derivatives, it also highlights a major weakness: the difficulty to control the spiro-stereocenter. Analyzing the situation for jatrophone itself, it becomes apparent that substrate control of the dithiane addition is unlikely to the desired product. Hegedus later on confirmed this potential problem (see the next section).

2.3. (\pm)-*epi*-Jatrophone and (\pm)-jatrophone (Hegedus, 1990)

Hegedus published a racemic synthesis of jatrophone (**8**) in 1990,⁶⁰ nine years after the publication of Smith's report. The goal of Hegedus' synthesis was to showcase the new palladium-mediated chemistry that had been developed by his late coworker Stille at Colorado State University.

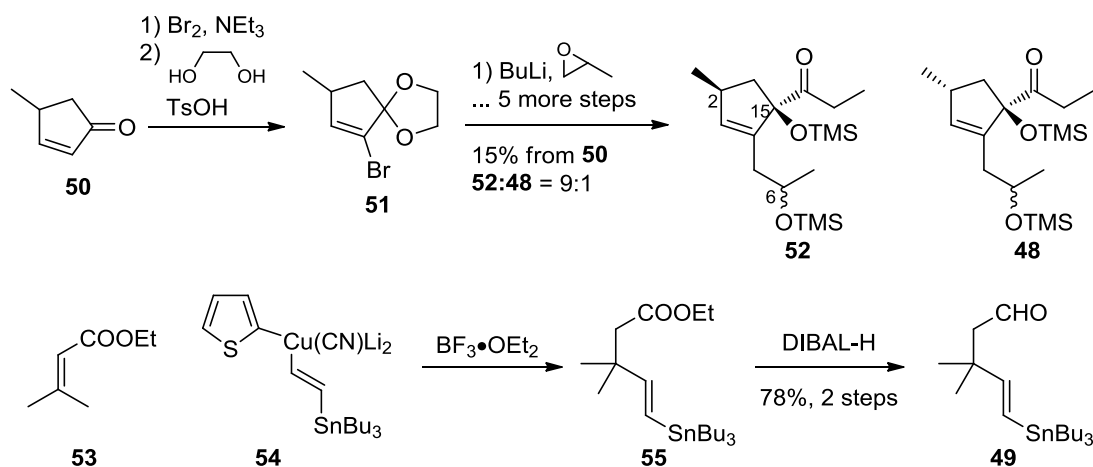


Scheme 8: Hegedus' retrosynthesis of jatrophone

His retrosynthetic analysis of the natural product is shown in Scheme 8. The core idea was to utilize a carbonylative Stille coupling^{61,62} to close the macrocycle starting from a compound such as **46**. Since Smith's spirocycle formation protocol worked smoothly, Hegedus intended to apply it, leading to **47** as precursor. Again, similar to Smith's

synthesis, he planned to access **47** *via* an aldol coupling of a five-membered ring fragment **48** and a “chain” fragment **50**.

The synthetic route is shown in Scheme 9. The synthesis of **48** is analogous to Smith’s earlier work, with two modifications. First, Hegedus starts with 4-methylcyclopentene **50** to access jatrophone instead of normethyljatrophone. Second, his retrosynthesis requires two more carbon atoms on fragment **48**. Consequently, he employs ethoxypropane instead of formaldehyde as electrophile after the lithium-halogen exchange of **51**.



Scheme 9: Synthesis of Hegedus' fragments

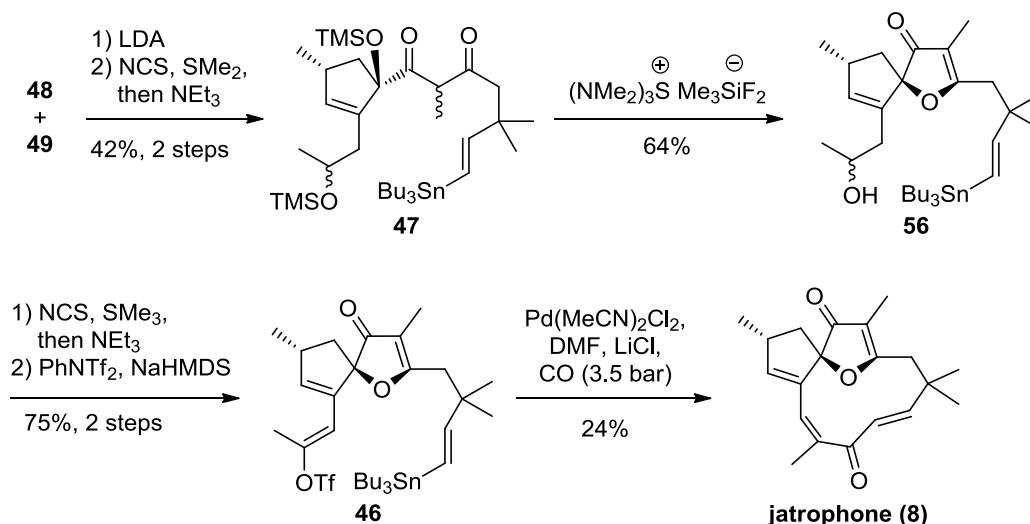
A problem arises at this stage, since a mixture of **52** and **48**, differing in the relative stereochemistry between C2 and C15, is obtained. While the stereochemistry of the C6 OTMS remains inconsequential (as this position is oxidized later on), the relationship between C2 and C15 is crucial. Continuing with **52** results in *epi*-jatrophone, **48** gives jatrophone. However, a 9:1 ratio favoring the undesired isomer is obtained.

Hegedus developed the synthesis with the undesired isomer and only switched to the correct one as success was certain. The following schemes depict the route leading to jatrophone, starting from the disfavored isomer **48**.

The second fragment **50** is accessed *via* 1,4-addition of cuprate **54** to α,β -unsaturated ester **53**. The resulting ester **55** is then reduced to aldehyde **50**.

Scheme 10 shows the completion of the synthesis. Following Smith’s lead, **48** and **50** are coupled using an aldol reaction. Corey-Kim oxidation⁶³ then leads to **47**. While Smith used catalytic amounts of HCl to effect closure of the spirocycle, those conditions

result in concomitant protodestannylation in Hegedus' route. As the tributyl tin group is essential for the upcoming ring closure, this leads to a dead end. However, the relatively obscure fluoride source tris(dimethylamino)sulfur (trimethylsilyl)difluoride⁶⁴ effects spirocyclization to yield **56** without cleavage of the stannane. As expected, the second TMS group of the molecule is also removed during this step, thus, setting the stage for the conversion to the enol triflate. First, Corey-Kim oxidation delivers the ketone, which is then converted to the enol triflate under thermodynamic conditions to yield **46**.



Scheme 10: Coupling of the fragments and completion of the synthesis

The final carbonylative Stille macrocyclization provided the natural product jatrophone (**8**), albeit in only 24% yield.

In summary, jatrophone is produced in 0.3% yield over 16 steps. The success of the final macrocyclization shows impressively what carbonylative Stille couplings are capable of. Although the yield is relatively low, a further carbon atom is incorporated and a difficult to form 11-membered ring is closed. The protodestannylation observed during acid-catalyzed spirocycle formation shows a limitation though: the rather low stability of the tin intermediates. While taking a Bu_3Sn group through a longer synthetic route is certainly possible, the more defensive option is to introduce the stannane only shortly before it is required.

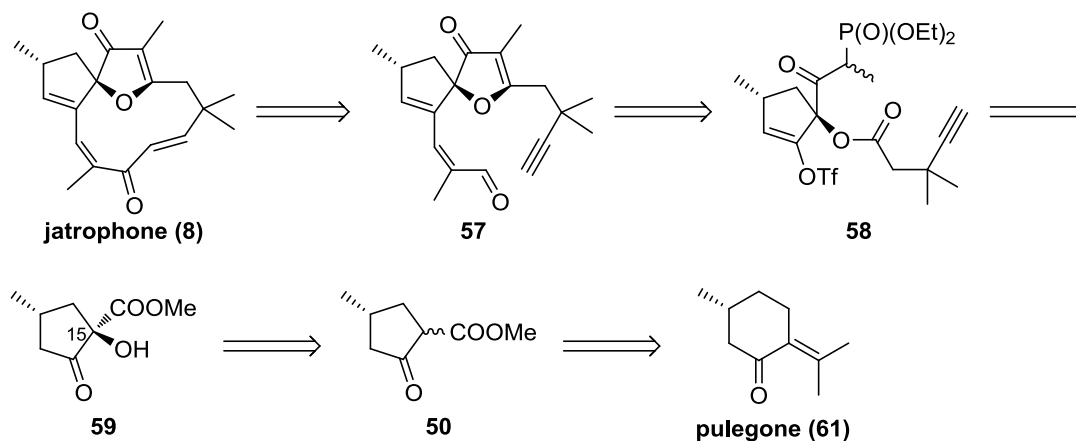
Despite demonstrating the capabilities of palladium catalyzed transformations very well, the total synthesis suffers from the 9:1 diastereomeric ratio toward the undesired isomer **52**. So, while Smith's cyclopentene methodology, which Hegedus adopted, may be a

great way to access (2H)-furan-3-ones in general, it may not be very helpful for making natural jatrophone.

2.4. (+)-Jatrophone (Wiemer, 1992)

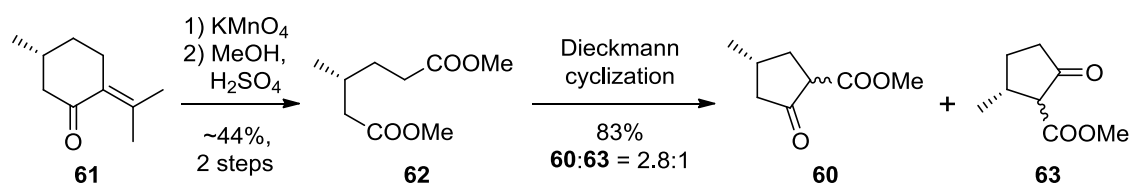
In 1992, the first nonracemic route to jatrophone was published by Wiemer.⁶⁵ It built upon usage of a chiral pool starting material and a clever substrate-directed dihydroxylation to set the two required stereogenic centers. It also features a completely different retrosynthetic analysis as the preceding syntheses, evading some of the problems encountered previously.

The retrosynthesis is shown in Scheme 11. Wiemer intended to close the macrocycle by intramolecular addition of an alkyne to an aldehyde within **57**. That in turn was deemed accessible from **58** *via* a palladium catalyzed coupling to install the propenal chain and a Horner-Wadsworth-Emmons (HWE) reaction^{66,67} to close the spirocycle. Relatively simple retrosynthetic operations led back from **58** to cyclopentanone **59**. To set the correct stereochemistry on C15, Wiemer used the already present methyl group to direct a dihydroxylation step to occur from the correct face of the cyclopentanone. The starting point for that procedure was **60**, which was derived from pulegone (**61**).



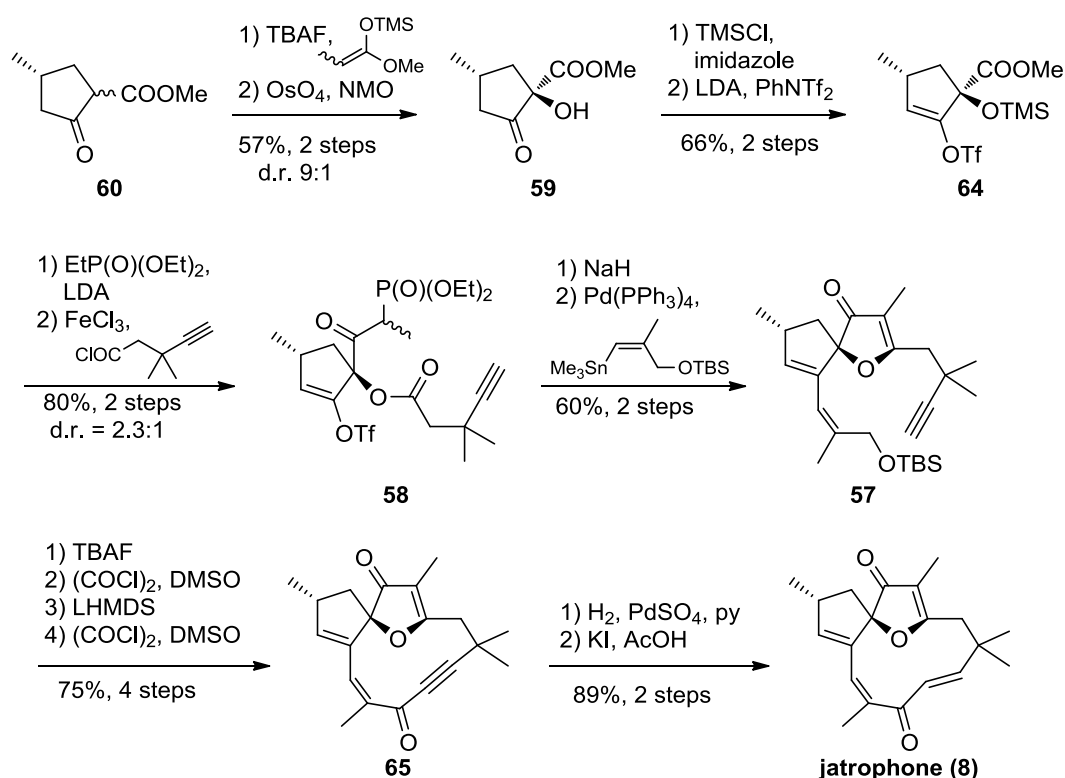
Scheme 11: Wiemer's retrosynthetic analysis of jatrophone

The synthesis commences⁶⁸ with oxidative ring opening of pulegone (**61**) and conversion of the resulting diacid to the methyl esters under acidic conditions to yield **62** (Scheme 12).



Scheme 12: First steps of Wiemer's jatrophone synthesis

The following Dieckmann cyclization yields a 2.8:1 mixture of regioisomers, **60** and **63**. In accordance with literature precedent,⁶⁹ the desired isomer is found in excess. While the mixture is not separated at this stage, it is shortly thereafter. The following schemes depict only the desired isomer **60**.



Scheme 13: Mid- and endgame of Wiemer's route to jatrophone

To install the second stereogenic center, Wiemer generates a silyl enol ether using a protocol developed by Kita,⁷⁰ as shown in Scheme 13. Dihydroxylation of the resulting double bond from the less hindered face of the cyclopentene then delivers **59** in good diastereoselectivity. Alcohol protection and triflation of the ketone yields **64**. Elaboration of the methyl ester is followed by FeCl_3 catalyzed esterification, allowing isolation of **58**. The TMS ether is cleaved in-situ under Lewis-acidic conditions. The observed 2.3:1 mixture of diastereomers next to the phosphonate is inconsequential, as it is removed in the next step. Thus, generation of the spirocycle is effected cleanly by

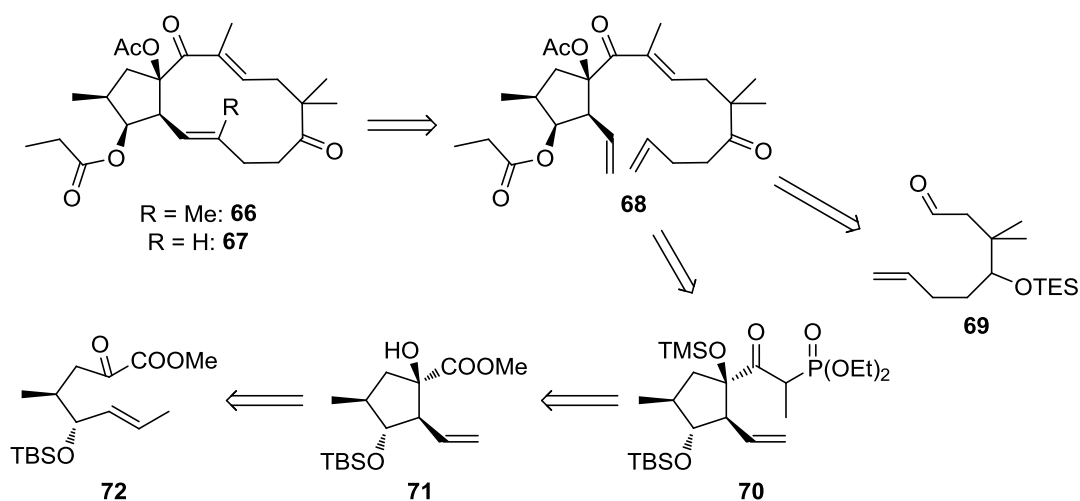
treatment with sodium hydride. The remaining carbon atoms missing for completion of the natural product are introduced *via* a Stille coupling, which results in **57**.

For the completion of the synthesis, only macrocyclization and several oxidation state adjustments remain. The sequence begins with deprotection of the TBS ether, followed by oxidation to the aldehyde. Addition of lithium bis(trimethylsilyl)amide (LHMDS) to this intermediate cleanly triggers the ring closure. A second Swern oxidation⁷¹ then delivers **65**. From here on, Wiemer follows the footsteps of Smith, who obtained an analogous intermediate without the methyl group in his normethyljatrophone synthesis. Reduction of the alkyne over PdSO₄ in pyridine first delivers the (*Z*) double bond, which is then isomerized to the (*E*) geometry for the completion of (+)-jatrophone.

Overall, enantiopure jatrophone is obtained in 3% overall yield over 17 steps from pulegone. This is an impressive feat when compared to the earlier syntheses, especially given the fact that previously, racemic material was the target.

2.5. (-)-15-O-Acetyl-3-propionyl-17-O-norcharaciol (Hiersemann, 2006)

After 14 years without a new, completed total synthesis of a jatrophane, Hiersemann published a route to (-)-15-*O*-acetyl-3-*O*-propionyl-17-norcharaciol (**67**) in 2006.^{72,73} The original intention was to target the natural product (-)-15-*O*-acetyl-3-*O*-propionyl-characiol (**66**), which proved elusive, though. One reason for the choice of these objectives was to show the power of carbonyl ene reactions which he had previously developed.^{74–77}

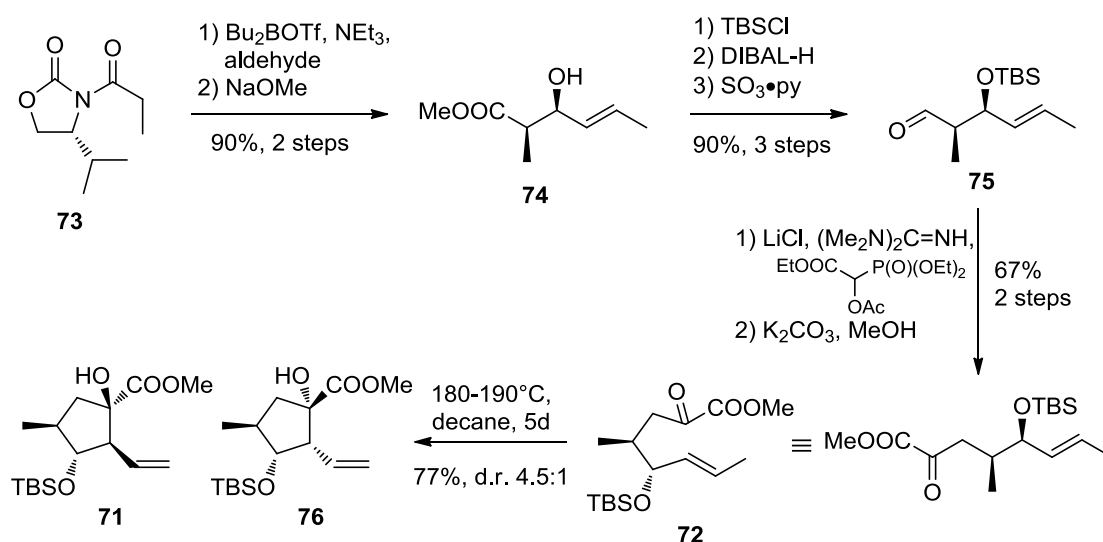


Scheme 14: Hiersemann's retrosynthetic analysis

Scheme 14 shows Hiersemann's retrosynthetic analysis. He envisaged a late-stage macrocyclization under ring closing metathesis (RCM) conditions, leading back to **68** as new sub-target. To access this intermediate, a HWE olefination joining two smaller fragments, **70** and **69** seemed appropriate. Phosphonate **70** should be available from ester **71**, which could potentially be generated by a carbonyl ene reaction from acyclic precursor **72**.

For the sake of brevity, the detailed synthetic operations leading to fragment aldehyde **69** are omitted here, they can be found in the supporting information of the original publication.⁷² Thus, Scheme 15 shows the route toward intermediate **71**. The synthesis commences with an Evans⁷⁸ aldol reaction of **73** followed by removal of the auxiliary to give **74**. Protection of the secondary alcohol as TBS ether and a reduction-oxidation⁷⁹ sequence leads to aldehyde **75**. C₂-elongation is performed using a HWE^{66,67} reaction under Masamune-Roush conditions⁸⁰ to yield the enol acetate, which is directly methanolized, resulting in cyclization precursor **72**.

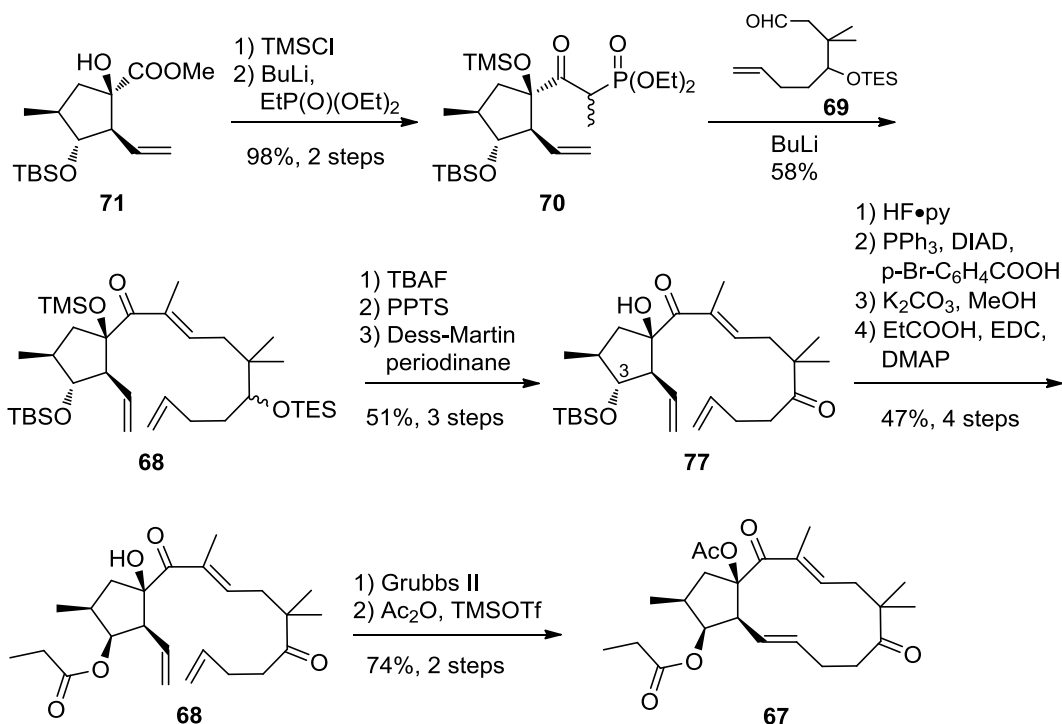
The subsequent thermic carbonyl ene reaction is effected by heating in decane for 5 days in a sealed tube. It results in isolation of a 4.5:1 diastereomeric mixture of **71** and **76** in 77% yield, favoring the desired isomer. With a total of 8 steps, this is the shortest route to the more functionalized jatrophone 5-membered rings.



Scheme 15: Synthesis of the 5-membered ring fragment

For the planned fragment coupling under HWE conditions, a phosphonate needs to be installed, as shown in Scheme 16. First, the tertiary alcohol in **71** is TMS protected, and

then the ethylphosphonate is introduced *via* addition to the methyl ester to produce **70**. The olefination with **69** reaction proceeds smoothly, yielding 58% of **68**. The TMS and TES ethers are cleaved and the resulting secondary alcohol is oxidized to ketone **77** under Dess-Martin conditions.^{81,82}



Scheme 16: Completion of Hiersemann's route to **67**

Before the final cyclization step, the stereochemistry on C3 is adjusted over 4 steps. Deprotection followed by a Mitsunobu reaction⁸³ leads to the desired inversion of the chiral center. Hydrolysis of the newly introduced *p*-bromobenzoate liberates the secondary alcohol, which is in turn esterified again with propanoic acid to give **68**.

With the 17-nor system, the macrocyclization using Grubbs' 2nd generation catalyst⁸⁴ works well and produces the target **67** after acetylation of the tertiary alcohol on C15.

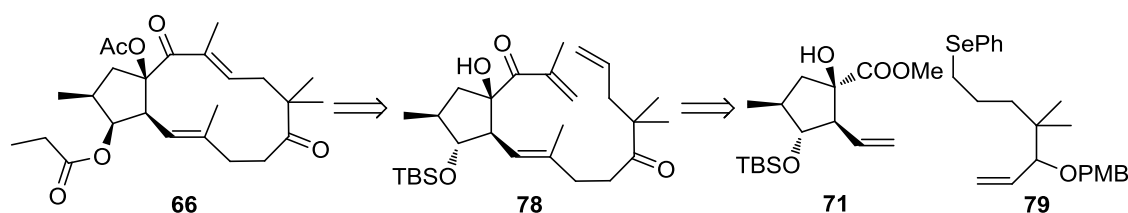
Overall, (-)-15-*O*-Acetyl-3-*O*-propionyl-17-norcharaciol **67** is obtained in 7% yield over 20 steps. The synthesis illustrates some advantages and drawbacks of methodology-driven total synthesis. The 8 step route to the cyclopentane is fascinating in its rapid buildup of complexity. On the other hand, the synthesis of fragment **69** is rather lengthy, and the endgame involves a 3 step oxidation state adjustment and a 4 step sequence to correct the stereochemistry on C4. Nevertheless, this synthesis still represents a great

contribution to the collection of total syntheses of the jatrophanes, especially given the complexity of the target.

2.6. (-)-15-O-Acetyl-3-O-propionylcharaciol (Hiersemann, 2009)

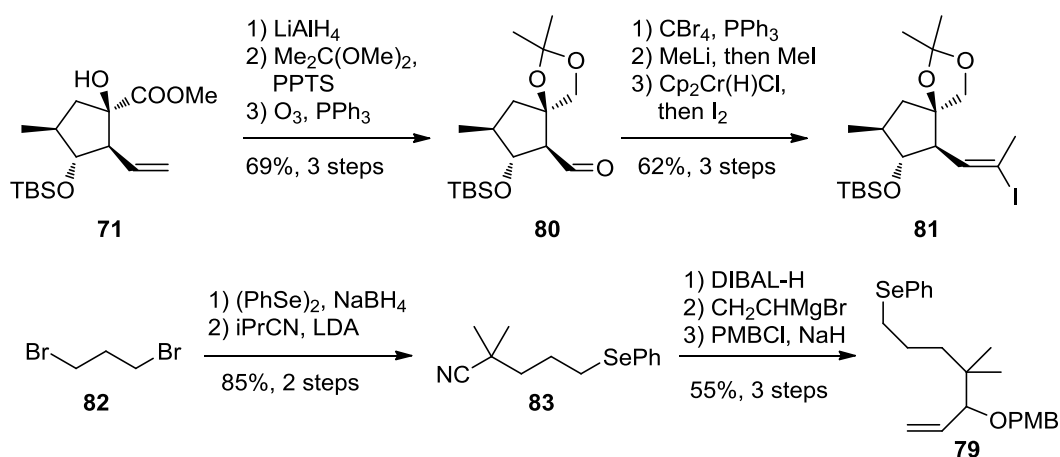
Three years later, Hiersemann published a second generation synthesis of (-)-15-O-acetyl-3-O-propionylcharaciol (**66**).⁸⁵

The updated retrosynthetic analysis is shown in Scheme 17. In the previous attempt, macrocyclization by ring-closing metathesis at the southern double bond failed for the fully substituted precursor. Sticking to RCM as ring closure protocol, Hiersemann planned to apply it to the enone in the northern end of the molecule, leading him to intermediate **78**.



Scheme 17: Second-generation retrosynthesis by Hiersemann

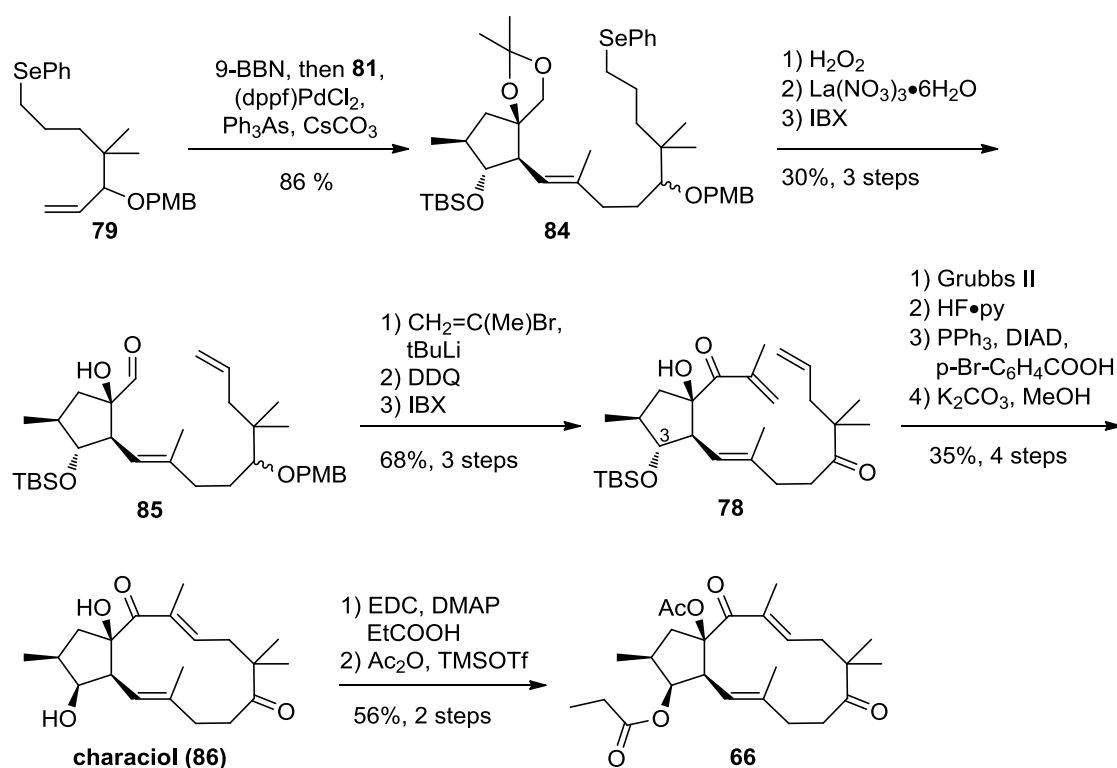
Several functional group modifications and a fragment coupling *via* Suzuki-Miyaura coupling result in the two fragments **71** and **79**, where the first one is already known from his previous synthesis.



Scheme 18: Routes to the fragments used by Hiersemann

The sequence (Scheme 18) begins with the cyclopentane **71**, which was described earlier (see chapter 2.5). First, the ester is reduced and the resulting diol is protected as acetonide. The following ozonolysis of the double bond yields **80**. A Corey-Fuchs sequence then forms the alkyne, which is methylated in-situ. The coupling partner **81** is then obtained by hydrozirconation and an iodine quench.

The synthesis of the second fragment starts from **82**, which is elaborated into **83** over 2 steps. The nitrile is then reduced to the aldehyde, which is exposed to vinyl-Grignard reagent. The resulting alcohol is finally *p*-methoxybenzyl (PMB) ether protected to yield **79**.



Scheme 19: Completion of the synthesis of **66** according to Hiersemann

Suzuki-Miyaura coupling is effected *via* hydroboration of the double bond in **79**, followed by addition of **81**, palladium catalyst and base (see Scheme 19). The resulting intermediate **84** is elaborated by oxidative elimination of the phenylselenenyl group. Lanthanum(III) nitrate hexahydrate is then used to selectively cleave the acetonide in presence of the TBS and PMB ethers. The liberated primary alcohol is oxidized with 2-iodoxybenzoic acid (IBX) to yield **85**. Next, 2-lithiopropene is added to the aldehyde. After PMB deprotection using 2,3-dichloro-5,6-dicyano-1,4-benzoquinone (DDQ), both secondary alcohols are oxidized to the ketone using IBX. The cyclization precursor **78**

is then treated with Grubbs' second generation catalyst⁸⁴ to trigger ring-closing metathesis. Over the next 3 steps, the stereochemistry on C3 is inverted using Mitsunobu conditions⁸³ to deliver charciol (**86**). The target **66** is finally obtained after esterification in 0.5% overall yield over 27 steps.

Aside from (-)-15-*O*-acetyl-3-*O*-propionylcharaciol (**66**), more jatrophane diterpenes and derivatives can be derived from characiol (**86**) by selective esterification of the two alcohols. This enables systematic SAR studies to investigate the effect of the cyclopentane substitution pattern on the MDR inhibition potency. Indeed, such an effort was published by Wiese and Hiersemann two years later.⁸⁶

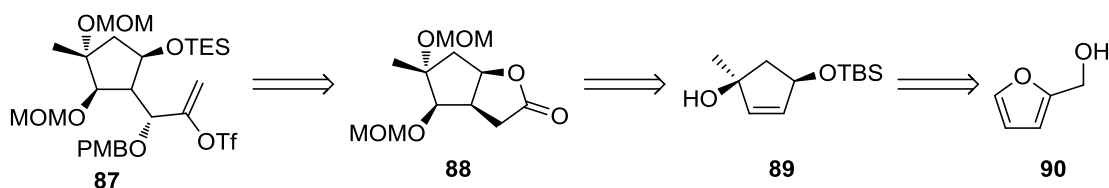
The synthesis of the natural product **66** is considerably longer compared to that of the nor-derivative **67** and the yield is smaller by a factor of 14. However, this work shows how minor structural changes can make or break a synthetic route. One additional methyl group can force the retrosynthetic analysis into a different direction, necessitating a different approach strategy. The target **66** is the most complex jatrophane synthesized up to now, and the completion of this synthesis is a testament to Hiersemann's persistence.

2.7. Other approaches toward jatrophane derivatives

More approaches to jatrophane diterpenes or derivatives thereof have been published, but no other total synthesis was completed.⁸⁷⁻⁹⁴ Since many of these publications detail the preparation of cyclopentane, which is not the main focus of this thesis, they are omitted for the sake of brevity.

The single exception is of course the preparation of a 5-membered ring fragment leading to euphosalicin (**1**) published by the Mulzer group in 2004.^{95,96}

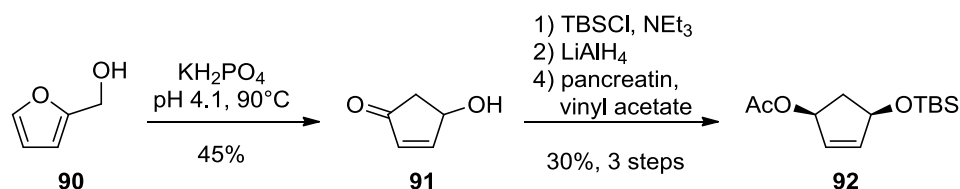
The retrosynthetic analysis for the 5-membered ring is outlined in Scheme 20. The complete retrosynthesis of euphosalicin leading back to **87** is discussed in chapter 3.



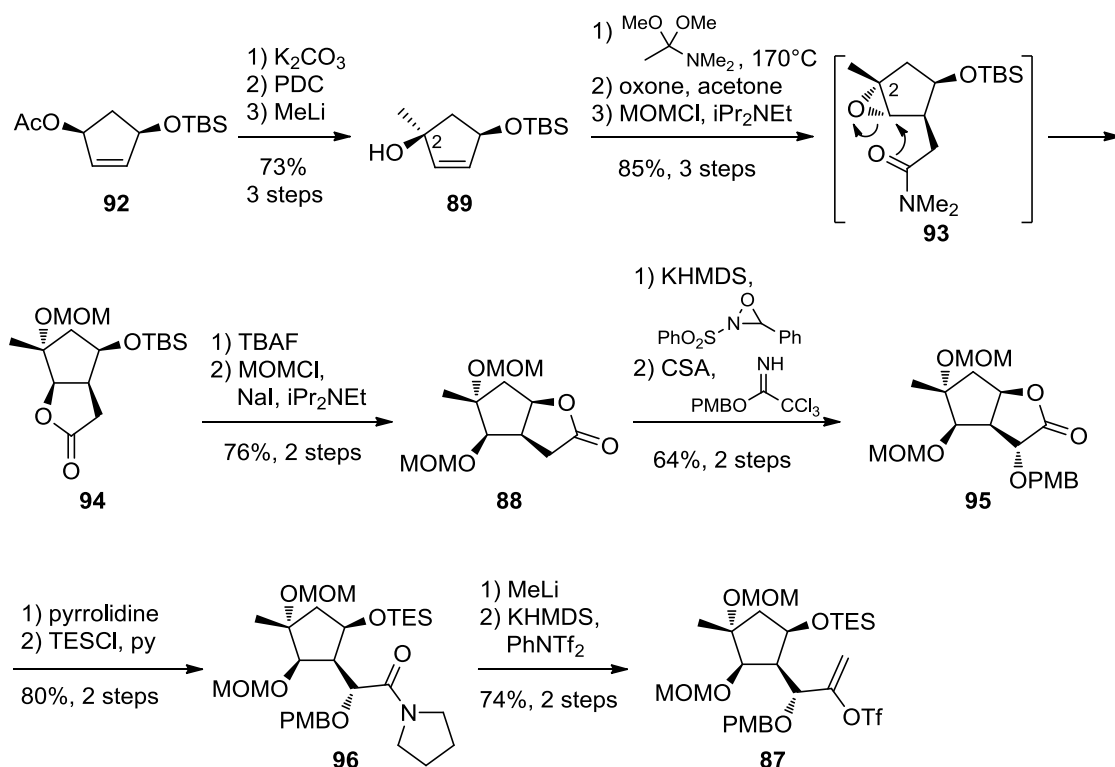
Scheme 20: Retrosynthetic analysis for the complex cyclopentane **87**

The target fragment **87** was thought to be available from **88** *via* α -oxygenation of the ester and subsequent ring opening. The bicyclic **88** in turn can in theory be obtained from the much simpler **89**, with the crucial steps being a Claisen rearrangement to install the C₂ side chain and an epoxidation/epoxide opening to introduce hydroxy groups in the desired positions. The starting material of the synthesis was cheap and readily available furfuryl alcohol **90**, which was already known to rearrange into a suitable carbocycle that can be elaborated to **89**.⁹⁷

Thus, **90** is subjected to acidic conditions, whereupon the furan opens, then closes to give carbocycle **91** (Scheme 21). After TBS protection and reduction, the racemate is resolved using pancreatin to obtain ester **92**.



Scheme 21: Furfuryl alcohol rearrangement and racemate resolution



Scheme 22: Completion of an advanced 5-membered ring fragment

The further elaboration of **92** is shown in Scheme 22. First, the acetate introduced during resolution is cleaved and the resulting alcohol is oxidized to the ketone using pyridinium dichromate (PDC). Methyl lithium addition from the less hindered side of the ring then gives **89**. Addition of *N,N*-dimethylacetamide dimethyl acetal, followed by heating then triggers an Eschenmoser-Claisen rearrangement.⁹⁸ The shifted double bond is epoxidized using in-situ generated dimethyldioxirane to generate the unstable **93**. Upon exposure to silica gel during flash chromatography, the epoxide is directly opened by the adjacent dimethylamide, and after methoxymethyl (MOM) protection of the resulting tertiary alcohol, **94** is obtained. It is interesting to note the effective inversion of the C2 stereocenter in the process.

Upon cleavage of the TBS ether, the **94** ester is rearranged to the less sterically hindered bicycle, which after MOM protection is obtained as **88**. This process proved fortunate, as α -oxygenation of the ester using Davis' reagent⁵⁷⁻⁵⁹ now proceeds with the desired stereochemical outcome. Subsequent PMB protection of the generated alcohol using Bundle's protocol leads to **95**. The next steps toward **87** are opening of the ester using pyrrolidine and, again, protection of the liberated alcohol to give **96**. Methyl lithium addition to the amide then delivers the methyl ketone, which is transformed to the enol triflate under standard conditions, yielding **87**.

Overall, fragment **87** is obtained in 2.3% overall yield over 18 steps. Compared to the other syntheses of 5-membered rings shown so far, this is a relatively long sequence, however, the resulting cyclopentane is also the most complex shown so far.

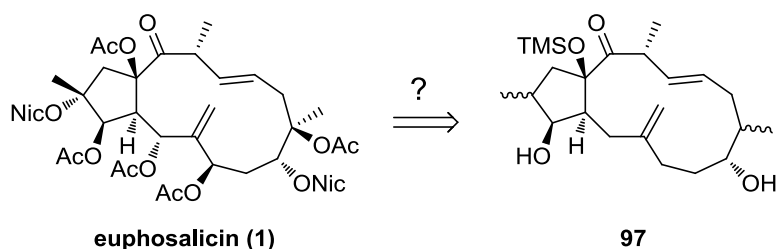
3. Results and discussion

3.1. Retrosynthetic analysis of euphosalicin

Planning a total synthesis of euphosalicin brought a number of challenges, such as when to introduce the ester side chains? Is it advantageous to introduce oxygenation right at the start or would a cyclase phase/oxidase phase approach be better?⁹⁹ How should the macrocycle be closed? How to construct the quaternary stereogenic centers?

Working through this list, we opted to install the esters at a late stage. Otherwise the synthetic operations to our disposal would be greatly limited for much of the synthesis, due to the presence of the relatively sensitive acetates.

We also chose a traditional “early oxygenation” approach, instead of the more cutting-edge cyclization/oxidation strategy popularized by Phil S. Baran. Scheme 23 shows a potential intermediate **97**, which could be obtained at the end of the cyclase phase.



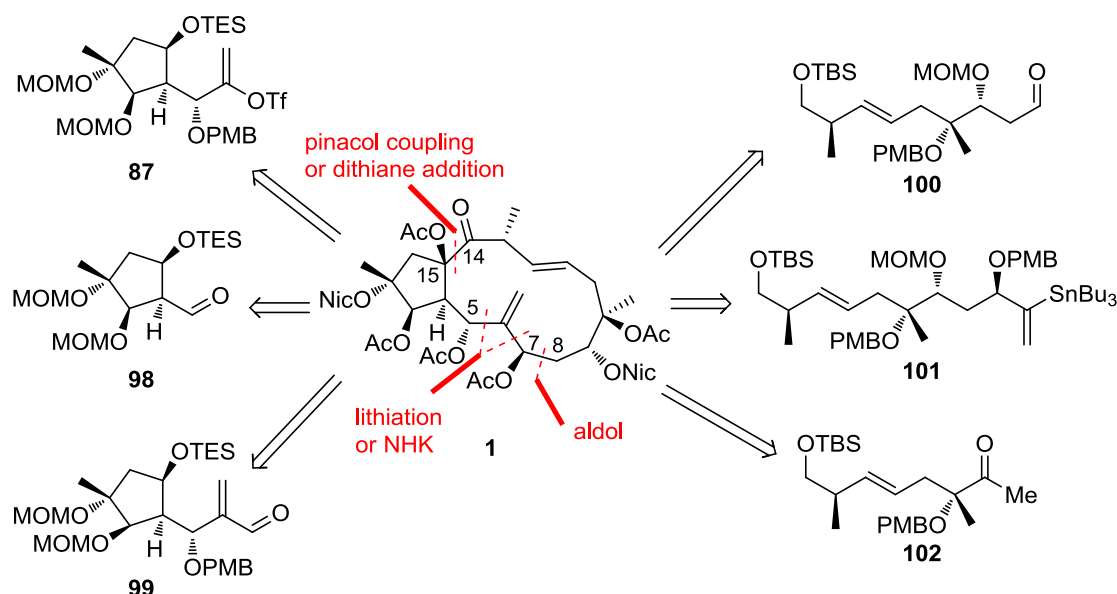
Scheme 23: A possible precursor for a cyclase phase/oxidation phase approach

While euphosalicin itself is reasonably rigid due to steric crowding caused by the large number of substituents, **97** and similar oxidation phase precursors are more flexible. This lack of stiffness raises questions about the regio- and stereoselectivity of the required oxidation reactions, and about the workability of this strategy as a whole. Indeed, such a 2-phase approach has mostly been applied to the targets with rigidly interlocked rings and without large, flexible, appendages. The two double bonds in **1** also pose a further challenge in obtaining selectivity of the requisite oxidations. Overall, while this plan was intriguing, it was deemed unworkable for the task at hand.

The previous two decisions, early oxygenation with late introduction of the ester appendages, coupled with the large number of oxygen atoms in euphosalicin, made it necessary to use protection groups in the synthesis. The choices for the protecting group strategy were mainly driven by the reactions used for the construction of the fragments.

Thus, for ease of understanding, details of this aspect will be discussed later in this chapter.

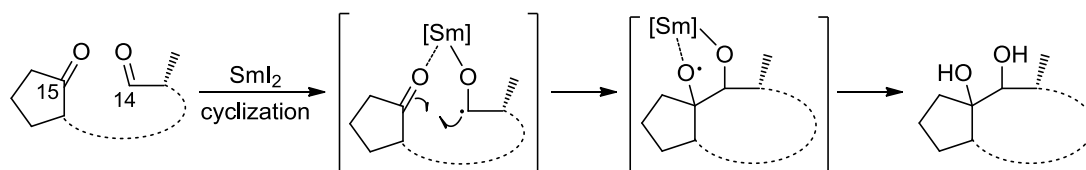
Plans for macrocyclization are shown in Scheme 24. The intention was to split the molecule into two halves by retrosynthetic cuts in the northern and southern part of the molecule. For closing the C14-C15 bond, an intramolecular pinacol¹⁰⁰ cyclization or a dithiane^{101,102} addition seemed feasible. On the southern side, three distinct fragment coupling or cyclization sites were considered (C5-C6, C6-C7 and C7-C8), applying lithiation/addition,¹⁰³ Nozaki-Hiyama-Kishi (NHK)^{104,105} or aldol reactions.¹⁰⁶



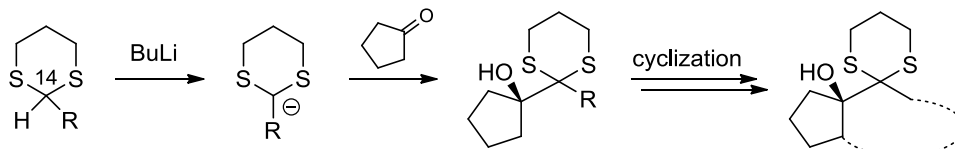
Scheme 24: Options for fragment coupling and ring closure

The order of these reactions (coupling north/cyclization south or coupling south/cyclization north) depends on the reaction chosen for forming the C14-C15 bond. A pinacol-type addition cannot be a fragment coupling step and thus must be a macrocyclization, as an intermolecular pinacol coupling has low chances of success. This is due to the unfavorable entropic factor as well as due to the likely formation of homo-coupling products. Conversely, a dithiane addition must be a fragment coupling, where the dithiane is separately deprotonated before addition of the ketone partner. Otherwise, the lower pK_A of the carbonyl group would lead to the formation of enolates before formation of the dithiane anion, resulting in elimination and decomposition of the five-membered ring fragment. Scheme 25 visualizes these requirements.

Intramolecular pinacol reaction: better thermodynamics and suppression of homocoupling



Intermolecular dithiane addition: umpolung requires deprotonation without presence of the ketone



Scheme 25: Closing the C14-C15 bond *via* pinacol reaction or dithiane addition

In the southern part of the molecule, the synthesis plan included several options to perform the fragment coupling or ring closure. The best position for this retrosynthetic cut was considered to be the C5-C6 bond. Previous work by Gilbert, Mulzer⁹⁵ and Rinner showed that the more elaborate 5-membered ring fragments, such as **87** or **99** (in Scheme 24), were difficult to produce in quantities required for the completion of the natural product. Thus, we focused on a fragment coupling at the C5-C6 junction under lithiation/addition or NHK conditions. This plan yielded roughly equally large fragments, while requiring 5-membered rings that were easier to produce in quantity, such as **98**. Conversely, this entailed a larger and more complex “side chain fragment” **101**, as opposed to the shorter **100** and **102** intermediates.

Obviously, stannane **101** will not work well in an NHK reaction. It is however suitable for lithiation chemistry, and can easily be transformed into the corresponding vinyl iodide **103** (Figure 13), which would be a viable NHK substrate. Conversely, **103** or bromide **104** could potentially be converted to stannane **101**, should the need arise.^{107–109} Thus, all three compounds, **101**, **103** and **104**, are appropriate sub-targets, and which of them is pursued is largely a matter of synthetic convenience.

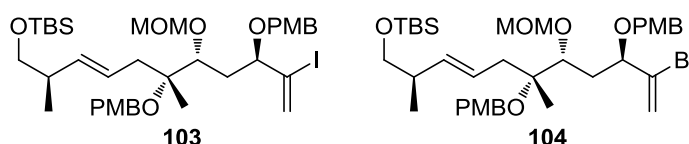
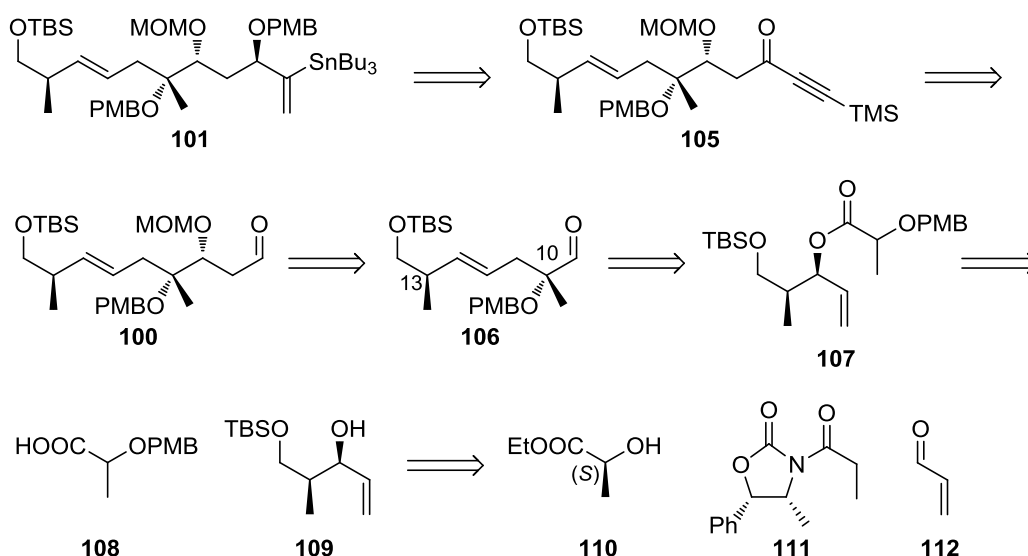


Figure 13: Synthetic equivalents to **101**

Since the retrosynthesis of the 5-membered ring fragments has already been discussed in a previous chapter, the main open question was how to approach **101** or one of its

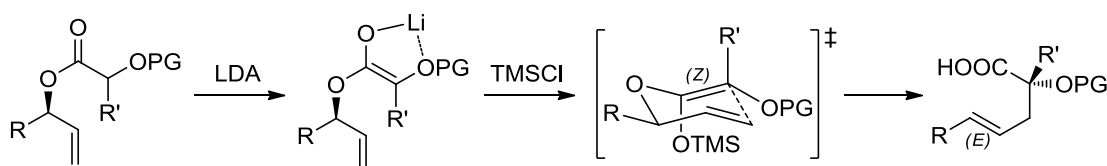
equivalents, as well as the shorter chain fragments. Scheme 26 depicts the linear approach that was ultimately selected. The final coupling partner should be accessible from **105** or a related compound. The plan for this reaction was either a regioselective hydrostannylation to give **101**, or a hydrometallation followed by an iodine quench to give **103**. Further simplification led to **114**, which was planned to be obtained from **106** via an asymmetric acetate aldol reaction. Noting the γ - δ -unsaturated carbonyl functionality in **106**, the possibility of constructing it by a Claisen rearrangement of **107** was intriguing. If this reaction proved feasible, it would present an elegant solution for the construction of the C10 quaternary stereogenic center. The chiral information present on adjacent carbon atoms in **107** could potentially be introduced in a single reaction step, with the rearrangement relaying this chirality to the distant position. Further, a Claisen reaction would naturally ensure the required (*E*)-configuration of the double bond.



Scheme 26: Retrosynthetic analysis of **99**

A major obstacle for chirality transfer using Claisen reactions is obtaining the desired (*E*)/(*Z*)-configuration of the intermediate enolate. Its geometry determines the stereochemistry of the newly formed chiral center, but is difficult to control using conventional enolization methods. However, Ireland-Claisen rearrangements^{110,111} of α -oxygenated esters deliver good selectivities, as shown by Kallmerten.^{112,113} The (*Z*) enolate geometry is obtained by chelation of the metal by the ester and the α -oxygen (Scheme 27). The subsequent rearrangement proceeds through a chair transition state, with the rest R on the allylic fragment occupying an equatorial position. This gives rise

to the (*E*) geometry of the double bond in the product and controls the absolute configuration of the newly formed quaternary center.



Scheme 27: General mechanism of Kallmerten's variant of the Ireland-Claisen reaction

After formulating a viable plan to access **106** from precursor **107**, further retrosynthetic simplification leads to **108** and **109**. Acid **108** is easily obtained from the inexpensive and readily available (*S*)-ethyl lactate (**110**). Allylic alcohol **109** should be available from the corresponding diol through selective mono-protection of the primary alcohol. This diol is known to be accessible from an Evans aldol reaction^{78,114} of **111** with acrolein (**112**). Finally, **111** has been used extensively in other syntheses^{115,116} and is obtained starting from (1*S*,2*R*)-norephedrine.

At last, at the protection strategy needs to be examined. As stated earlier, the vast number of oxygen substituents in euphosalicin required the use of protecting groups. Indeed, our approach required 3 different groups that were orthogonally cleavable due to the following requirements:

1. The C14 alcohol must be accessible separately for closing the C14-C15 bond in the northern part of the target.
2. Oxygen atoms of the two nicotinoyl esters must be selectively addressable for esterification in the endgame of the synthesis.
3. Likewise, oxygen atoms of the acetates in the product need to be protected, without interfering with the previous two prerequisites.

Based on these premises, *p*-methoxybenzyl (PMB) ether was selected for protecting the nicotinoyl ester oxygen atoms. This choice was dictated by the Claisen rearrangement of **107**, which required a coordinating α -oxygen, corresponding to a nicotinoyl ester in euphosalicin. Indeed, all published examples of this reaction employed either -OMe, -OBn, or -OPMB ethers in this position. Thus, we opted for the PMB group, as it should be more readily cleavable late-stage than benzyl (Bn) or methyl ethers.

For the remaining two protecting groups, we singled out silyl ethers and MOM groups as promising candidates, due to their stability in light of the anticipated reaction conditions, along with good protocols for late-stage removal. We chose a TBS ether to protect the primary C14 alcohol, as it can be selectively cleaved in the presence of MOM and PMB groups. Furthermore, it is introduced in a selective mono-protection of a primary over a secondary alcohol to give **109**. The bulkier silyl group thus promised better results than a protection with the sterically less demanding MOMCl.

Hence, we selected the methoxymethyl ether for protecting oxygen atoms carrying acetyl groups in the natural product. More bulky silyl groups would also have been an option, but we considered the reduced steric demands of the MOM group to be of advantage here. However, we were aware of the number of additional coordinating oxygen atoms introduced through MOM ethers, which might interfere with certain reactions.

We considered several other protecting groups as well, foremost those allowing simultaneous protection of 1,2- or 1,3-diols, such as acetonides, benzylidene acetals or silyl diethers. The arrangement of acetyl and nicotinoyl esters in euphosalicin makes this approach difficult, as Figure 14 shows. Except around the southern coupling point at C6, neighboring oxygen atoms never carry the same esters, but consistently follow an A-B pattern. Since all adjacent oxygen atoms must be differentiated later on for selective esterification, a common protecting group for neighboring hydroxy groups was not advantageous.

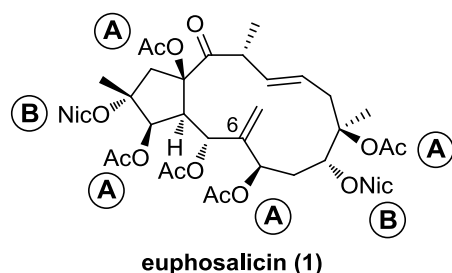


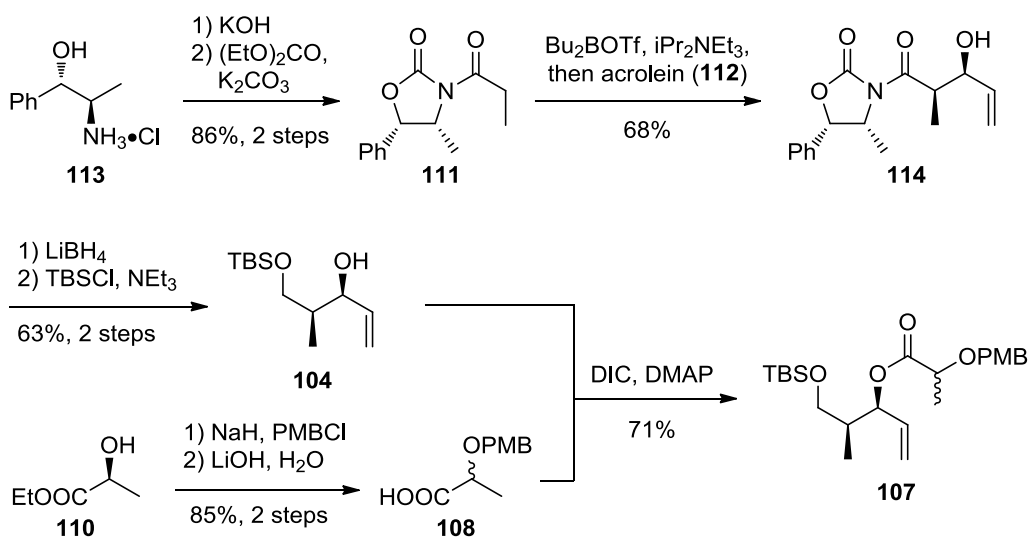
Figure 14: A-B-A pattern of acetate and nicotinoyl groups in euphosalicin

The option of using a common protecting group for all esters in the natural product, hoping for late-stage differentiation, was also investigated. That idea was discarded, as both acetyls and nicotinoyls occupy secondary as well as tertiary positions, requiring orthogonal protection right from the start.

Several other protecting groups were also considered. Mostly, they were ruled out due to their reactivity (e.g. acetyl groups) or their cleavage conditions being incompatible with other functionality present in the late-stage intermediates (e.g. methyl ethers, pivaloates and allyl ethers) or simply due to other options being preferable (e.g. PMB was chosen over benzyl ethers and TBS- over other silyl groups).

3.2. The first-generation approach

The first generation approach followed the general retrosynthetic route outlined above. The synthetic sequence started off with production of **114** from (1*S*,2*R*)-norephedrine hydrochloride **113**, as shown in Scheme 28. Cyclization was achieved by refluxing in neat diethylcarbonate over K_2CO_3 ,¹¹⁷ which consistently gave high yields without elaborate purification – in contrast to other protocols. Amide formation was effected by deprotonation of **113** with BuLi followed by quenching with EtCOCl to deliver **111**. The subsequent Evans aldol reaction worked smoothly, producing **114** in reasonable yield after high-performance liquid chromatography (HPLC) purification to remove traces of the undesired *anti* product. Reductive removal of the auxiliary worked flawlessly, and allowed recovery of the oxazolidinone. Selective mono-TBS protection gave **109** without any trace of regioisomers or the bis-silylated product.

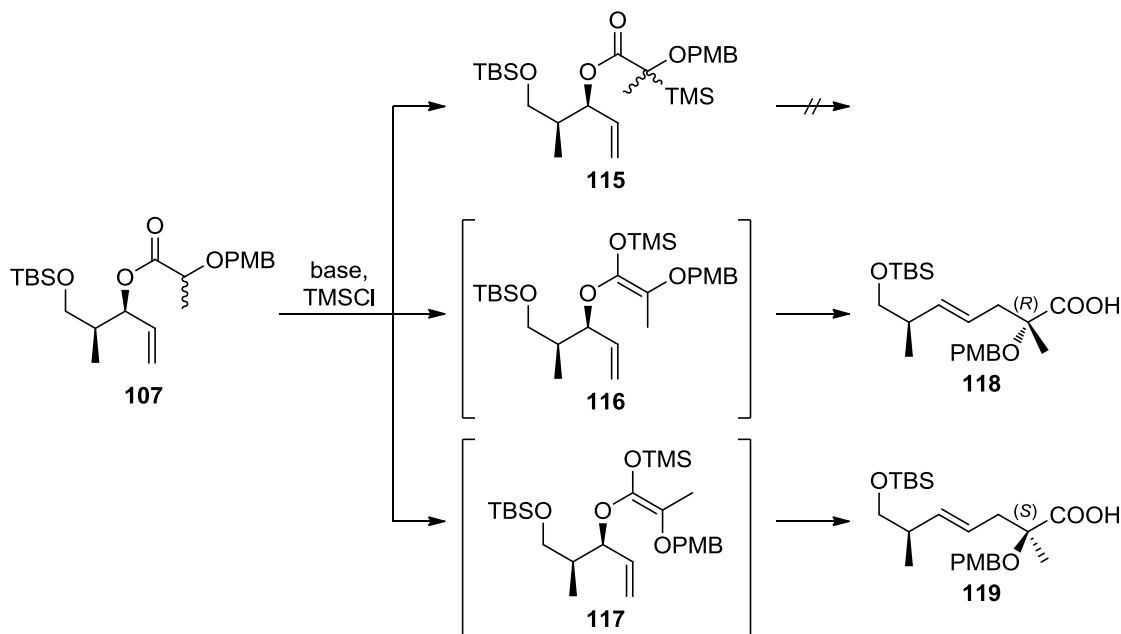


Scheme 28: Synthesis of the Claisen rearrangement precursor **107**

Intermediate **108** was produced from (*S*)-ethyl lactate **110** via PMB protection followed by saponification of the ester under basic conditions. Interestingly, the α -stereocenter was racemized to a significant degree during hydrolysis. Nuclear magnetic resonance (NMR) analysis of diastereomeric esters of **108** indicated a remaining enantiomeric

ratio (e.r.) of about 1.4:1. This was inconsequential, as that chiral center was destroyed during the following Claisen reaction. Despite the racemization, (*S*)-ethyl lactate **110** used as starting material as it was often cheaper than racemic ethyl lactate. Esterification of the two fragments **109** and **108** was performed using Steglich conditions¹¹⁸ and gave the rearrangement precursor **107** in good yield.

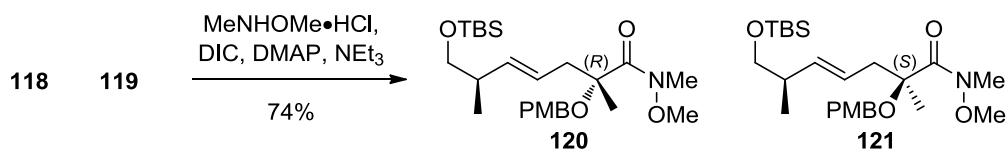
With this compound in hand, numerous rearrangement protocols were tested, starting with the Ireland-Claisen conditions described by Kallmerten. They comprised of addition of LDA to a precooled (-78°C) solution of the ester, followed by immediate quenching with TMSCl.^{112,113} The three possible silylation products **115**, **116**, and **117**, as well as rearrangement products arising from them are shown in Scheme 29. At first, no rearrangement was observed, and only C-silylated **115** was obtained. This problem was overcome by pre-cooling the base and the chlorosilane as well as the starting material to -78°C. These changes led to an effectively quantitative yield of the diastereomeric acids **118** and **119**. Determination of the diastereomeric ratio was difficult at this stage, due to the challenging purification of the acids.



Scheme 29: Claisen enolate geometry and stereochemical outcome

Thus, the crude mixture was directly converted to the corresponding Weinreb amides **120** and **121** under standard conditions using *N,N'*-diisopropylcarbodiimide (DIC), 4-dimethylaminopyridine (DMAP) and triethylamine (Scheme 30). Flash column chromatography gave a single product in 74% yield. Analytical HPLC with UV

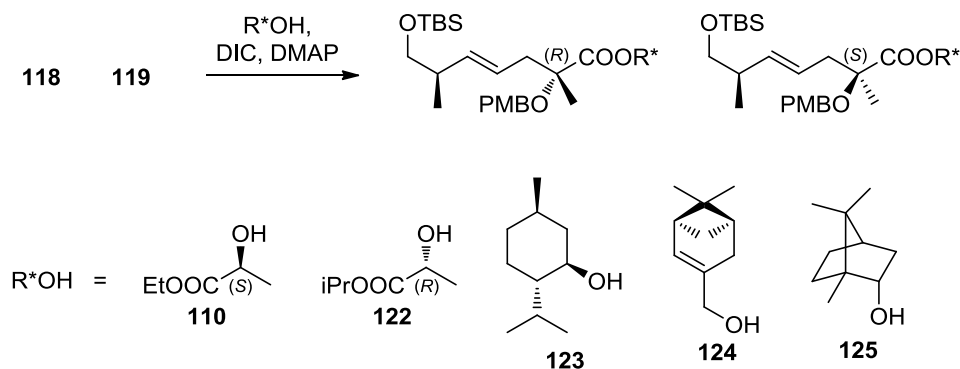
detection and HPLC/MS showed only a single peak, and IR data was also consistent with the presence of only a single diastereomer. ^1H - and ^{13}C -NMR spectra also showed a single compound, with the exception of a small unexplained signal in the ^{13}C data, which was initially not regarded as a serious problem.



Scheme 30: Conversion of the crude acids **118** and **119** to the corresponding Weinreb amides

For several more synthetic steps (see below), all analytical data were promising, indicating a single diastereomer, though sometimes a small unexplained signal was present in ^{13}C -NMR. Only when the intermediates got more complex, it became clear that a diastereomeric mixture was present. Retracing the synthetic steps, we found that the Ireland-Claisen rearrangement under the conditions described by Kallmerten did not produce diastereomerically pure material. Instead, **118** and **119** were generated in a ratio of about 3:1.

To preserve the value of already present rearranged material, later separation of the diastereomers was considered. HPLC analysis of all subsequent intermediates did not allow separation of the isomers, however. Esterification of the mixture of **118** and **119** with a number of chiral alcohols (**110**, **122–125**) was evaluated, as shown in Scheme 31. The alcohols were selected mostly by price and ready availability, since the Ireland-Claisen rearrangement was performed on 10 g scale, necessitating large amounts of chiral alcohol. Ultimately, none of the esters that could be obtained in reasonable yield permitted separation of the diastereomeric mixture.



Scheme 31: Esterification of **118** and **119** to separate the diastereomeric mixture

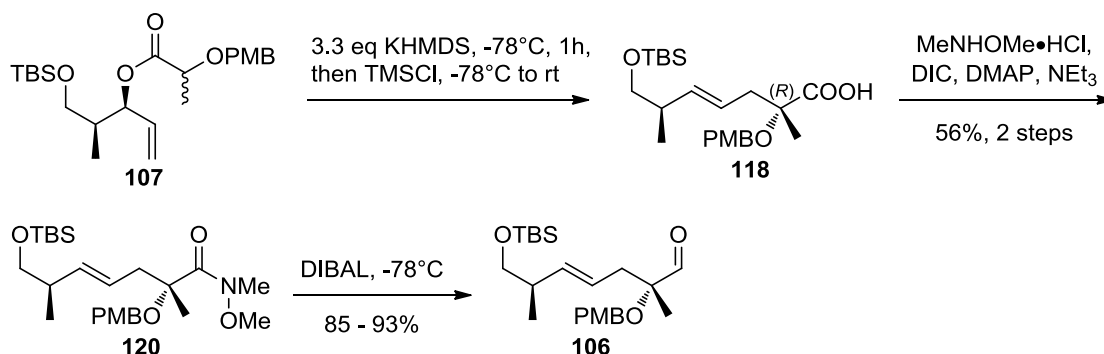
After these experiments, it became clear that diastereomer separation would not be feasible after the mixture had been produced. Thus, the only option left was to investigate alternative conditions for the Ireland-Claisen reaction, in order to generate one isomer. Revisiting previous publications showed that Kallmerten's approach yielded very good results with glycolate esters, but delivered lower selectivities with lactates, mandelates, and other higher esters.¹¹⁹ Bartlett's earlier studies on lactate esters also showed lower selectivities,¹²⁰ as did later applications in total syntheses.¹²¹ While all of these conditions favored the formation of the desired (*Z*)-enolate, none of them increased the selectivity beyond about 5:1 to 7:1. Introduction of a chiral auxiliary on the α -oxygen atom¹²² of the lactate might have improved the diastereomeric ratio, but was deemed impractical, due to concerns about cost, auxiliary removal, and the difficulties of re-protecting the resulting tertiary alcohol.

A possible solution was finally found in a publication by Langlois.¹²³ He examined the effect of different bases on the Ireland-Claisen rearrangement of an α -OPMB hexenoate ester and observed that using potassium bis(trimethylsilyl)amide (KHMDS) as a base led to excellent selectivity in the formation of the (*Z*)-enolate and consequently a large diastereomeric ratio (d.r.) after the rearrangement.

Applying those conditions to intermediate **107**, the reaction proceeded smoothly, although some unreacted starting material remained. Conversion to the Weinreb amide allowed purification and detailed analysis, which showed only one diastereomer, without any traces of a second isomer. Additionally, the resulting compound was identical to the major isomer previously obtained under the classic Kallmerten conditions, indicating that it was indeed the desired **120**. Although the overall yield of the product was lower (56% over 2 steps), remaining starting material could be recovered. Further experiments aimed at improving conversion – with as prolonged reaction times and altered temperature profiles – did not give superior results. Scheme 32 shows the final Claisen rearrangement conditions, along with the next reactions in the sequence.

Weinreb amide **120** was smoothly reduced to aldehyde **106** using diisobutylaluminium hydride (DIBAL). The yield fluctuated slightly between reactions, and traces of over-reduction were sometimes observed. Presumably, temperature and water content of the solvent (absolute ether) contributed to this phenomenon. Aldehyde **106** was stable for

several days at room temperature (rt), and indefinitely at -18°C. Larger batches of up to 6 grams of **106** were routinely prepared and stored.



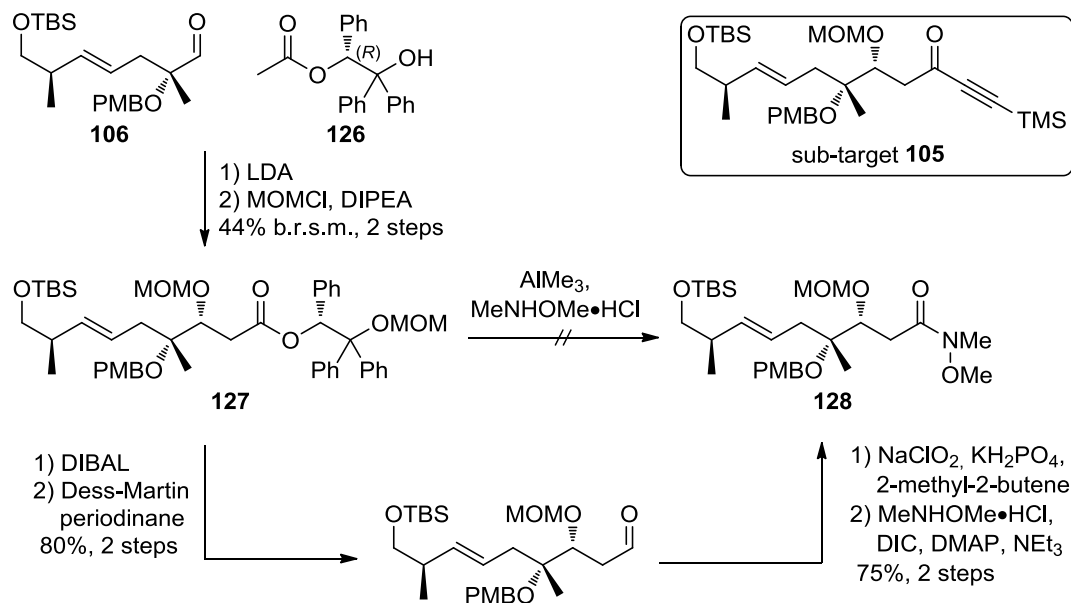
Scheme 32: Final conditions for the Ireland-Claisen rearrangement and further steps toward **106**

With a practical, economic, and scalable route to **106** established, the next task was C₂ elongation to obtain aldehyde **100**, which might be achieved using an acetate aldol reaction. However, many of the common asymmetric aldol reactions perform poorly with acetate enolates, especially in regards to stereoselectivity. Romea and Urpí observed:

*Indeed, pioneering studies soon recognized that the asymmetric installation of a single stereocenter in such aldol reactions was much more demanding than the simultaneous construction of two new stereocenters in the related propionate counterparts.*¹²⁴

Manfred Braun's (*R*)-2-hydroxy-1,2,2-triphenylethyl acetate ((*R*)-HYTRA, **126** in Scheme 33) quickly emerged as the most promising option.^{125–127} In practice, double deprotonation of HYTRA using LDA, followed by aldolization at -100 °C gave a mixture of the desired product along with unreacted starting materials. Due to the low solubility of the triphenylethanol moiety, purification was difficult. Flash column chromatography required large amounts of silica compared to the crude product mass. HPLC separation was necessary due to the low R_f value difference between leftover HYTRA and the product, and required consequently large amounts of solvent. Therefore, the crude material was commonly moved on, and purification was performed after the following MOM protection, which was effected using MOMCl and diisopropylethylamine (DIPEA). Slightly more soluble material was obtained this way, and purification by flash column chromatography and HPLC yielded 44% **127** based on recovered starting material (b.r.s.m.). Typically, 14% starting material was recovered

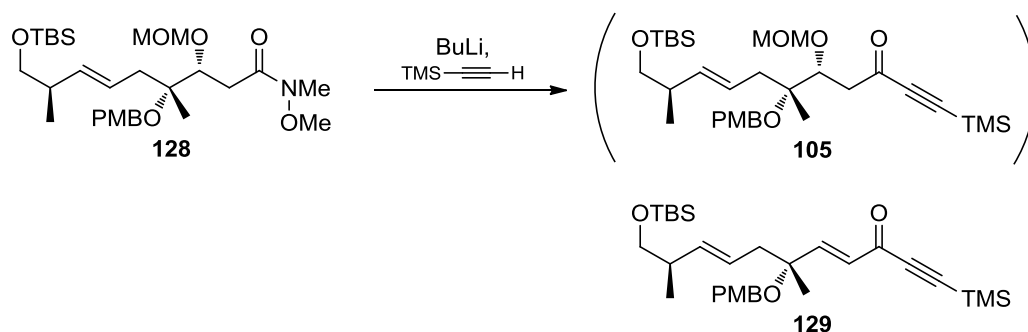
and subsequently recycled. Although this solution was not ideal, it allowed exploration of the next reactions in the planned sequence.



Scheme 33: Second part of our first approach to **105**

To obtain sub-target **105**, the most straight-forward route would have been a direct conversion of **127** to Weinreb amide **128**. However, all such transformations¹²⁸ failed when applied to **127**, most likely due to the steric crowding by the bulky ester group. Further, saponification under basic conditions did not yield the desired product. Thus, we developed a slightly circuitous route. First, the ester was reduced with DIBAL, followed by oxidation to aldehyde **100** using the Dess-Martin periodinane.^{81,82} Then, **100** was further oxidized under Pinnick conditions¹²⁹ and finally converted to the Weinreb amide **128**.

The last step to convert **128** to the desired sub-target **105** was addition of an acetylene anion equivalent. However, this conversion proved difficult to achieve (Scheme 34).



Scheme 34: Addition of trimethylsilylethynyl lithium to **128**

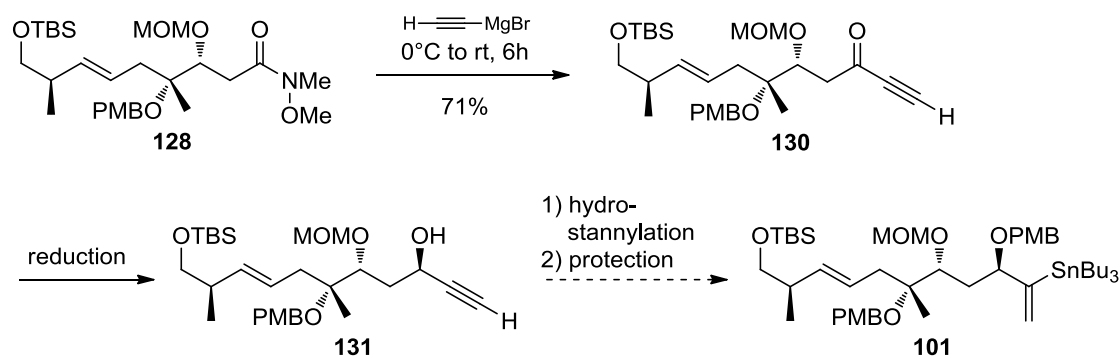
After initial attempts¹³⁰ led to re-isolation of starting material, the first step was ascertaining that deprotonation of trimethylsilylacetylene was proceeding as expected. Indeed, a D₂O quenching experiment showed near-complete deuteration, indicating that deprotonation was not the issue. Exposure of simpler model compounds to the reaction conditions gave the expected products, suggesting that the problem might be a peculiarity of **128**. Table 1 summarizes the conducted experiments, along with their outcome.

Table 1: Surveyed reaction conditions for addition of trimethylsilylethynyl lithium to **128**

Anion Eq.	Solvent	Time / Temperature	Additives	Outcome
1.5	THF	3 h, -10°C	-	No reaction
3	THF	3 h, -10°C	-	No reaction
3	THF	3 h, rt	-	No reaction
3	THF	6 h, reflux	-	No reaction
3	Et ₂ O	6 h, reflux	-	No reaction
1.5	THF	6 h, -10°C to reflux	TMEDA	No reaction
1.5	THF	6 h, -10°C to reflux	HMPA	129 (60%)

Standard reaction conditions only led to re-isolation of starting material, even after prolonged heating. Addition of tetramethylethylenediamine (TMEDA) had no effect on the outcome. Upon addition of hexamethylphosphoramide (HMPA) and prolonged heating, a new compound was isolated. It was identified as the elimination product **129**, which was presumably formed *via* an E1cB mechanism. Interestingly, the corresponding Weinreb amide could not be recovered, suggesting that either elimination occurred only after successful addition of the alkyne to **128**, or that an α,β -unsaturated Weinreb amide intermediate was formed and reacted quantitatively with the lithiated ethyne under the reaction conditions. To conclude, no variation of these conditions allowed access to the desired product.

To circumvent these issues, other organometallic protocols were investigated. Indeed, exposure of **128** to ethynyl magnesium bromide at 0°C to rt for 6 h gave the adduct **130** in 71% yield, as shown in Scheme 35.



Scheme 35: Grignard addition to **128** and planned route toward stannane **101**

At this stage, only the following three steps remained for obtaining the final fragment **101**:

- reduction of the ketone
- hydrostannylation of the triple bond and
- protection of the resulting alcohol.

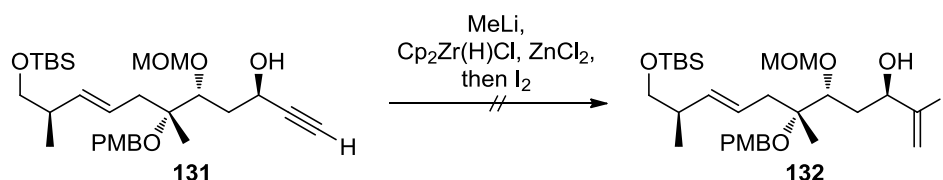
Originally, our plan was to use a Noyori reduction,^{131,132} which is reported to give excellent yields and stereoselectivities on similar systems.¹³³ This relied on the TMS protecting group on the alkyne, however, as unprotected ynones are known to impede the catalytic reduction process. While there are several methods to generate trimethylsilylethynyl Grignard reagents,^{134,135} it seemed prudent to explore other asymmetric reductions first. This was especially enticing, as it would remove the need for subsequent TMS cleavage, saving one step along the reaction sequence. Reduction conditions and results are shown in Table 2.

Table 2: Conditions for ynone reduction

Catalyst / reducing agent	Time / Temperature	Outcome
Noyori catalyst / iPrOH	12 h, rt	No reaction
Alpine borane	12 h, rt	No reaction
Me-CBS / BH ₃ •SMe ₂	1 h, -30°C	Mixture of 131 and its epimer
Me-CBS / BH ₃ •SMe ₂	1 h, -78°C	No reaction

As expected, the Noyori catalyst did not promote reduction of the unprotected ynone. Reduction using alpine borane^{136,137} also failed to give any reduction product. Corey-Bakshi-Shibata (CBS) reduction^{138,139} led to a 1.4:1 mixture of epimers at -30°C in 68% yield. Attempts to improve the low selectivity by decreasing the temperature did not succeed, as only starting material could be isolated.

Next, we aimed for the crucial hydrometallation of the triple bond. The first route to explore was Ready's hydrozirconation protocol to obtain **132** (Scheme 36),¹⁴⁰ since it promised good regioselectivity, which is difficult to achieve in the functionalization of alkynes. Preliminary experiments showed that the double bond of **131** was attacked more readily than the triple bond. Thus, a mixture of products missing the crucial *E*-alkene was obtained, while the alkyne stayed intact.



Scheme 36: Ready's hydrozirconation conditions

At this point, before investigating the path toward stannane **101** or iodide **103** any further, it became clear that the HYTRA aldol reaction would not be able to supply enough material to continue toward the natural product on this route. The major problem was the purification of the aldol mixture. Performing column chromatography and HPLC of tens of grams of hardly soluble crude product was found to be impossible with the available methods.

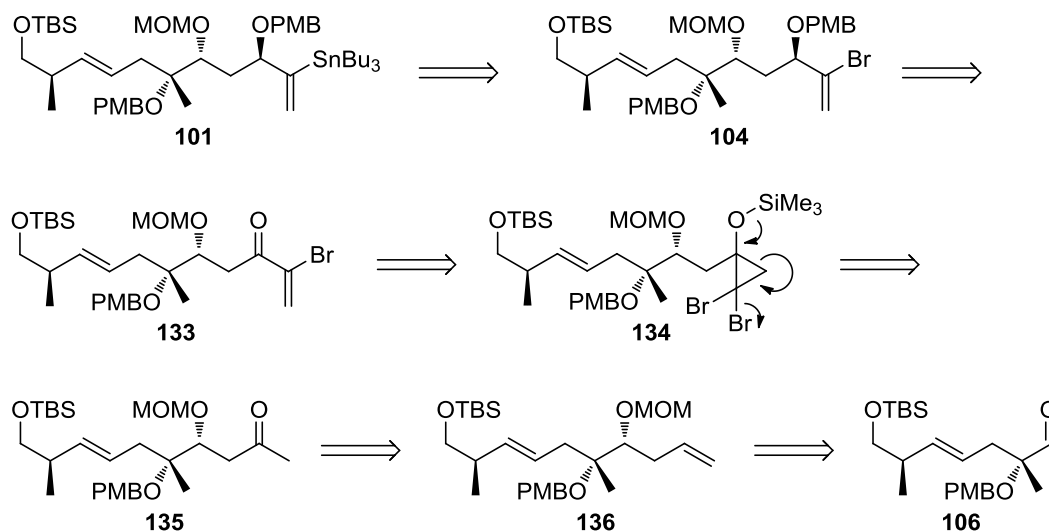
As one of the key reactions of this approach was discovered to be unviable, we turned our attention to a new strategy.

3.3. **Second-generation approach: retrosynthetic analysis**

An alternative route was sought to evade the problems encountered during the first generation approach. The goal was

- to perform the reactions at the required scale, without an excessive amount of practical difficulties.
- to keep the well-working reaction sequence up to aldehyde **106**.
- to ideally find a route offering more convenient access to the stannyl-alkene moiety. While obtaining this class of compounds from terminal double or triple bonds is possible, side products are often observed.
- to possibly obtain a shorter linear sequence toward **101**.

The core retrosynthetic ideas behind this strategy are shown in Scheme 37.



Scheme 37: Second-generation retrosynthetic analysis

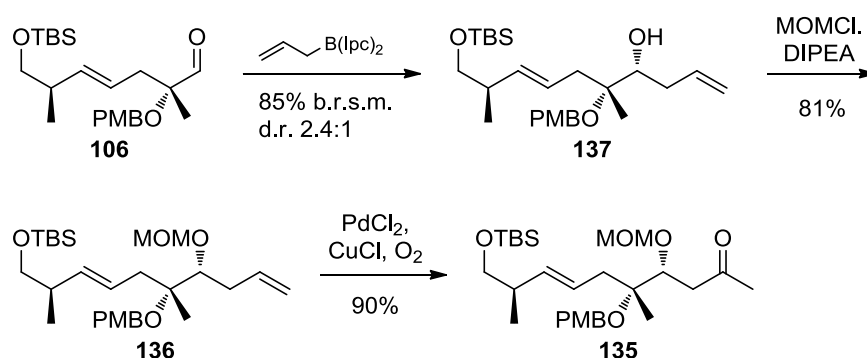
Stannane **101** could be obtained from **104** either *via* lithiation/stannylation¹⁰⁷ or palladium-catalyzed methods.^{108,109} Alternatively, **104** itself could be used directly as a coupling partner with the previously published 5-membered ring fragments. Possible options for such a coupling would include lithium-halogen exchange or an NHK reaction.^{104,105} It should be possible to derive **104** from intermediate **133** by functional group interconversion. Bromoenone **133** could conceivably arise from a rearrangement of intermediate **134**, which could be obtained by a dibromocyclopropanation of a silyl enol ether of **135**.¹⁴¹ Methyl ketone **135** should be the product of a Wacker oxidation¹⁴² of homoallyl alcohol **136**, which may result from an allylation of the already known aldehyde **106**.

Although the reliability the rearrangement from a dibromocyclopropane to the desired α -bromoenone was uncertain, this strategy nevertheless seemed appealing. First, it started from an already known, easily accessible intermediate **106**. Further, if workable, it would solve the problem of generating the bromoalkene moiety in a very direct and elegant way. And finally, apart from the unknown rearrangement, all other reactions were considered robust and amenable to scale-up.

3.4. Second generation-approach: forward synthesis

The first step that deviated from the previous approach was allylation of aldehyde **106**, as shown in Scheme 38. Several methods were tried for the stereoselective allylation of

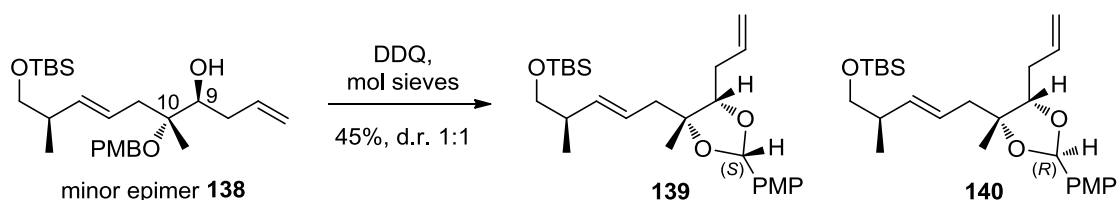
106. Brown's isopinocampheyl (Ipc) based borane¹⁴³ gave **137** in good yields b.r.s.m., albeit at only low stereoselectivities. Separation of the epimers was feasible using normal flash column chromatography, so the selectivity issue was less problematic compared to the Ireland-Claisen rearrangement described earlier. Other conditions resulted in better selectivities, for example using the Duthaler-Hafner catalyst¹⁴⁴, but their low yields precluded larger scale use.



Scheme 38: Route to the methyl ketone **135**

The subsequent protection of the newly generated alcohol with MOMCl proceeded smoothly to give **136** and set the stage for the Wacker oxidation of the terminal double bond. Ketone **135** was obtained in excellent yield after bubbling oxygen through a mixture of **136**, palladium (II) chloride and copper (I) chloride for 24 hours.

Before turning to the crucial enolization and rearrangement, it seemed prudent to ascertain the relative stereochemistry of the adjacent chiral centers in **137**. To that end, the PMB protecting group of an analytical amount of the minor epimer **138** was oxidized to the cyclic p-methoxyphenyl (PMP) acetal using DDQ under anhydrous conditions, as shown in Scheme 39.



Scheme 39: Oxidation of the PMB protecting group to the cyclic PMP acetal

This gave a mixture of two new compounds, **139** and **140**, roughly in a 1:1 ratio. Separation was achieved by flash column chromatography. NMR, mass spectrometry

(MS) and detailed nuclear Overhauser effect (NOE) analysis of the two products gave consistent results and showed that:

- The two compounds were isomeric and only differed in the configuration on the newly formed acetal C.
- The relative configuration of C9 and C10 in **138** is as shown above. Thus the major epimer **137** was shown to possess the desired relative stereochemistry.

An overview of the key NOE signals observed for **139** and **140** is shown in Figure 15. Red arrows indicate NOEs on the “top” side of the ring (above the paper plane); blue arrows indicate NOEs on the “bottom” side (below the paper plane). As can be seen, no inconsistent or unexpected NOE signals were detected.

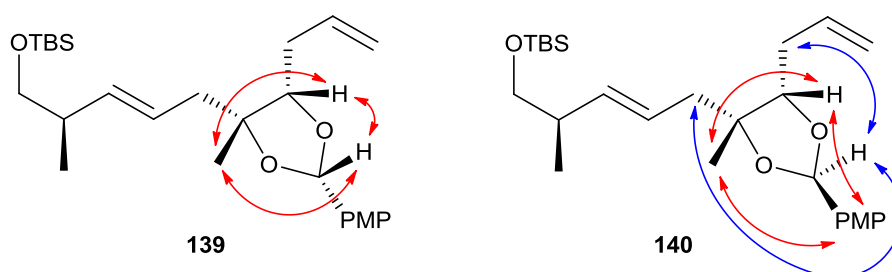
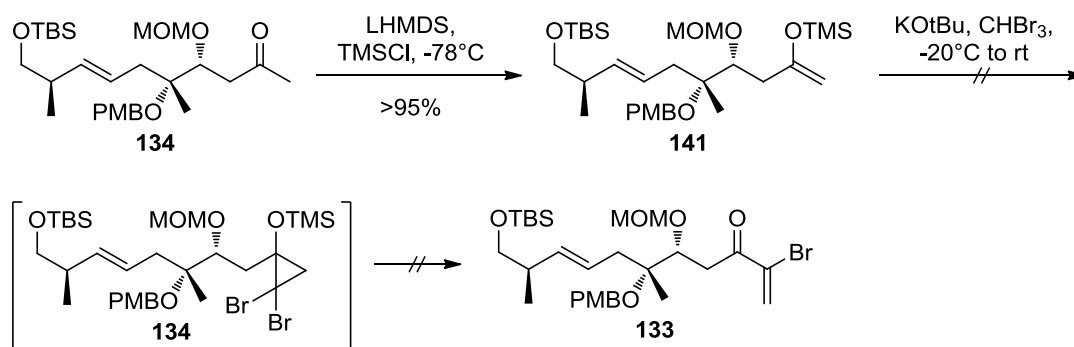


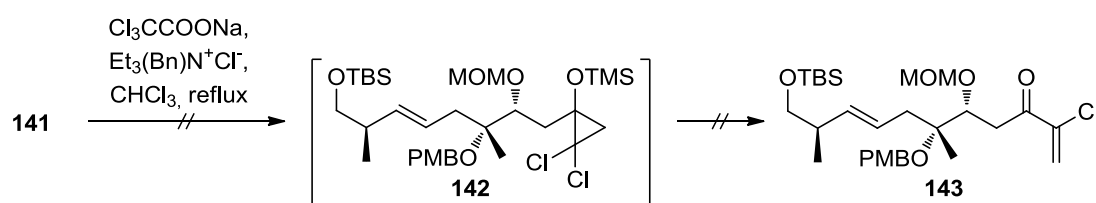
Figure 15: Key NOE signals in **139** and **140**

With the correct relative stereochemistry in **137** ascertained, the crucial rearrangement was examined. The reaction conditions are shown in Scheme 40. Conversion of methyl ketone **135** to silyl enol ether **141** was effected by kinetic deprotonation at -78°C using LHMDS, followed by quenching with TMSCl. The resulting silyl enol ether was unstable on silica, so the crude mixture was moved on to the next stage without further purification.



Scheme 40: Enolization of **135** and rearrangement

Treatment of this material with KOtBu and CHBr₃, which should form the electron-deficient dibromocarbene CBr₂, did not allow isolation of either the cyclopropane **134** or the rearranged product **133**. Instead, either methyl ketone **135** was re-isolated after workup, or complete decomposition was observed when applying more forcing conditions. Switching to other carbene sources, such as generating dichlorocarbene CCl₂ by thermal decomposition of sodium trichloroacetate, did not result in the desired product **143** via rearrangement of **142**, either (Scheme 41). Ultimately, despite various attempts, neither cyclopropanation of the silyl enol ether, nor the rearrangement could be observed.



Scheme 41: Treatment of **141** with dichlorocarbene

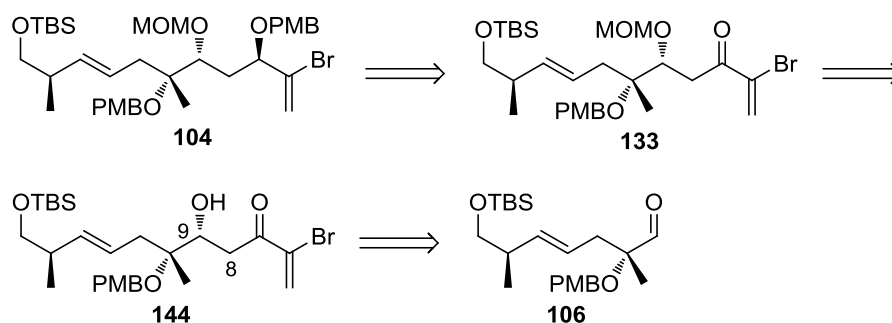
Clearly, this reaction carried the highest risk of being a stumbling block for this route. That risk was accepted, since the reward would have been a particularly elegant route toward the fragment coupling partner **101**. Ultimately this problem could not be solved, which is why this approach had to be abandoned.

3.5. *Third-generation approach: retrosynthetic analysis*

After the more ambitious rearrangement strategy described in the previous section, the third approach is more conventional and, in a way, similar to the first generation route. The core idea was to use an aldol reaction to form the C8-C9 bond, as in the first approach. Previously, a C₂ unit was installed using an auxiliary based method. The new approach aimed to introduce a larger fragment at this stage, with the help of auxiliary-free asymmetric aldol protocols. This would alleviate the need for further carbon-carbon bond forming steps later along the route to **101**. Further, if workable, it might circumvent the practical problems often encountered with acetate aldol reactions.¹²⁴

The retrosynthesis is depicted in Scheme 42. As shown, the target is bromoalkene **104**, which also appeared in the second-generation approach. For fragment coupling purposes, **104** and the corresponding stannane **101** can be considered practically equivalent, and both may be useful, depending on the type of reaction desired to couple

the fragments (lithiation versus NHK conditions). A simple functional group interconversion leads further back from **104** to intermediate **133**, which should be available *via* MOM protection of aldol **144**. Further, **144** might be constructed in a single step starting from the previously described aldehyde **106** using a direct catalytic asymmetric aldol reaction.¹⁴⁵

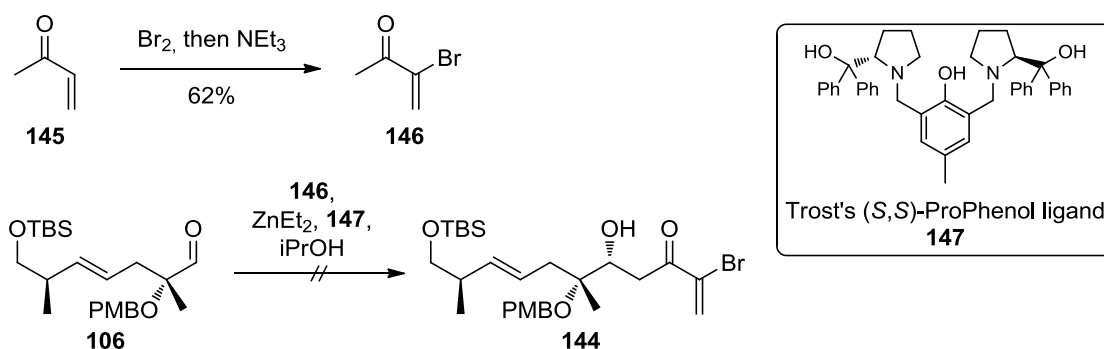


Scheme 42: Third-generation retrosynthetic analysis

The term “direct catalytic asymmetric aldol reaction” encompasses transformations where aldolization is effected by an external promoter, or catalyst. Crucially, that promoter also carries chiral information, which should influence the stereochemical outcome of the reaction. The most prominent example is the proline catalyzed aldol reaction.^{146,147} However, for the task at hand, Trost’s zinc based methodology¹⁴⁸ seemed better suited, as it was already demonstrated to work well with methyl vinyl ketone as reactant.¹⁴⁹

3.5.1. Third approach: forward synthesis

Bromobutenone **146** was obtained from methyl vinyl ketone **145** in a single step after purification by distillation (Scheme 43). The subsequent aldol reaction using the Trost (*S,S*)-bis-ProPhenol ligand **147** and diethylzinc did not produce any product. Despite numerous experiments with different reaction conditions, no aldolization was observed. Instead, only starting material was recovered. Application of other direct catalytic asymmetric aldol methodologies did not result in better yields, so right at the start this approach had to be revised.

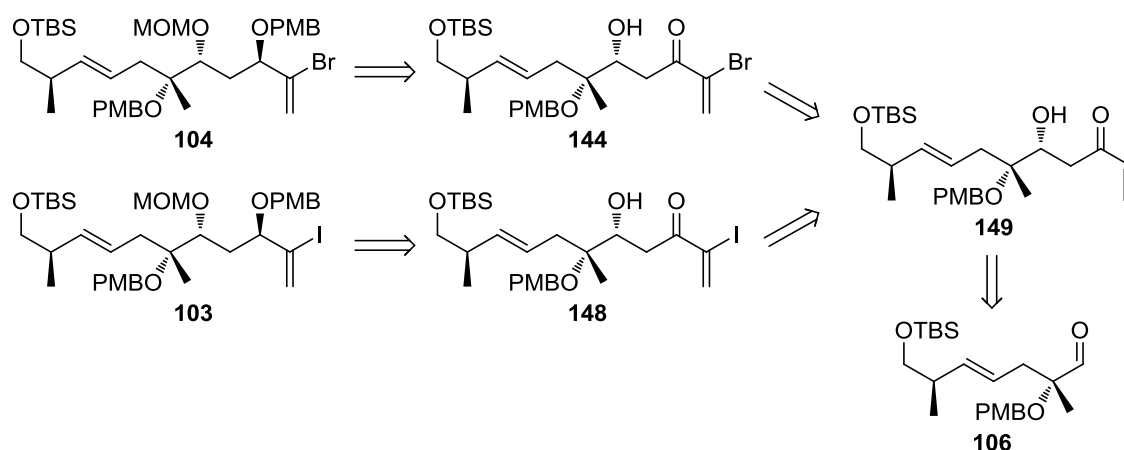


Scheme 43: Synthesis of bromobutenone **146** and the following aldol reaction

3.5.2. Third approach: revised retrosynthesis – methyl vinyl ketone aldol

Trost had demonstrated reasonable substrate scope for “aldol acceptors” (electrophilic aldehydes). In contrast, only a few different compounds were ever used as “aldol donor” (i.e. as enolizable ketone). Thus, it seemed likely that steric or electronic differences between methyl vinyl ketone **145** and its bromo derivative **146** were enough to make the latter unviable as substrate in this reaction.¹⁴⁹

This line of thought naturally led to the idea that methyl vinyl ketone **145** itself could be used in the aldol reaction. While this required the introduction of a substituent on the alkene later on, it offered a lower-risk path overall. This strategy was still a major improvement over the original acetate aldol approach, as the carbon backbone is constructed in a convergent manner. Scheme 44 shows the revised retrosynthetic analysis.



Scheme 44: Revised retrosynthesis for **104** and **103**

The intermediates **104** and **103** are both viable for coupling to a five-membered ring fragment, such as **98**. It should be possible to access them *via* relatively simple transformations from **144** and **148**, respectively. Those two might, in turn, be derived from **149**, which should be the product of an aldol reaction of **106** with methyl vinyl ketone **145**.

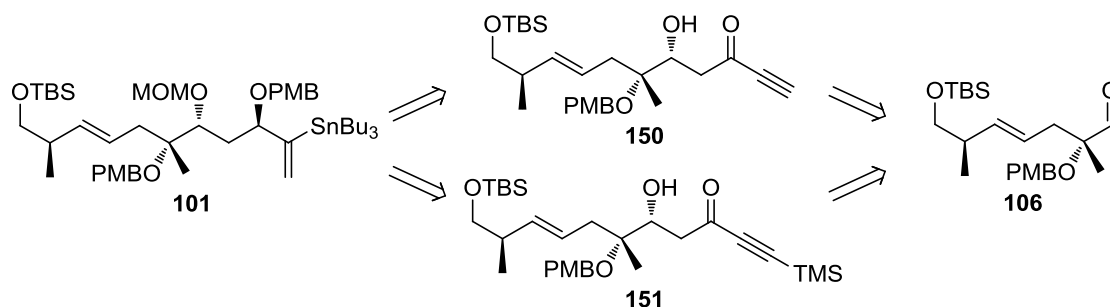
The presence of the ketone functional group in **149** was crucial at this stage, because it offered a way to effect a regioselective bromination or iodination of the terminal alkene, without the need for harsher conditions possibly attacking the internal *E* double bond as well. In the halogenation of enones, there are two typical reaction modes:¹⁵⁰

1. A Baylis-Hillman-type 1,4-addition of a nucleophile generating an enolate, which is halogenated. Subsequently, a β -elimination restores the double bond.
2. An electrophilic halogenation of the alkene, followed by β -elimination of a halogen.

As the second option would likely halogenate the more electrophilic internal alkene first, conditions favoring a Baylis-Hillman-type mechanism seemed preferable. Despite the fact that such reactions work only sluggishly for acyclic enones,^{151,152} access to **149** should be facile enough to warrant exploring those conditions.

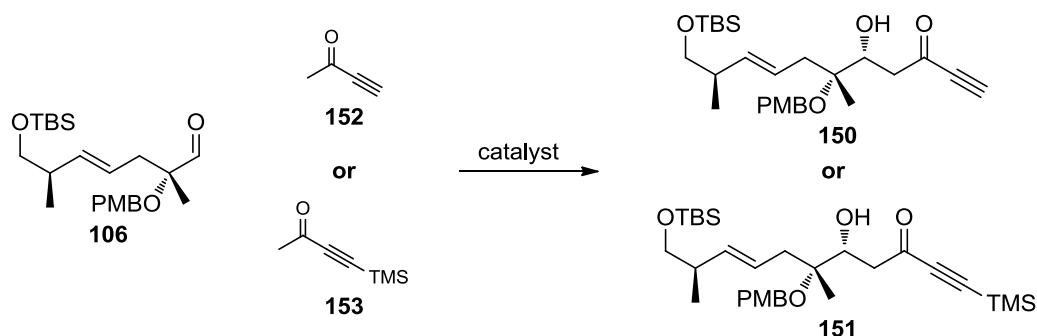
3.5.3. Third approach: revised retrosynthesis – butynone aldol

In light of the risks surrounding the halogenation of the double bond, it seemed prudent to additionally investigate a closely related approach, as shown in Scheme 45.



Scheme 45: Retrosynthesis for the butynone aldol strategy

Here, instead of using methyl vinyl ketone in an aldol reaction with **106**, butynone **152**, or 4-(trimethylsilyl)but-3-yn-2-one **153** could be employed instead (Scheme 46).



Scheme 46: The envisioned aldol reaction of **106** with butynones **152** and **153**

Compared to the methyl vinyl ketone approach, this strategy offered a greater selection of reactions available to introduce a halogen or stannane substituent. Along with Ready's hydrosilylation protocol, hydrosilylations (both, transition-metal catalyzed and *via* a radical mechanism) and other hydrometallations were considered to be promising options. This implied increased chances of finding a synthetically viable path toward **101**.

Overall, this strategy aimed to:

- functionalize the alkyne
- reduce the ketone
- protect the hydroxy groups.

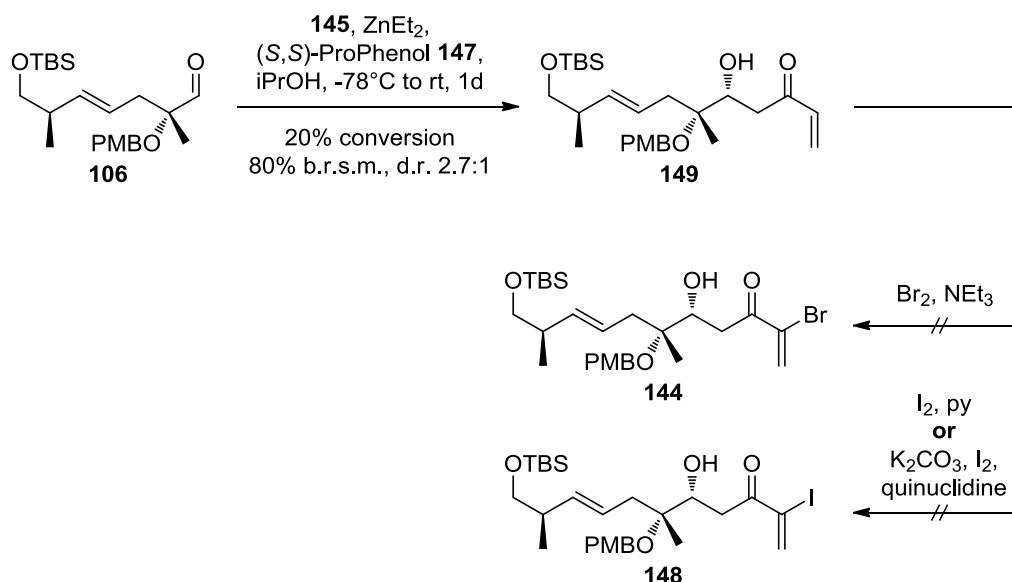
The different hydrometallation protocols necessitated different substrates, however. Some might work on unprotected, ynones, such as **150**, while others would require prior reduction and protection of the ketone. Obviously, this would impact the sequence of the synthetic steps. In practice, several different approaches were tested, with slight changes to the order of steps. Those adjustments will be discussed directly in the context of the forward syntheses (see below), along with the evaluated reaction conditions themselves.

3.5.4. Third approach: forward synthesis – methyl vinyl ketone aldol

The revised route toward **150** started off with a Trost aldol of the previously synthesized aldehyde **106** with methyl vinyl ketone **145** (Scheme 47).¹⁴⁹ The reaction was performed with a catalyst loading of 10 mol% from -78°C to rt overnight. Under these conditions, only 20% conversion was observed. Based on recovered starting material,

yield was good however, and an acceptable diastereomeric ratio was found. Longer reaction times or higher catalyst loadings did not result in higher conversion, but led to decomposition of starting material and product. Optimization was further complicated by the fact that methyl vinyl ketone **145** was used as co-solvent, and increasing its amount in the reaction mixture resulted in solidification upon cooling to -78°C .

As no variations to increase conversion could be developed, several recycling steps were performed to obtain sufficient amounts of **149** to proceed with the halogenation reactions. All the evaluated reaction conditions led to decomposition however.^{151,153} It seemed likely that, at the complexity level of **149**, with several protecting groups and a second double bond, common halogenation conditions were too harsh to be practical.

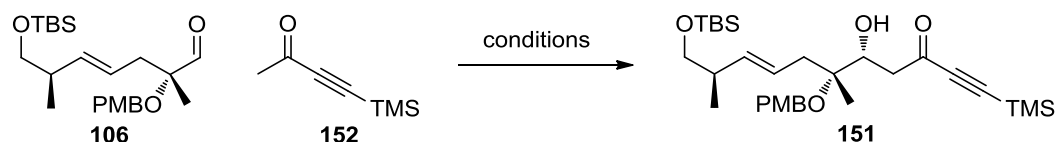


Scheme 47: Trost aldol reaction and attempts at halogenation of the double bond

In parallel with these studies, the aldol reactions of the butynones were investigated. So, after the relatively poor results obtained in the Trost aldol reaction, and the complete failure in the subsequent step, this approach was abandoned and work was focused on the butynone aldol reactions.

3.5.5. Third approach: forward synthesis – butynone aldol

For the direct catalytic asymmetric aldol reaction of **106** with protected butynone **152**, several options were evaluated (Scheme 48). The reaction conditions and results are shown in Table 3.

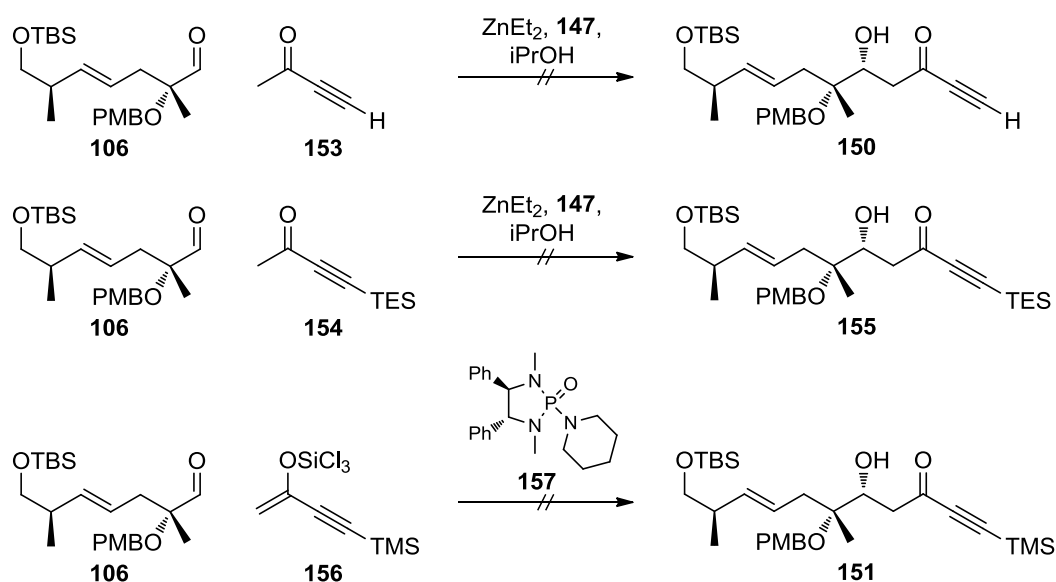


Scheme 48: Direct catalytic asymmetric aldol reaction of **106** with **152**

Experiments using proline as organocatalyst did not result in any observable reaction.^{146,147} Similarly, Trost's zinc based methodology with the (*S,S*)-ProPhenol ligand gave no traces of product.¹⁵⁴ Initial attempts at using Shibasaki's conditions with $\text{LaLi}_3((S)\text{-binaphthoxide})_3$ (*(S)*-LLB, **158**) as catalyst led to the desired product **151** in low yields in a 1.6:1 diastereomeric ratio.^{155–157}

Table 3: Reaction conditions and results for the aldol reaction shown above

Catalyst (mol%)	Conditions	Outcome
L-Proline (35 mol%)	DMSO, rt to 45°C, 1d	No reaction
L-Proline (40 mol%)	Neat in ketone, rt to 45°C, 1d	No reaction
ZnEt ₂ , ProPhenol 147 (3 mol%)	THF, -78°C to rt overnight	No reaction
(<i>S</i>)-LLB (15 mol%)	THF, -45°C to -30°C overnight	~35% yield, d.r. 1.6:1

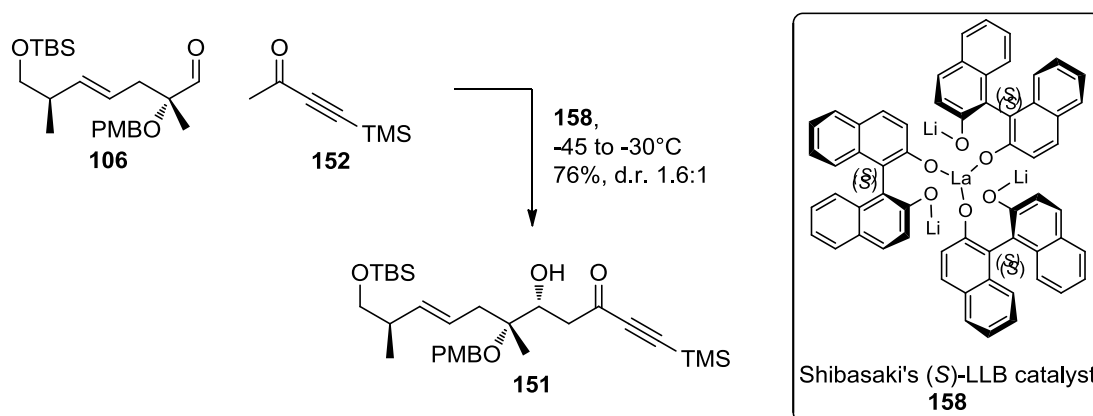


Scheme 49: Further aldol reaction attempts

Two further attempts at effecting an aldol reaction of **106** with butynone equivalents **153** and **154** under Trost conditions are shown in Scheme 49. Both ketones are known to be viable substrates under these reaction conditions.¹⁴⁹ Unexpectedly, as with **152**,

the desired products **150** and **155** were not obtained; no reaction was observed and only starting material could be recovered. Scheme 49 also depicts an aldol reaction using Denmark's Lewis-base catalyst **157** to react trichlorosilyl enol ether **156** with **106**.^{158,159} Again, no reaction was observed.

After this first screening of protocols to access aldols **150**, **151** or **155**, Shibasaki's (*S*)-LLB catalyzed reaction seemed to be the only way forward (Scheme 50). The main problems with this were, obviously, the low yield and diastereoselectivity. Investigating these issues, it became clear that the reaction itself was working smoothly, giving good yield based on crude product NMR. Careful analysis showed that the reaction product **151** was unstable on silica gel, and that decomposition during column chromatography was responsible for the low yield. Despite several attempts at isolating and characterizing the decomposition products, they could not be identified.



Scheme 50: Shibasaki's direct asymmetric aldol reaction and LLB catalyst

The search for alternate purification methods was challenging due to the large reaction scale (typically > 10 g crude product mass) and the necessity to separate the diastereomeric mixture at this stage. Epimer separation at a later stage was precluded by the difference in retardation factors (R_f values) of the epimers growing smaller with subsequent steps. Several different solid phases were evaluated in the hope of suppressing decomposition. On florisil, no separation was obtained, while most other solid phases (deactivated silica,^{160,161} alumina) led to even faster decomposition. Moreover, additives in the eluent (AcOH, TfOH or NEt_3) did not improve stability of the product during chromatography. Using reversed phase chromatography was not considered practical, as no sufficiently large reversed phase HPLC columns were available.

Ultimately, two protocols were developed:

- 1) Separation by preparative HPLC, preferably on a cold day or with pre-cooled solvent. This provided excellent separation of the diastereomers and increased the combined yield to roughly 50%.
- 2) Flash chromatography on a column cooled to -20 to -25°C , with precooled solvent. While this posed considerable practical challenges, it was the preferred method, as it allowed mostly clean diastereomer separation, while giving 76% overall yield. Figure 16 shows a schematic representation of the apparatus, along with a photograph.

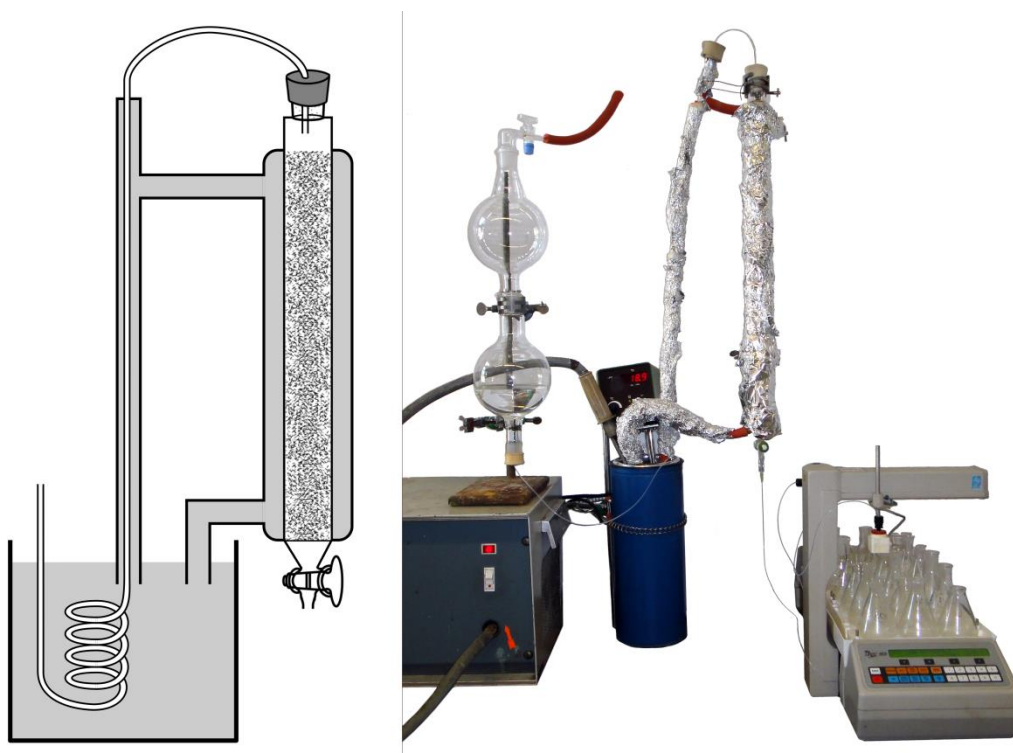


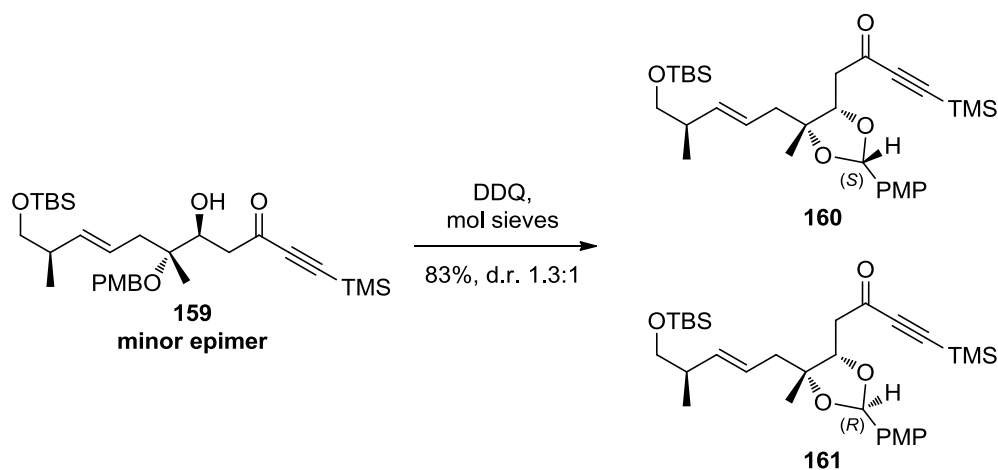
Figure 16: Column chromatography at -20°C

Pressure was applied to the solvent reservoir *via* an air pump, forcing the eluent through Teflon tubing running through a cold bath onto the top of the column. The column itself was cooled by a cooling mantle, through which coolant from the cold bath was cycled. After equilibrating the column, the crude mixture was loaded onto the column with a syringe, and elution was continued until both product diastereomers had eluted. This procedure is described in more detail in the experimental section.

Thus, a method was at hand to obtain the desired aldol product **151** in good yield, albeit with only low stereoselectivity. Attempts to improve the diastereomeric outcome of the reaction were met with failure. Alterations of the reaction conditions, such as changing the solvent, temperature, or reaction time led to decreased yields and did not significantly alter the d.r. of the product.

Despite the difficult purification, the reaction was very reproducible and gave consistent results, even when performed on multi-gram scale. Despite the low selectivity, the ability to separate the isomers enabled exploration of the next steps along the synthetic route.

Before doing so, however, it was important to ascertain the relative stereochemistry of the newly formed chiral center. This was done by oxidation of the PMB protecting group to the PMP acetal, using DDQ under anhydrous conditions. This time, both isomers were separately subjected to oxidation conditions. The results are shown for the minor epimer **159** (Scheme 51). In accordance with previous experience with such a cyclization, a 1.3:1 mixture of compounds **160** and **161**, epimeric on the PMP acetal position, was obtained in good yield. For the analogous reaction of **151**, a 1.1:1 mixture of isomers was produced. Subjection of all 4 resulting diastereomers to detailed NOE NMR experiments gave consistent results and ascertained that the major isomer **151** produced in the aldol reaction does indeed possess the desired relative stereochemistry.

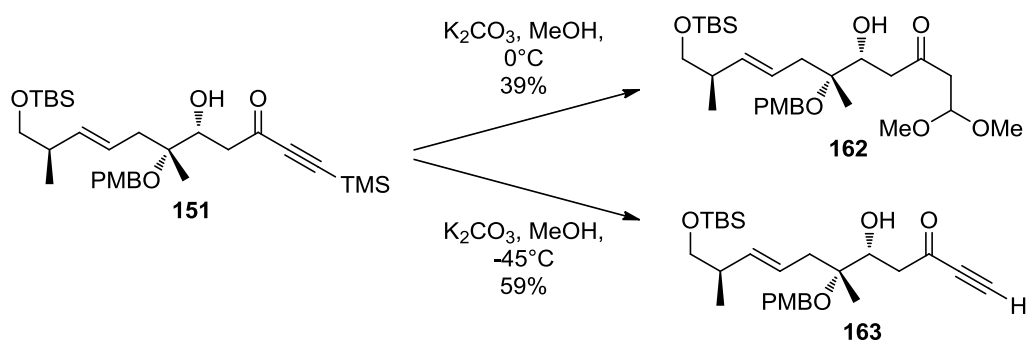


Scheme 51: Determining the relative stereochemistry of the newly formed stereogenic center

From here, the possible next steps (apart from protection of the alcohol), were reduction of the ketone and functionalization of the alkyne. The initial focus was to investigate

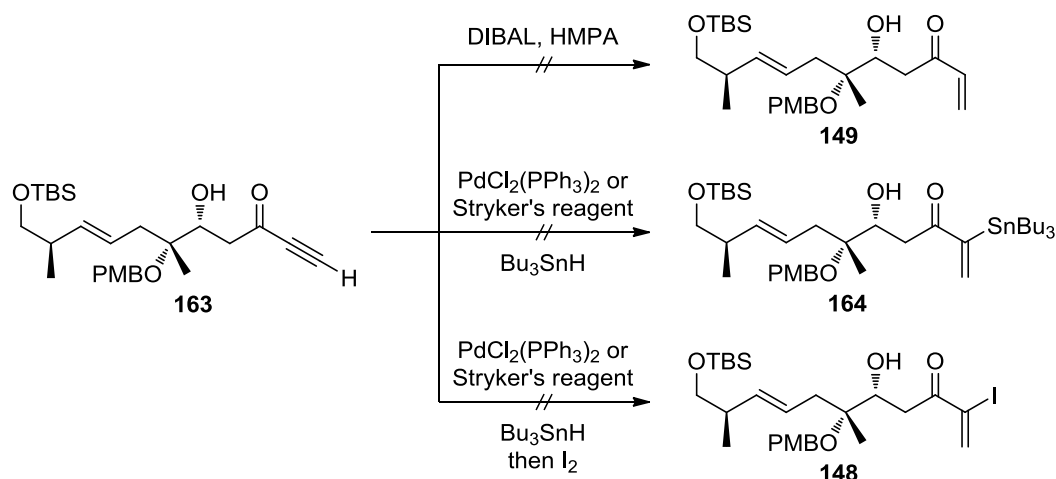
methods to introduce a halogen or stannane directly at the ynone stage, before reduction of the ketone.

The first step toward this goal was cleavage of the TMS group protecting the terminal alkyne. Remarkably, under standard conditions (K_2CO_3 , MeOH, 0°C), the main product was **162**, the result of double 1,4-addition of methanol across the ynone (Scheme 52). Lowering the temperature to -45°C led to the desired unprotected alkyne **163**, albeit in moderate yield. This outcome suggested that the ynone system represents good 1,4-acceptor and is highly electrophilic, which may have been responsible for the instability of **151**. The unprotected **163** was more stable on silica than the parent compound, and could be purified by flash chromatography at room temperature, given that contact time was limited. Prolonged exposure to silica gel still led to decay, though. Again, no definite decomposition products could be identified.



Scheme 52: Cleavage of the C-TMS protecting group

The reactions explored to effect a hydroalumination, hydrostannylation or hydrostannylation/iododestannylation of the ynone are summarized in Scheme 53. A reduction based on DIBAL using HMPA as additive¹⁶² resulted exclusively in 1,2-reduction, instead of the desired 1,4-pathway giving **149**. Palladium catalyzed hydrostannylation conditions¹⁶³ led to slow decomposition, the expected stannane **164** was not formed. The same results were obtained using Stryker's reagent,^{164–166} the hexameric copper hydride complex $[(\text{PPh}_3)\text{CuH}]_6$: at short reaction times and lower temperatures, no reaction was observed, while longer reaction times at rt led to decomposition. To exclude that instability of the stannane caused these setbacks, several experiments were performed where the presumed stannane intermediate was quenched in-situ with iodine. However, the desired product **148** could not be isolated in any of the experiments.



Scheme 53: Attempts to functionalize the alkyne moiety in **163**

3.5.6. Third approach: 1,3-*anti* reduction

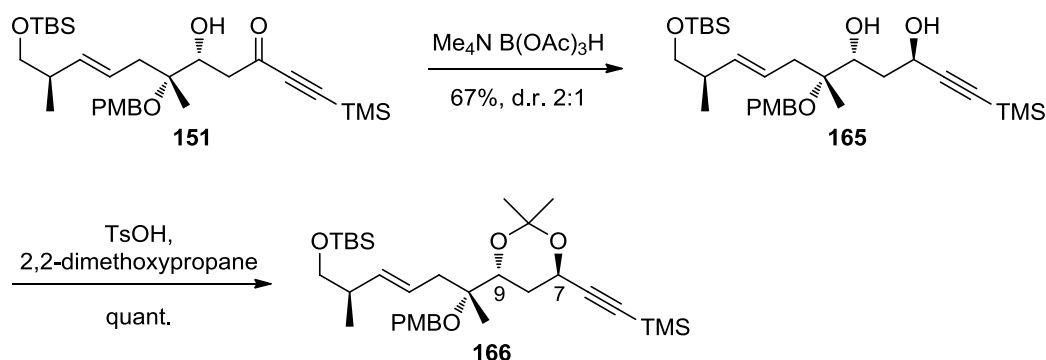
After these failures, the most promising approach was deferring the introduction of the tin or halogen substituent to a later stage, and to reduce the ketone and protect the free hydroxy groups before that step.

To control the stereoselectivity of the reduction step, two options were considered:

- using the free hydroxy group to direct the diastereofacial selectivity, or
- using an asymmetric reduction reagent or catalyst.

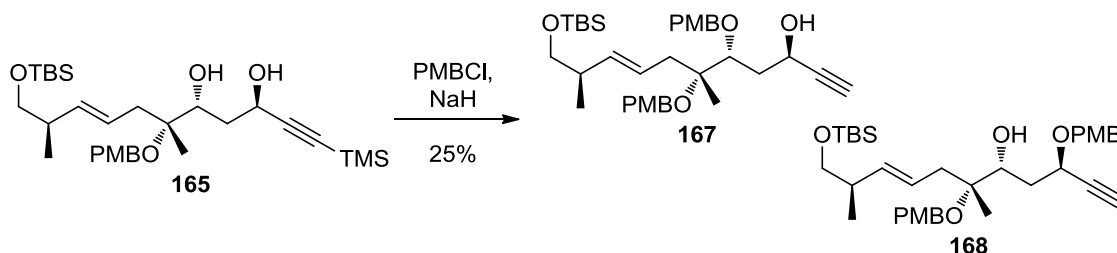
From a theoretical and aesthetic point of view, the first option was preferable, as it meant using chiral information already present in the molecule to control the reaction. To obtain the correct stereochemistry for the target molecule, a 1,3-*anti*-reduction was required. In contrast to 1,3-*syn* reductions, where several methods exist that typically give good diastereoselectivities, *anti*-reduction methodologies are scarce. Tetramethylammonium triacetoxyborohydride was considered to be the promising option available, usually resulting in a d.r. of 2:1 to 4:1.¹⁶⁷

Proceeding with that protocol, the desired reduction product **165** was obtained in 67% yield with a d.r. of 2:1 (Scheme 54). The relative stereochemistry of the resulting epimers was determined by acetonide protection of the diol, to give **166**, which was subjected to NMR NOE analysis. As expected, the desired *anti*-reduction product was the major isomer.



Scheme 54: 1,3-*anti*-reduction and acetonide formation

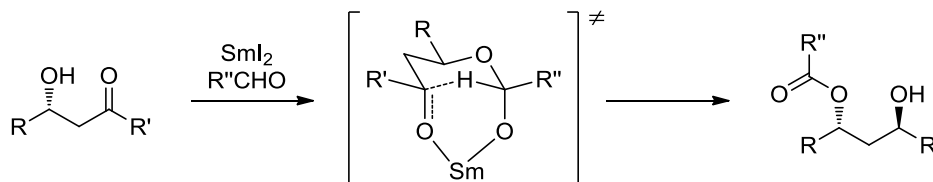
Although the resulting acetonide was a useful tool to deduce the relative stereochemistry, synthetically, it was a dead end. The two oxygen substituents in position 7 and 9 carry different esters in the natural product: 9-ONic and 7-OAc. Thus those two positions needed to be distinguished at one point, and deferring this issue to a later stage was considered too risky. Consequently, a method was sought to differentially protect the two hydroxy groups in **165**. The results of PMB protection under basic conditions are shown in Scheme 55. PMB ether formation was accompanied by cleavage of the alkyne TMS group, and a mixture of mono-protected regioisomers **167** and **168** was obtained in a 1:1 ratio. Separation was not possible *via* flash column chromatography or by HPLC. Similar results were obtained using other protecting groups or conditions or when TMS cleavage was performed as a separate step before protection. Therefore, differentiation of the hydroxy groups in **165** seemed impossible, and another reduction strategy that would allow easier differentiation of those two positions was considered.



Scheme 55: Mono-PMB-protection of **165** gave a mixture of regioisomers

The Evans-Tishchenko reaction, typically promoted by SmI_2 , appeared to be promising.^{168–171} Its starting materials are a β -hydroxyketone and an aldehyde; the ketone is reduced while the aldehyde is oxidized. The initial hydroxy group is transformed into the ester of the added aldehyde (Scheme 56). The reaction proceeds

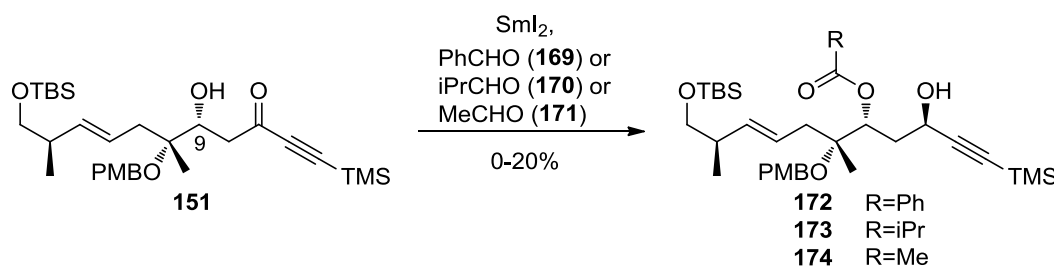
under very mild conditions and tolerates a large variety of functional groups. Due to its bicyclic, intramolecular hydrogen transfer, it offers excellent diastereoselectivity in favor of the 1,3-*anti* product.



Scheme 56: The Evans-Tishchenko reaction

The catalytically active species is presumed to be a samarium(III) pinacolate complex, formed *via* a pinacol coupling reaction between SmI_2 and the starting aldehyde. Typically, this transformation occurs in-situ as SmI_2 is added to a mixture of the starting materials. Alternatively, the complex can also be pre-formed before addition of the hydroxyketone, to achieve milder reaction conditions. This modification also allows screening of different pinacolate ligands, independent of the aldehyde used in the actual Evans-Tishchenko transformation.

In initial studies, a mixture of **151** and benzaldehyde **169** was treated with SmI_2 and the desired ester **172** was obtained in low yields (Scheme 57). Increasing reaction time and catalyst loading did not improve the outcome. Due to the high sensitivity of SmI_2 , traces of water or oxygen, as well as the quality of commercially available SmI_2 solutions, were seen as potential sources of the problem. However, the yields did not improve using careful Schlenk technique and rigorous drying of starting materials and solvents. The particular batch of SmI_2 used did influence the outcome, but no synthetically viable results were ever obtained (see the experimental section for details).



Scheme 57: Evans-Tishchenko reactions of **151**

After it became apparent that the yield could not be improved by tweaking the reaction conditions, using a different aldehyde was considered a promising way forward. Apart

from benzaldehyde (**169**), isobutyraldehyde **170** is another common reactant. Similar reaction conditions as above applied to a mixture of **151** and **170** gave **173** in better yields than before, but still below 20%. Again, despite extensive optimization attempts, the yield could not be increased further. While the exact reason for the low yields was not entirely clear, it seemed plausible that steric congestion around the C9 stereocenter was part of the problem. Thus, the use of a smaller aldehyde was investigated: performing the reaction with acetaldehyde **171** improved the yields to around 20% of **174**, but no further.

In these experiments, the samarium pinacolate complex was generated using the same aldehyde that was used for the Evans-Tishchenko transformation itself. Both, in-situ pinacol coupling and pre-formation of the catalyst before addition of **151** were investigated, with only slight differences between the two procedures. One final promising modification was preparing the samarium pinacolate catalyst using benzaldehyde, which is known to react quickly and smoothly with SmI₂, followed by addition of acetaldehyde **171** and **151**, as shown in Scheme 58. Unfortunately, this variant did not improve the product yields in any way.

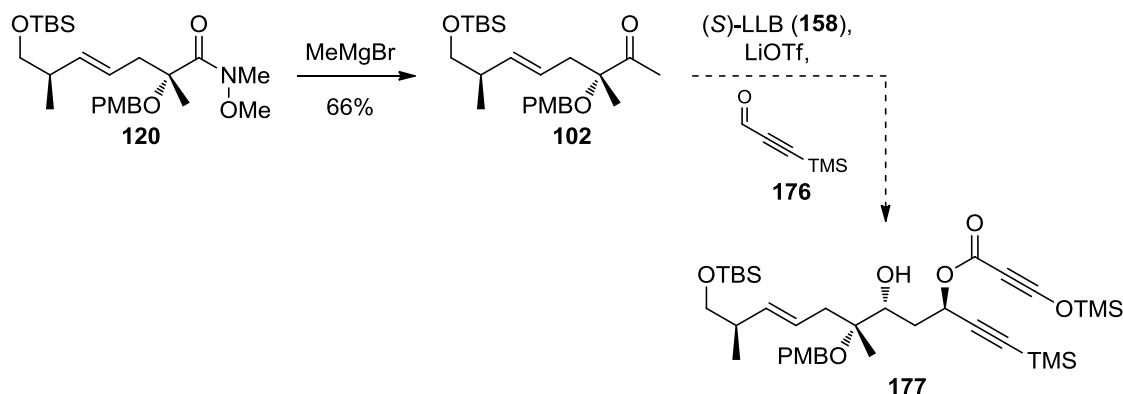


Scheme 58: Pre-forming the samarium pinacolate **175** before the Evans-Tishchenko reaction

After these failures with SmI₂, other conventional Evans-Tishchenko reactions mediated by scandium and zirconium complexes were briefly considered, but discarded due to limited functional group compatibility.¹⁶⁹ However, a protocol developed by Shibasaki to combine a direct catalytic, asymmetric aldol reaction with an Evans-Tishchenko reaction seemed worthy of investigation.¹⁷² The addition of LiOTf to Shibasaki's (*S*)-LLB catalyst **158** generates a new species that can promote both transformations in a single synthetic step. If this reaction was workable, it would offer quick access to an advanced intermediate in a stereocontrolled fashion, as well as side-step the laborious purification of aldol **151**.

Instead of the aldehyde **106**, this transformation required the corresponding methyl ketone **102** as starting material. It was obtained from the known Weinreb amide **120** by

addition of methylmagnesium bromide in moderate yield, as shown in Scheme 59. The subsequent aldol-Tishchenko cascade reaction with aldehyde **176** did not give the desired product **177**. In all attempts, starting material was reisolated, and no sign of successful catalysis was observed.

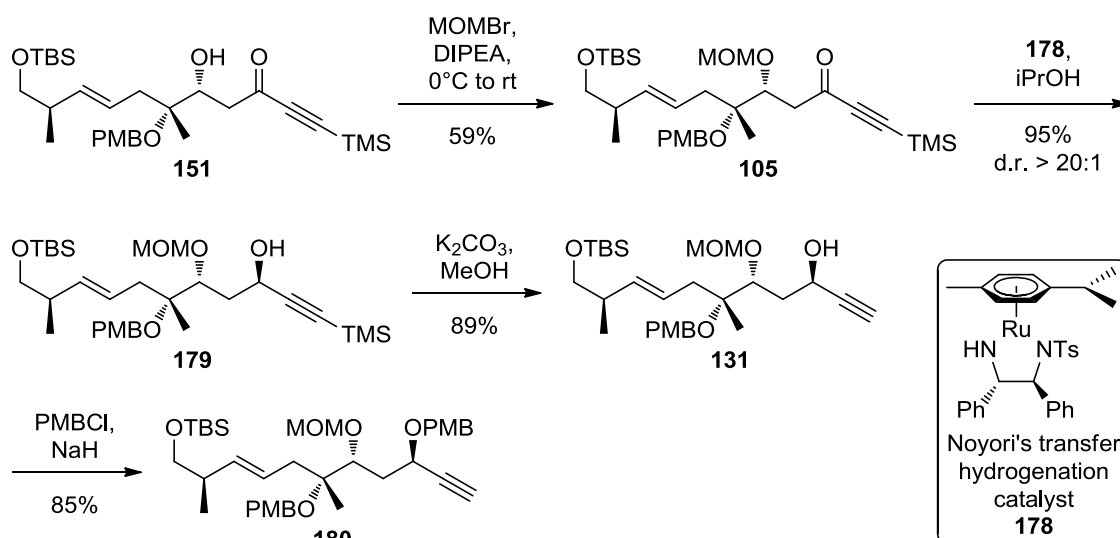


Scheme 59: Synthesis of methyl ketone **102** and attempted aldol-Tishchenko cascade

3.5.7. Third approach: Route toward the stannane **101**

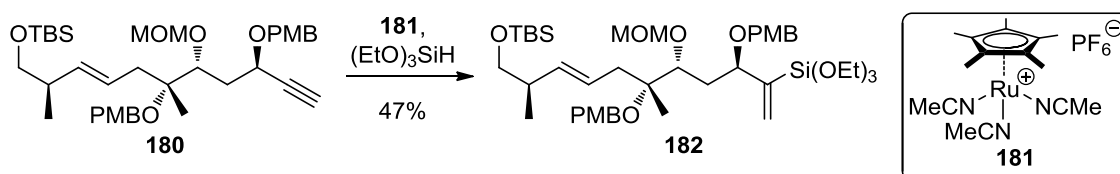
Since the C7 stereogenic center could not be set in a substrate controlled fashion, reagent-controlled reductions provided a path forward. Prior to that step, the hydroxy group in **151** had to be protected in order to differentiate the two alcohols (Scheme 60). Initial experiments with MOMCl gave low yields. Therefore, various protecting groups and protection protocols were surveyed, until ultimately MOMBr/DIPEA emerged as the best option. As the resulting ketone **105** was unstable when exposed to silica gel, column chromatography was performed at low temperatures to avoid decomposition. Noyori's transfer hydrogenation protocol¹³² using **178** as catalyst gave **179** in excellent yield and diastereoselectivity. Indeed, a second epimer was not detectable. Purification was greatly facilitated, since **178** was stable on contact with silica gel during flash chromatography.

Trimethylsilyl deprotection using K_2CO_3 in methanol led to alkyne **131**, which was converted to the PMB ether under standard conditions, giving the fully protected **180**.



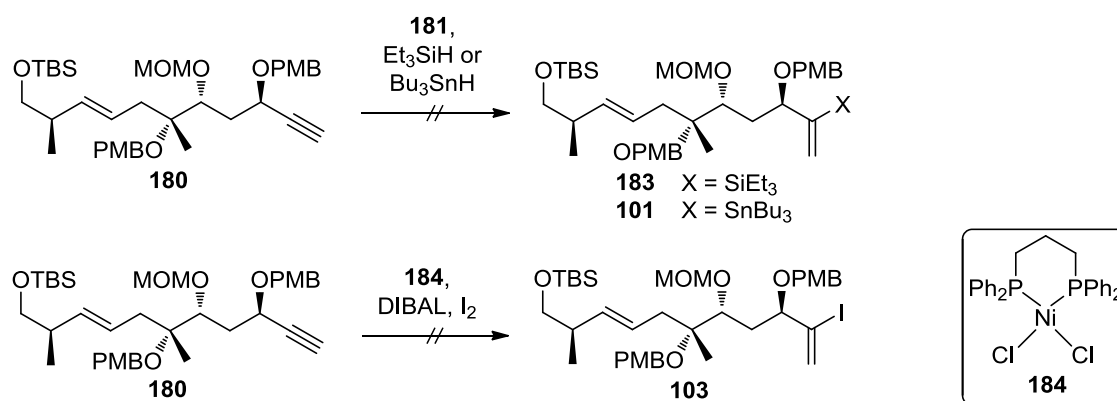
Scheme 60: Synthesis of fully protected alkyne **180**

The remaining step to a suitable coupling partner for the five-membered ring fragments was the hydrofunctionalization of the triple bond. Initial experiments using Trost's ruthenium complex **181** to add triethoxysilane across the alkyne¹⁷³ showed promising results (Scheme 61). However, further transformation of the resulting silane **182** into a stannane or a halogenide better suited for metal-catalyzed cross couplings could not be achieved. For example, treatment with KHF_2 and iodine led to rapid decomposition instead of iodo-desilylation. Thus, triethoxysilane **182** was a dead end.



Scheme 61: Ruthenium catalyzed hydrosilylation

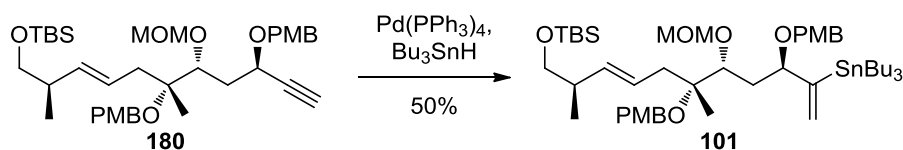
Next, reactions of the same catalyst **181** with triethylsilane or tributyltin hydride as reactants were explored (Scheme 62). Neither of these modifications delivered the desired product **183** or **101**. In another attempt, Hoveyda's nickel-based hydroalumination/iodination protocol¹⁷⁴ – which relies on catalyst **184** – was evaluated, but the desired reaction of **180** to iodide **103** was not observed.



Scheme 62: Failed hydrosilylation and hydrostannylation reactions

Subsequently, these reactions were repeated with the free alcohol **131** before PMB protection, but did not produce better results with this starting material. Further experiments conducted in our group suggested that Hoveyda's protocol in particular is limited to substrates without oxygenation in the propargylic position, and thus unsuitable for substrates such as **180**.

To overcome this obstacle, traditional transition-metal catalyzed hydrostannylation reactions were surveyed. When **180** was exposed to tributyltin hydride in the presence of Pd(PPh₃)₄, PdCl₂(PPh₃)₂ or RhCl(CO)(PPh₃)₂, a mixture of stannylated products was obtained. After extensive optimization, Pd(PPh₃)₄ in THF at 0°C was found to give the best tradeoff of overall yield and regioselectivity, as shown in Scheme 63. The desired chain fragment **101** could thus be obtained in 50% yield.



Scheme 63: Successful hydrostannylation to produce the completed chain fragment **101**

Finally, a coupling partner for the 5-membered ring fragments was at hand. The sequence to **101** was reproducible and delivered sufficient material to enable investigation of the fragment coupling and steps beyond. In summary, the longest linear sequence to **101** starting from norephedrine hydrochloride **113** was 16 steps, with an overall yield of 1.2%.

4. Conclusion

Euphosalicin (**1**) is an interesting compound due to its biological profile and its intriguing bicyclic structure. The diterpene provides promising biological activity, as it prominently inhibits P-glycoprotein, which often shows overexpression in cancer cells leading to increased efflux of xenobiotica. The resulting multidrug-resistance is a major cause of chemotherapy failure. Thus, euphosalicin possesses remarkable potential as a lead structure for drug development to overcome resistance to chemotherapy.

Synthesis of this compound entails supreme challenges due to its high degree of oxygenation. Previous work directed at the synthesis of euphosalicin's five-membered ring fragments was published in 2005 and 2006. Consequently, the focus of this thesis was the generation of complementary coupling partners for the already known fragments.

Several different approaches were devised and carried out. They all shared the initial route to aldehyde **106**, which started with an Evans aldol reaction to install two neighboring stereocenters. During a subsequent Ireland-Claisen rearrangement, this stereochemical information relayed to set the geometry of a new, distant quaternary stereocenter. Careful choice of deprotonation conditions was necessary to control the enolate geometry prior to the rearrangement to ensure reliable stereoinduction.

Initially, **106** was C₂-elongated using a HYTRA aldol reaction. Although several subsequent steps were developed, this strategy was soon abandoned due to the impracticalities of handling the aldol products in large scale which were caused by the low solubility of the auxiliary.

Accessing the desired coupling fragments *via* the rearrangement of a dibromocyclopropane to a bromoenone was investigated next. Several steps were successful, but the key dibromocyclopropanation/ring opening cascade could not be triggered, which led to the development of a new strategy.

The ultimately successful third approach centered on the use of an Ireland-Claisen rearrangement and a Shibasaki catalytic, asymmetric aldol reaction to construct the carbon backbone in an expedient and convergent fashion. Although several dead-ends – such as the substrate-controlled reduction of the C7 ketone – were encountered, these

difficulties could ultimately be overcome. The resulting fragment for the euphosalycin macrocycle is orthogonally protected and should serve as a base for the completion of the total synthesis in the future.

Further studies are now warranted to investigate the fragment coupling and the following cyclization. With the fragment developed in this work, macrocyclization can be achieved in multiple locations. This allows great flexibility in the final steps of the synthetic route, moving a completion of the total synthesis within reach. Therefore, this work makes an important contribution to the drug development of chemotherapeutics and may offer an intriguing platform to overcome multi-drug resistance in cancer cells in the future.

5. Experimental procedures

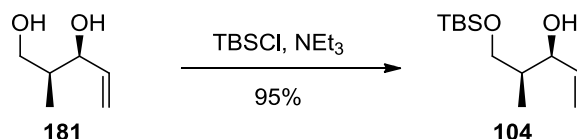
Reactions under water-free conditions were performed with oven-dried glassware under argon in anhydrous solvents. Petroleum ether (PE), CH₂Cl₂ and EtOAc were distilled for routine applications. THF abs. was distilled from potassium under argon. Et₂O abs. and toluene abs. were distilled over Na/benzophenone ketyl radical. CH₂Cl₂ abs. was distilled over phosphor pentoxide and passed through a column of neutral aluminium oxide. DIPEA, NEt₃, diisopropylamine (DIPA) and isopropanol were freshly distilled under argon from CaH₂. TMSCl was freshly distilled prior to use. Acrolein was freshly distilled prior to use, with hydroquinone added to the distillation and receiving flasks as stabilizer. Unless otherwise noted, *n*-butyllithium was used as 2.5 M solution in hexanes. All other chemicals were used as received.

Analytical thin layer chromatography (TLC) was carried out on Merck “TLC Silica Gel 60 F₂₅₄” or Macherey-Nagel “ALUGRAM Xtra SIL G/UV₂₅₄” plates. Typical solvent systems for development of the plates were PE/EtOAc or toluene/EtOAc mixtures. UV active spots were detected with UV light at 254 nm. TLC plates were stained with I₂/silica or ceric ammonium molybdate (0.3 g Ce(SO₄)₂, 20 g phosphomolybdic acid, 400 mL 10% H₂SO₄). Preparative column chromatography was performed on Macherey Nagel “MN Silica Gel 60 M” (40-63µm).

NMR spectra were recorded on Bruker Avance AV 400, DPX 400 or DRX 600 spectrometers operating at ¹H frequencies of 400, 400 and 600 MHz, respectively. ¹³C NMR spectra were recorded at 100, 100 or 150 MHz in *J*-modulated mode; signals were assigned as C, CH, CH₂ or CH₃. Chemical shifts δ are reported in ppm relative to the residual peaks of the deuterated solvent. Unless otherwise noted, samples were dissolved in CDCl₃. Spectra recorded in CDCl₃ are referenced to 7.26 (¹H) and 77.00 (¹³C). MS and high resolution mass spectrometry (HRMS) determinations were carried out on Finnigan MAT 8230 or Bruker maXis spectrometers. Electron ionization (EI) and electrospray ionization (ESI) were used as ionization methods. For EI, the acceleration energy was typically 70 eV, the exact value is included for each measurement. ESI was performed with acetonitrile/methanol/water in a 1:1:0.01 ratio as solvent. Infrared (IR) spectroscopic data are reported in wave numbers (per cm) and were obtained on a Bruker Vertex 70 FTIR spectrometer using a single reflection diamond ATR module. Polarimetry data were measured on a Perkin-Elmer P 341 unit

with a 10 cm cell length at 20°C. The wavelength was 589 nm (the sodium D line doublet). Values are reported in the format “[α]_D = specific rotation (concentration, solvent)”.

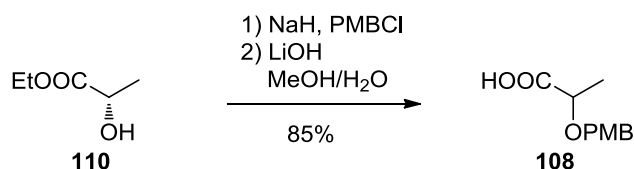
5.1. (3*S*,4*S*)-5-((*tert*-butyldimethylsilyl)oxy)-4-methylpent-1-en-3-ol (**104**)



Diol **181**¹⁷⁵ (17.7 g, 152 mmol) was dissolved in CH₂Cl₂ (400 mL) and cooled to 0°C. Triethylamine (27.4 mL, 198 mmol) and TBSCl (25.2 g, 167 mmol) were added and the solution was left to warm to room temperature overnight. The mixture was quenched with NH₄Cl aq. sat. (250 mL), the phases were separated and the aqueous layer was extracted with CH₂Cl₂ (3 times 150 mL). The combined organic phases were washed with brine, dried over Na₂SO₄, and the solvents were removed. Flash chromatography (hexanes:EtOAc 9:1) delivered **S1** (33.2 g, 95%) as a clear oil.

¹H-NMR (CDCl₃) δ 5.88 (1H, ddd, J = 17.2, 10.6, 5.4 Hz), 5.29 (1H, dt, J = 17.2, 1.7 Hz), 5.17 (1H, dt, J = 10.6, 1.7 Hz), 4.28 (1H, m), 3.67 (2H, m), 3.26 (1H, d, J = 5.3 Hz), 1.93 (1H, m), 0.90 (9H, s), 0.86 (3H, d, J = 7.1 Hz), 0.07 (6H, s). ¹³C-NMR (CDCl₃) δ 138.60 (CH), 115.00 (CH₂), 75.76 (CH), 67.21 (CH₂), 39.46 (CH), 25.83 (CH₃), 18.13 (C), 11.09 (CH₃), -5.64 (CH₃), -5.66 (CH₃). HRMS (EI, 70 eV): [M-tBu]⁺ m/z calcd for C₈H₁₇O₂Si 173.0998; found 173.1006. IR(film): 3451, 2930, 1472, 1255, 1094, 921, 837, 776 cm⁻¹. [α]_D = -12.0° (10 mg/mL, CHCl₃). These data are consistent with previously reported¹⁷⁵ values.

5.2. 2-((4-methoxybenzyl)oxy)propanoic acid (**108**)



Sodium hydride (2.2 g, 94 mmol) was dissolved in THF abs. (120 mL) and cooled to 0°C. (*S*)-Ethyl lactate **110** (10.0 g, 85 mmol) was added slowly. After the hydrogen evolution had stopped, PMBCl (12.7 mL, 94 mmol) was added and the solution was

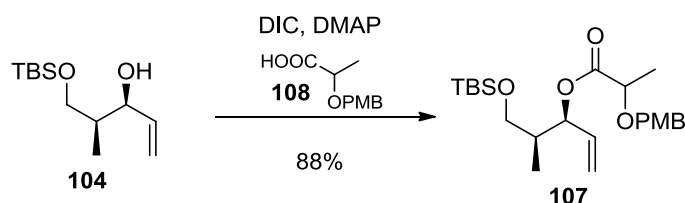
warmed to room temperature overnight. The reaction was quenched by slow addition of NH_4Cl aq. sat. (150 mL). The layers were separated and the aqueous phase was extracted with EtOAc (3 times 100 mL). The combined organics were washed with brine, dried over Na_2SO_4 , and the solvents were removed.

The crude PMB ether was dissolved in MeOH (200 mL) and cooled to 0°C before water (200 mL) and LiOH (4.1 g, 170 mmol) were added. The mixture was warmed to room temperature overnight. The reaction mixture was washed with Et_2O before the pH of the aqueous phase was adjusted to 4. The aqueous layer was extracted with Et_2O (3 times 200 mL), the combined organics were washed with brine, dried over Na_2SO_4 and the solvents were removed to give 15.2 g (85%) of **108** as pale orange solid. The crude product was moved on without further purification.

Note: Later results showed that during saponification, the α -stereocenter partially racemized, which was ultimately without consequence as this chiral center is destroyed in the Ireland-Claisen step (see below).

^1H -NMR (CDCl_3) δ 10.21 (1H, br. s), 7.29 (2H, d, $J = 8.6$ Hz), 6.89 (2H, d, $J = 8.7$ Hz), 4.63 (1H, d, $J = 11.3$ Hz), 4.48 (1H, d, $J = 11.3$ Hz), 4.09 (1H, q, $J = 6.9$ Hz), 3.81 (3H, s), 1.47 (3H, d, $J = 6.9$ Hz). HRMS (ESI): $[\text{M}+\text{Na}]^+$ m/z calcd for $\text{C}_{11}\text{H}_{14}\text{O}_4\text{Na}$ 233.0790; found 233.0783. These data are consistent with previously reported values.^{176,177}

5.3. (3*S*,4*S*)-5-((*tert*-butyldimethylsilyl)oxy)-4-methylpent-1-en-3-yl 2-((4-methoxybenzyl)oxy)propanoate (**107**)

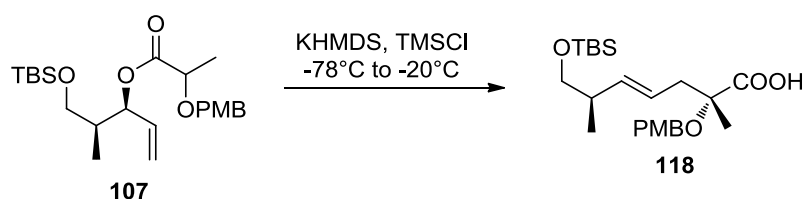


To **108** (13.0 g, 61.9 mmol) in THF (50 mL) was added *N,N*-diisopropylcarbodiimide (9.6 mL, 61.9 mmol) at 0°C . After 10 min, a heavy precipitate had formed. A solution of **104** (9.5 g, 41.3 mmol) in THF (20 mL) was added, followed by 4-dimethylaminopyridine (0.5 g, 4.1 mmol). The mixture was allowed to warm to room temperature overnight. The urea was filtered off and the solvents were removed under

vacuum. Flash chromatography (PE:EtOAc 19:1, dry load) afforded 20.9 g (88%) of **107** as slightly yellow oil.

$^1\text{H-NMR}$ showed a mixture of diastereomers. HRMS (EI): $[\text{M-tBu}]^+$ m/z calcd for $\text{C}_{19}\text{H}_{29}\text{O}_5\text{Si}$ 365.1784; found 365.1774. IR (film): 2930, 2858, 1750, 1613, 1514, 1464, 1389, 1303, 1250, 1194, 1112, 1037, 939, 838, 777, 671 cm^{-1} .

5.4. (2*R*,6*R*,*E*)-7-(*tert*-butyldimethylsilyloxy)-2-(4-methoxybenzyloxy)-2,6-dimethylhept-4-enoic acid (**118**)

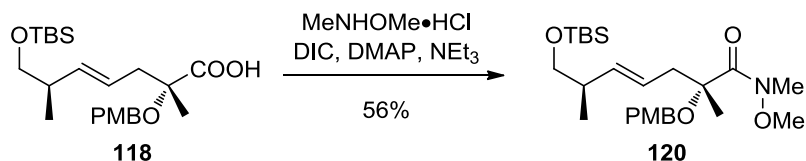


Rearrangement precursor **107** (1.00 g, 2.26 mmol) was dissolved in toluene (15 mL) and cooled to -78°C under argon. KHMDS (1.56 g, 7.81 mmol) in toluene (15 mL) was slowly added at -78°C , whereupon the mixture turned yellow. After 1 h of stirring at the same temperature, TMSCl (0.93 mL, 7.34 mmol) was added *via* syringe and the solution was left to warm to rt overnight. The reaction was quenched by addition of NH_4Cl aq. sat. (~50 mL) and the pH was adjusted to 4 using 1 M HCl aq. The phases were separated and the aqueous layer was extracted with EtOAc (5 times 75 mL). The combined organic phases were washed with brine, dried over Na_2SO_4 , and the solvents were removed. The crude product was used in the next step. A small amount of material was subjected to column chromatography and HPLC purification to obtain pure material for analytical data.

$^1\text{H-NMR}$ (CDCl_3) δ 9.24 (1H, s), 7.26 (2H, d, $J=8.6$ Hz), 6.89 (2H, d, $J=8.7$ Hz), 5.53 (1H, dd, $J=15.5, 7.1$ Hz), 5.42 (1H, dd, $J=14.7, 7.8$ Hz), 4.49 (1H, d, $J=10.1$ Hz), 4.43 (1H, d, $J=10.1$ Hz), 3.82 (3H, s), 3.48 (1H, dd, $J=9.8, 6.0$ Hz), 3.37 (1H, dd, $J=9.7, 7.1$ Hz), 2.59 (2H, m), 2.31 (1H, m), 1.54 (3H, s), 0.98 (3H, d, $J=6.8$ Hz), 0.88 (9H, s), 0.03 (6H, s). $^{13}\text{C-NMR}$ δ 174.59 (C), 159.56 (C), 138.19 (CH), 129.45 (C), 129.21 (CH), 122.55 (CH), 114.00 (CH), 80.85 (C), 67.95 (CH_2), 65.63 (CH_2), 55.32 (CH_3), 39.95 (CH), 39.45 (CH_2), 25.93 (CH_3), 21.50 (CH_3), 18.35 (C), 16.62 (CH_3), -5.33 (CH_3). HRMS (ESI): $[\text{M}+\text{Na}]^+$ m/z calcd for $\text{C}_{23}\text{H}_{38}\text{O}_5\text{SiNa}$ 445.2386; found 445.2382. IR

(film): 2928, 1713, 1615, 1515, 1463, 1250, 1108, 835, 777, 749, 532, 442, 404 cm^{-1} .
 $[\alpha]_{\text{D}} = +8.2^{\circ}$ (10 mg/mL , CHCl_3).

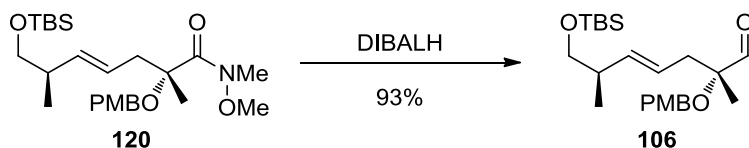
5.5. (2*R*,6*R*,*E*)-7-(*tert*-butyldimethylsilyloxy)-*N*-methoxy-2-(4-methoxybenzyloxy)-*N*,2,6-trimethylhept-4-enamide (**120**)



Crude **118** (100% yield assumed, 2.37 mmol) was dissolved in CH_2Cl_2 (10 mL) under argon and cooled to 0 $^{\circ}\text{C}$. Then, DIC (0.40 mL, 2.60 mmol) was added and the mixture was stirred at 0 $^{\circ}\text{C}$ for 20 minutes, whereupon a precipitate formed. NEt_3 (0.40 mL, 2.84 mmol), *N,O*-dimethylhydroxylamine hydrochloride (277 mg, 2.84 mmol) and DMAP (29 mg, 0.24 mmol) were added. The solution was allowed to warm to rt overnight. The methylene chloride was removed and the residue was re-dissolved in THF. The insoluble urea was filtered and extracted with THF. The solvents were removed from the combined organic phases. The crude product was purified by flash chromatography (PE:EtOAc 5:1, dry load) to yield 1331 mg (56% over two steps) of the amide **120** as a slightly yellow oil.

$^1\text{H-NMR}$ δ 7.25 (2H, d, $J = 8.4$ Hz), 6.87 (2H, d, $J = 8.6$ Hz), 5.45 (2H, m), 4.41 (1H, d, $J = 10.6$ Hz), 4.35 (1H, d, $J = 10.5$ Hz), 3.80 (3H, s), 3.66 (3H, s), 3.48 (1H, dd, $J = 9.7$, 5.9 Hz), 3.36 (1H, dd, $J = 9.7$, 7.2 Hz), 3.34 (3H, s), 2.62 (2H, m), 2.31 (1H, m), 1.48 (3H, s), 0.98 (3H, d, $J = 6.7$ Hz), 0.89 (9H, s), 0.03 (6H, s). $^{13}\text{C-NMR}$ δ 172.18 (C), 159.09 (C), 137.22 (CH), 130.39 (C), 129.05 (CH), 123.82 (CH), 113.78 (CH), 81.24 (C), 68.11 (CH_2), 65.77 (CH_2), 60.47 (CH_3), 55.26 (CH_3), 40.51 (CH_2), 39.50 (CH), 35.56 (CH_3), 25.92 (CH_3), 21.67 (CH_3), 18.34 (C), 16.72 (CH_3), -5.34 (CH_3). HRMS (EI, 70 eV): $[\text{M-tBu}]^+$ m/z calcd for $\text{C}_{21}\text{H}_{34}\text{NO}_5\text{Si}$ 408.2206; found 408.2192. IR (film): 2930, 1778, 1656, 1614, 1515, 1463, 1383, 1250, 1173, 1087, 1035, 837, 777 cm^{-1} . $[\alpha]_{\text{D}} = +6.0^{\circ}$ (2.8 mg/mL , CHCl_3).

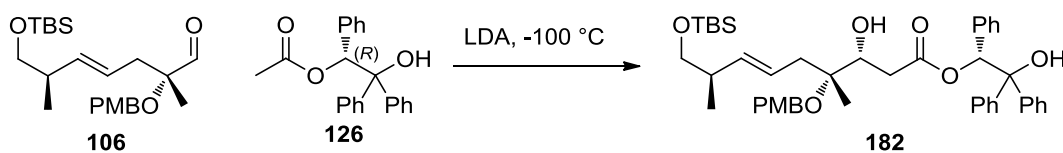
5.6. (2R,6R,E)-7-(tert-butyldimethylsilyloxy)-2-(4-methoxybenzyloxy)-2,6-dimethylhept-4-enal (106)



To a solution of the amide **120** (7.80 g, 16.8 mmol) in diethylether (170 mL) was added DIBAL-H (1.0 M in heptanes, 26.8 mL, 26.8 mmol) dropwise at -78°C . After 1 h of stirring at -78°C , the mixture was quenched with NH_4Cl aq. sat. (~100 mL). Saturated Rochelle salt solution (100 mL) was added and the biphasic mixture was vigorously stirred for 90 minutes. The phases were separated and the aqueous layer was extracted with CH_2Cl_2 (3*100 mL). The combined organic phases were washed with brine and dried over Na_2SO_4 . The solvents were removed and the crude product was purified by flash chromatography (hexanes:EtOAc 5:1) to give 6.32 g of **106** (93%) as a colorless oil.

^1H -NMR δ 9.62 (1H, s), 7.28 (2H, d, $J = 8.6$ Hz), 6.88 (2H, d, $J = 8.6$ Hz), 5.44 (2H, m), 4.44 (1H, d, $J = 10.7$ Hz), 4.38 (1H, d, $J = 10.7$ Hz), 3.81 (3H, s), 3.47 (1H, dd, $J = 9.7, 6.2$ Hz), 3.38 (1H, dd, $J = 9.7, 6.9$ Hz), 2.50-2.26 (3H, m), 1.30 (3H, s), 0.97 (3H, d, $J = 6.7$ Hz), 0.89 (9H, s), 0.03 (6H, s). ^{13}C -NMR δ 204.80 (C), 159.31 (C), 137.85 (CH), 130.32 (C), 129.14 (CH), 122.54 (CH), 113.89 (CH), 82.30 (C), 68.02 (CH_2), 66.09 (CH_2), 55.30 (CH_3), 39.48 (CH), 38.41 (CH_2), 25.92 (CH_3), 18.34 (C), 18.22 (CH_3), 16.63 (CH_3), -5.33 (CH_3). HRMS (ESI): $[\text{M}+\text{Na}]^+$ m/z calcd for $\text{C}_{23}\text{H}_{38}\text{O}_4\text{SiNa}$ 429.2437; found 429.2442. IR (film): 2929, 2856, 1733, 1615, 1515, 1464, 1386, 1250, 1173, 1110, 1038, 837, 776, 667, 415 cm^{-1} . $[\alpha]_{\text{D}} = +23.4^{\circ}$ (10 mg/mL, CHCl_3).

5.7. (3S,4R,8R,E)-((S)-2-hydroxy-1,2,2-triphenylethyl) 9-(tert-butyldimethylsilyloxy)-4-(4-methoxybenzyloxy)-3-(methoxymethoxy)-4,8-dimethylnon-6-enoate (182)

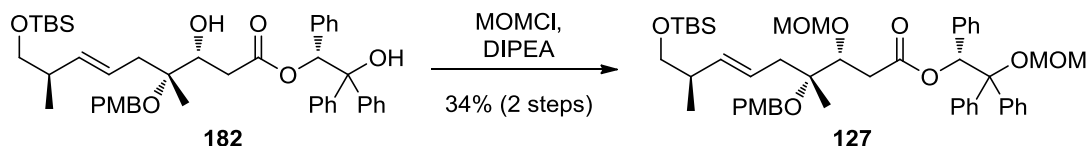


To a solution of (R)-HYTRA (944 mg, 2.84 mmol) in THF (20 mL) was added LDA (7.10 mmol) in THF (10 mL) at -78°C . After 30 min, the solution was warmed to -

20 °C. After the solution cleared, the mixture was cooled to -100 °C and **106** (462 mg, 1.136 mmol) in THF (5 mL) was added. After stirring for 1 h, the solution was warmed slowly to 0°C over 2 h. After quenching with NH₄Cl sat. aq., CH₂Cl₂ was added, the phases were separated, and the aqueous layer was extracted with CH₂Cl₂ (3*20 mL). The combined organic phases were washed with brine, dried over Na₂SO₄ and the solvents were removed. The crude product was moved on to the next step (100% yield were assumed). A small amount of material was subjected to column chromatography and HPLC purification to obtain pure material for analytical data.

¹H-NMR (CDCl₃) δ 0.04 (6H, s), 0.90 (9H, s), 0.98 (3H, d, *J* = 6.7 Hz), 1.11 (3H, s), 2.50-2.23 (6H, m), 2.93 (1H, s), 3.37 (1H, dd, *J* = 7.1, 9.7 Hz), 3.49 (1H, dd, *J* = 6.0, 9.7 Hz), 3.81 (3H, s), 3.88 (1H, m), 4.30 (1H, d, *J* = 10.6 Hz), 4.39 (1H, d, *J* = 10.6 Hz), 5.43 (2H, m), 6.68 (1H, s), 6.87 (2H, d, *J* = 8.6 Hz), 7.04 (2H, d, *J* = 7.0 Hz), 7.20-7.10 (11H, m), 7.26 (2H, m), 7.35 (2H, t, *J* = 7.6 Hz), 7.56 (2H, d, *J* = 7.3 Hz). ¹³C-NMR (CDCl₃) δ 171.30 (C), 159.03 (C), 144.69 (C), 142.60 (C), 136.73 (CH), 135.63 (C), 131.02 (C), 128.91 (CH), 128.36 (CH), 128.27 (CH), 127.89 (CH), 127.76 (CH), 127.44 (CH), 127.30 (CH), 127.02 (CH), 126.42 (CH), 126.27 (CH), 124.30 (CH), 113.77 (CH), 80.29 (C), 79.08 (CH), 78.59 (C), 72.17 (CH), 68.06 (CH₂), 63.66 (CH₂), 55.28 (CH₃), 39.44 (CH), 37.93 (CH₂), 37.03 (CH₂), 25.93 (CH₃), 19.27 (CH₃), 18.34 (C), 16.70 (CH₃), -5.30 (CH₃), -5.33 (CH₃). HRMS (ESI): [M+Na]⁺ *m/z* calcd for C₄₅H₅₈O₇SiNa 761.3850; found 761.3831. IR (film): 3524, 2929, 1734, 1613, 1514, 1449, 1384, 1249, 1154, 1081, 1034, 837, 780, 734, 696, 669, 644, 404 cm⁻¹. [α]_D = +111.2° (10 mg/mL, CHCl₃).

5.8. (3*S*,4*R*,8*R*,*E*)-((*S*)-2-(methoxymethoxy)-1,2,2-triphenylethyl) 9-(tert-butyldimethylsilyloxy)-4-(4-methoxybenzyloxy)-3-(methoxymethoxy)-4,8-dimethylnon-6-enoate (127**)**

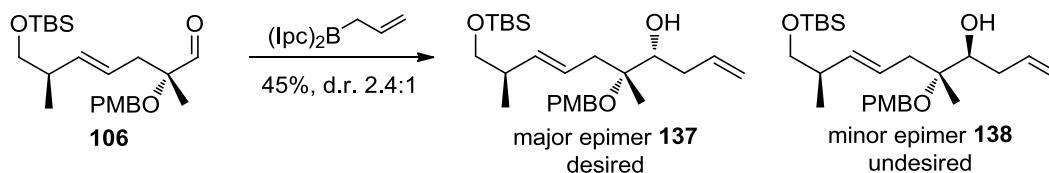


To a suspension of crude ester **182** (1.136 mmol) in CH₂Cl₂ (1 mL) was added DIPEA (3.96 mL, 22.72 mmol) and MOMCl (0.863 mL, 11.36 mmol) at 0°C. After stirring for

1 h at 0 °C, the mixture was warmed to 60°C for 1 h and stirred for 1 h, then reaction complete by TLC. After quenching with NH₄Cl sat. aq., the phases were separated and the aqueous layer was extracted with CH₂Cl₂ (3 times 10 mL). The combined organic phases were washed with brine, dried over Na₂SO₄ and the solvents were removed. The crude product was purified by preparative HPLC (silica, PE:EtOAc 80:20) to obtain 319 mg of **127** (34%) along with 185 mg unreacted **106** (22%).

¹H-NMR (CDCl₃) δ 7.19 (12H, m), 7.08 (1H, t, *J* = 7.3 Hz), 7.01 (2H, t, *J* = 7.4 Hz), 6.85 (2H, d, *J* = 7.3 Hz), 6.82 (2H, d, *J* = 8.7 Hz), 6.63 (1H, s), 5.47 (1H, m), 5.36 (1H, dd, *J* = 15.5, 6.9 Hz), 4.81 (1H, d, *J* = 5.7 Hz), 4.59 (1H, d, *J* = 5.7 Hz), 4.44 (1H, d, *J* = 6.4 Hz), 4.40 (1H, d, *J* = 10.8 Hz), 4.33 (1H, d, *J* = 6.6 Hz), 4.31 (1H, d, *J* = 10.8 Hz), 4.03 (1H, dd, *J* = 7.7, 2.9 Hz), 3.76 (3H, s), 3.48 (1H, d, *J* = 5.8 Hz), 3.45 (1H, d, *J* = 5.8 Hz), 3.32 (3H, s), 3.32 (1H, dd, *J* = 9.8, 7.2 Hz), 2.99 (3H, s), 2.77 (1H, dd, *J* = 16.6, 3.0 Hz), 2.40 (1H, dd, *J* = 16.6, 7.7 Hz), 2.25 (3H, m), 1.13 (3H, s), 0.94 (3H, d, *J* = 6.7 Hz), 0.86 (9H, s), 0.00 (6H, s). ¹³C-NMR (CDCl₃) δ 171.21 (C), 158.85 (C), 141.49 (C), 140.38 (C), 136.50 (C), 136.09 (CH), 131.42 (C), 128.85 (CH), 128.73 (CH), 128.62 (CH), 128.24 (CH), 127.63 (CH), 127.46 (CH), 126.89 (CH), 124.80 (CH), 113.67 (CH), 97.51 (CH₂), 92.90 (CH₂), 85.17 (C), 79.45 (CH), 78.61 (CH), 78.59 (CH), 68.15 (CH₂), 64.01 (CH₂), 56.00 (CH₃), 55.66 (CH₃), 55.23 (CH₃), 39.45 (CH), 37.89 (CH₂), 36.78 (CH₂), 25.92 (CH₃), 20.85 (CH₃), 18.33 (C), 16.74 (CH₃). HRMS (ESI): [M+Na]⁺ *m/z* calcd for C₄₉H₆₆O₉SiNa 849.4374; found 849.4367. IR (film): 2929, 1740, 1613, 1514, 1448, 1381, 1249, 1148, 1036, 837, 776, 701, 667, 413 cm⁻¹. [α]_D = +11.0° (10 mg/mL, CHCl₃).

5.9. (4*R*,5*R*,9*R*,*E*)-10-(*tert*-butyldimethylsilyloxy)-5-(4-methoxybenzyloxy)-5,9-dimethyldeca-1,6-dien-4-ol (137**) and (4*S*,5*R*,9*R*,*E*)-10-((*tert*-butyldimethylsilyl)oxy)-5-((4-methoxybenzyl)oxy)-5,9-dimethyldeca-1,7-dien-4-ol (**138**)**

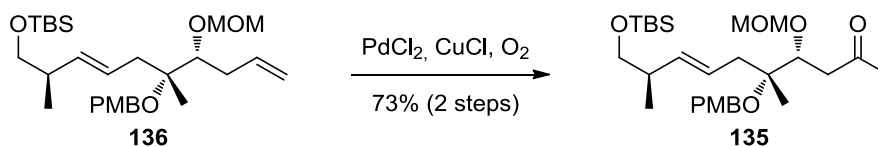


(+)-*B*-Allyldiisopinocampheylborane (1 M in pentane, 0.295 mL, 0.295 mmol) in Et₂O (0.8 mL) was cooled to -100°C using a methanol/liquid nitrogen bath. Aldehyde **106**

sat. (5 mL) and CH_2Cl_2 (5 mL) was added. The phases were separated and the aqueous layer was extracted with CH_2Cl_2 (3 times 5 mL). The combined organic phases were washed with brine and dried over Na_2SO_4 . The solvents were removed and the crude mixture was filtered over a silica plug. The product was moved on as is; an analytical amount was purified by flash chromatography to obtain analytical data.

¹H-NMR (CDCl₃) δ 7.24 (2H, d, *J* = 8.7 Hz), 6.86 (2H, d, *J* = 8.7 Hz), 5.93 (1H, m), 5.56 (1H, m), 5.42 (1H, dd, *J* = 15.5, 7.1 Hz), 5.09 (1H, dd, *J* = 17.1, 1.7 Hz), 5.03 (1H, d, *J* = 10.1 Hz), 4.72 (1H, d, *J* = 6.7 Hz), 4.68 (1H, d, *J* = 6.7 Hz), 4.48 (1H, d, *J* = 10.8 Hz), 4.40 (1H, d, *J* = 10.8 Hz), 3.80 (3H, s), 3.63 (1H, dd, *J* = 8.8, 2.9 Hz), 3.50 (1H, dd, *J* = 9.7, 5.8 Hz), 3.37 (3H, s), 3.36 (1H, dd, *J* = 9.7, 7.2 Hz), 2.50 (1H, dm, *J* = 13.2 Hz), 2.40–2.21 (4H, m), 1.23 (3H, s), 0.99 (3H, d, *J* = 6.7 Hz), 0.89 (9H, s), 0.03 (6H, s). ¹³C-NMR (CDCl₃) δ 158.78 (C), 136.76 (CH), 135.96 (CH), 131.75 (C), 128.64 (CH), 124.85 (CH), 116.23 (CH₂), 113.66 (CH), 97.88 (CH₂), 82.65 (CH), 79.75 (C), 68.20 (CH₂), 63.67 (CH₂), 56.06 (CH₃), 55.26 (CH₃), 39.51 (CH), 38.24 (CH₂), 35.54 (CH₂), 25.94 (CH₃), 20.01 (CH₃), 18.36 (C), 16.80 (CH₃), -5.31 (CH₃). HRMS (ESI): [M+Na]⁺ *m/z* calcd for C₂₈H₄₈O₅SiNa 515.3169; found 515.3165. IR (film): 2955, 2857, 1614, 1514, 1464, 1383, 1301, 1249, 1103, 1038, 918, 837, 776, 671 cm⁻¹. [α]_D = +16.0 (10 mg/mL, CHCl₃).

5.11. (4R,5R,9R,E)-10-(tert-butyldimethylsilyloxy)-5-(4-methoxybenzyloxy)-4-(methoxymethoxy)-5,9-dimethyldec-6-en-2-one (135)

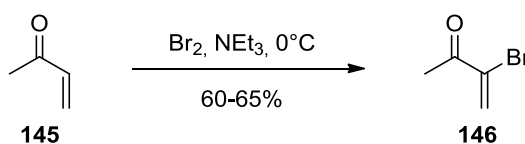


The crude alkene **136** (32 mg, 0.065 mmol) was dissolved in a THF (2 mL) / water (0.2 mL) mixture, and then cooled to 0°C. PdCl₂ (2.3 mg, 0.013 mmol) and CuCl (6.4 mg, 0.065 mmol) were added and oxygen was bubbled through the solution. The mixture was warmed to rt overnight while still passing oxygen through. The suspension was diluted with water/Et₂O (5 mL each), the phases were separated and the aqueous layer was extracted with Et₂O (times 5 mL). The combined organic phases were washed with brine and dried over MgSO₄, then the solvents were removed. The crude product

was purified by flash chromatography (PE:EtOAc 19:1) to give 24 mg (73 % over 2 steps) of **135** as a clear oil.

$^1\text{H-NMR}$ (CDCl_3) δ 7.22 (2H, d, $J = 8.5$ Hz), 6.85 (2H, d, $J = 8.5$ Hz), 5.56 (1H, m), 5.43 (1H, dd, $J = 15.5, 6.9$ Hz), 4.68 (1H, d, $J = 6.4$ Hz), 4.64 (1H, d, $J = 6.4$ Hz), 4.46 (1H, d, $J = 10.8$ Hz), 4.36 (1H, d, $J = 10.8$ Hz), 4.19 (1H, dd, $J = 7.4, 2.9$ Hz), 3.79 (3H, s), 3.51 (1H, m), 3.37 (1H, m), 3.33 (3H, s), 2.83 (1H, dd, $J = 16.8, 2.8$ Hz), 2.67 (1H, dd, $J = 16.8, 7.6$ Hz), 2.33 (3H, m), 2.14 (3H, s), 1.22 (3H, s), 0.99 (3H, d, $J = 6.7$ Hz), 0.89 (9H, s), 0.04 (6H, s). $^{13}\text{C-NMR}$ (CDCl_3) δ 207.17 (C), 158.86 (C), 136.07 (CH), 131.49 (C), 128.73 (CH), 124.96 (CH), 113.68 (CH), 97.81 (CH_2), 79.22 (CH), 78.83 (C), 68.17 (CH_2), 64.03 (CH_2), 55.87 (CH_3), 55.26 (CH_3), 45.25 (CH_2), 39.49 (CH), 38.04 (CH_2), 30.71 (CH_3), 25.94 (CH_3), 20.78 (CH_3), 18.35 (C), 16.79 (CH_3), -5.31 (CH_3). HRMS (ESI): $[\text{M}+\text{Na}]^+$ m/z calcd for $\text{C}_{28}\text{H}_{48}\text{O}_6\text{SiNa}$ 531.3118; found 531.3111. IR (film): 2929, 2856, 1719, 1614, 1515, 1464, 1362, 1249, 1149, 1102, 1039, 837, 777, 668 cm^{-1} . $[\alpha]_{\text{D}} = +25.6$ (7.2 mg/mL, CHCl_3).

5.12. 3-Bromobut-3-en-2-one (**146**)

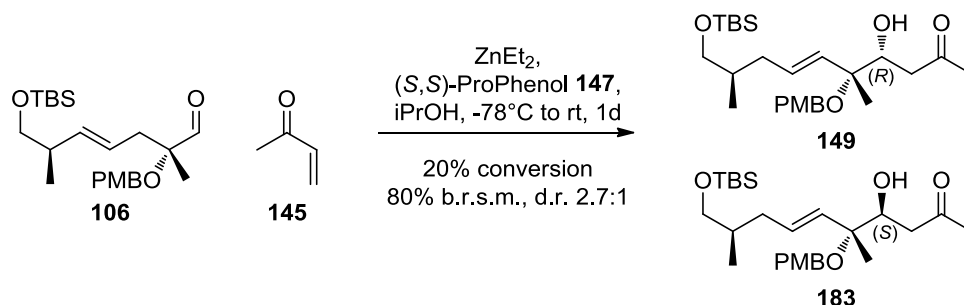


The preparation followed a previously published experimental procedure.¹⁷⁸

Methyl vinyl ketone (**145**, 24.0 mL, 288 mmol) in DCM (160 mL) was cooled to 0°C and bromine (15.0 mL, 291 mmol) in DCM (240 mL) was added dropwise. After 5 min of stirring at 0°C , NEt_3 (40.1 mL, 288 mmol) was added dropwise over 15 min, keeping the temperature at 0°C . Subsequently, the mixture was warmed to rt and stirred for 1 h. HCl aq. (2 M, 200 mL) was added, the phases were separated, and the organic layer was washed with NaHCO_3 sat. aq (200 mL). The organic phase was dried over MgSO_4 , filtered, and the solvents were removed. The crude mixture was purified by fractional vacuum distillation (45°C , 27 mbar) to give the **146** (26–28 g, 60–65%) as pale yellow oil. At room temperature, the neat product polymerized readily, thus it was stored at -18°C where it was stable for several months.

Experimental data were in agreement with previously published values.^{178,179}

5.13. (5*R*,6*R*,10*R*,*E*)-11-((*tert*-butyldimethylsilyl)oxy)-5-hydroxy-6-((4-methoxybenzyl)oxy)-6,10-dimethylundeca-1,7-dien-3-one (149**)**



Benzene was added to Trost's (*S,S*)-Bis-ProPhenol ligand **149**¹⁴⁸ (15.71 mg, 0.025 mmol) under argon. After cooling to 0°C , vacuum was applied to remove the solvent. This drying procedure was then repeated. After addition of THF abs. (0.25 mL), ZnEt_2 (1 M in hexanes, 0.049 mL, 0.049 mmol) was added slowly at rt, then the resulting solution was stirred for 30 min.

Molecular sieves (4 \AA , 50 mg) were added to a mixture of methyl vinyl ketone (**145**, 0.492 mL, 5.90 mmol), *i*PrOH (0.094 mL, 1.230 mmol) and aldehyde **106** (100 mg, 0.246 mmol). After cooling to -78°C , the previously prepared catalyst solution was added. Thereafter the solution was warmed to rt overnight and stirred for 15 h. Upon completion, 0.1 M HCl aq. was added, the phases were separated and the aqueous layer was extracted with Et_2O 4 times. The combined organic phases were washed with brine and dried over Na_2SO_4 . After removal of the solvents, the crude material was purified by column chromatography (PE:EtOAc 7:1) to give (in elution order) unreacted starting material (80 mg, 80%), the desired **149** (14 mg, 12%) and its epimer **183** (5 mg, 4%).

Data for **149** (major isomer, elutes first on normal-phase chromatography):

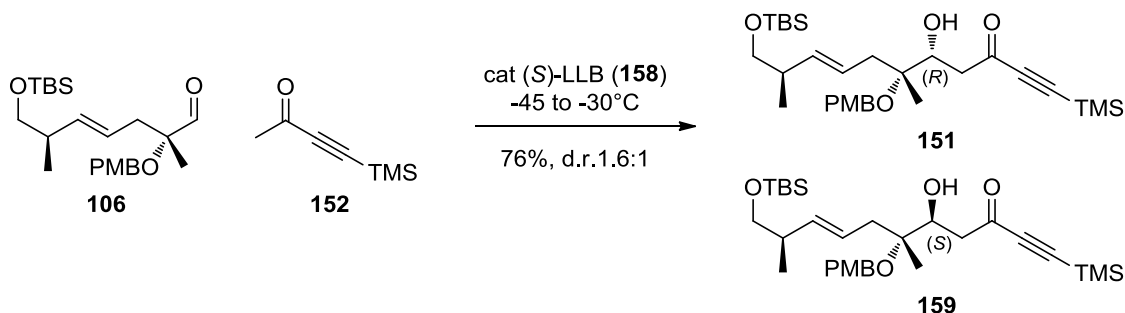
$^1\text{H-NMR}$ (CDCl_3) δ 7.23 (2H, d, $J = 8.7$ Hz), 6.86 (2H, d, $J = 8.7$ Hz), 6.36 (1H, dd, $J = 17.6, 10.4$ Hz), 6.22 (1H, dd, $J = 17.6, 1.0$ Hz), 5.84 (1H, dd, $J = 10.5, 1.0$ Hz), 5.50 (2H, m), 4.45 (1H, d, $J = 10.8$ Hz), 4.41 (1H, d, $J = 10.8$ Hz), 4.16 (1H, d, $J = 10.1$ Hz), 3.80 (3H, s), 3.49 (1H, m), 3.37 (1H, dd, $J = 9.7, 6.2$ Hz), 2.97 (1H, dd, $J = 17.1, 1.9$ Hz), 2.94 (1H, d, $J = 3.6$ Hz), 2.70 (1H, dd, $J = 17.0, 9.9$ Hz), 2.50 (1H, m), 2.34 (2H, m), 1.25 (3H, s), 0.98 (3H, d, $J = 6.8$ Hz), 0.89 (9H, s), 0.03 (6H, s). $^{13}\text{C-NMR}$ (CDCl_3) δ 201.56 (C), 158.97 (C), 136.85 (CH), 136.53 (CH), 131.33 (C), 128.80 (CH),

128.79 (CH₂), 124.56 (CH), 113.77 (CH), 78.50 (C), 71.02 (CH), 68.17 (CH₂), 63.53 (CH₂), 55.29 (CH₃), 40.66 (CH₂), 39.50 (CH), 38.43 (CH₂), 25.95 (CH₃), 18.51 (CH₃), 18.36 (C), 16.72 (CH₃), -5.30 (CH₃), -5.33 (CH₃). HRMS (ESI): [M+Na]⁺ m/z calcd for C₂₇H₄₄O₅SiNa 499.2856; found 499.2857.

Data for **183** (minor isomer, elutes last on normal-phase chromatography):

¹H-NMR (CDCl₃) δ 7.24 (2H, d, *J* = 8.6 Hz), 6.87 (2H, d, *J* = 8.7 Hz), 6.39 (1H, dd, *J* = 17.6, 10.5 Hz), 6.23 (1H, d, *J* = 16.6 Hz), 5.84 (1H, d, *J* = 9.6 Hz), 5.58–5.44 (2H, m), 4.50 (1H, d, *J* = 10.7 Hz), 4.42 (1H, d, *J* = 10.8 Hz), 4.18 (1H, m), 3.80 (3H, s), 3.49 (1H, m), 3.37 (1H, dd, *J* = 9.7, 7.1 Hz), 2.81 (3H, m), 2.47 (1H, dd, *J* = 14.3, 6.7 Hz), 2.34 (2H, m), 1.22 (3H, s), 0.99 (3H, d, *J* = 6.8 Hz), 0.89 (9H, s), 0.03 (6H, s). ¹³C-NMR (CDCl₃) δ 200.48 (C), 159.00 (C), 136.78 (CH), 136.65 (CH), 131.24 (C), 128.82 (CH), 128.70 (CH₂), 124.54 (CH), 113.79 (CH), 78.88 (C), 71.94 (CH), 68.08 (CH₂), 63.81 (CH₂), 55.28 (CH₃), 41.14 (CH₂), 39.49 (CH), 37.91 (CH₂), 25.93 (CH₃), 19.64 (CH₃), 18.35 (C), 16.72 (CH₃), -5.31 (CH₃), -5.34 (CH₃). HRMS (ESI): [M+Na]⁺ m/z calcd for C₂₇H₄₄O₅SiNa 499.2856; found 499.2856.

5.14. (5*R*,6*R*,10*R*,*E*)-11-((*tert*-butyldimethylsilyl)oxy)-5-hydroxy-6-((4-methoxybenzyl)oxy)-6,10-dimethyl-1-(trimethylsilyl)undec-8-en-1-yn-3-one (151)



To a solution of **17** (3.62 mL, 0.1 M in THF, 0.362 mmol) was added **18** (2.380 mL, 14.49 mmol) at -45°C and the mixture was stirred for 15 min. Then, a solution of **16** (0.982 g, 2.415 mmol) in 1.3 mL THF was added and the mixture was stirred at -30°C overnight. The mixture was quenched with NH₄Cl aq. sat. (10 mL), the phases were separated, and the aqueous layer was extracted with EtOAc three times. The combined organic phases were dried over sodium sulfate, filtered, and the solvents were removed. The crude product was purified using column chromatography (hexanes:EtOAc 9:1) at

low temperatures to give the undesired epimer **159** (384 mg, eluted first) and **151** (620 mg, eluted second), both as colorless oils, for a combined yield of 76% and a d.r. of 1.6:1.

The setup for low-temperature column chromatography is shown in Figure 16 on page 57. A cold bath was cooled to -30°C using a cooling finger. The eluent was run through the cooling bath in Teflon tubing, before being applied onto the top of a column with heating/cooling mantle through a septum. The column itself was additionally cooled by circulating the cooling mixture through its mantle using a pump. All tubing and the column itself was isolated using cotton wool and aluminium foil. Once the temperature had stabilized (usually around -25 °C), the crude mixture was dissolved in the eluent and applied to the top of the column through the septum using a syringe. Fractions were then collected until complete elution of the product.

Analytical data for the undesired isomer (**159**, eluting first):

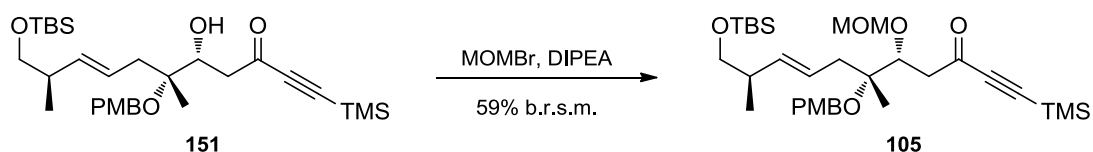
¹H-NMR (CDCl₃) δ 7.23 (2H, d, *J* = 8.6 Hz), 6.87 (2H, d, *J* = 8.7 Hz), 5.50 (2H, m), 4.42 (2H, s), 4.21 (1H, d, *J* = 9.7 Hz), 3.80 (3H, s), 3.49 (1H, m), 3.38 (1H, ddd, *J* = 9.7, 7.0, 1.3 Hz), 2.93 (1H, dd, *J* = 17.1, 2.2 Hz), 2.74 (1H, ddd, *J* = 17.1, 9.8, 1.9 Hz), 2.57 (1H, br s), 2.47 (1H, m), 2.32 (2H, m), 1.24 (3H, s), 0.99 (3H, d, *J* = 6.7 Hz), 0.89 (9H, s), 0.23 (9H, s), 0.04 (6H, s). ¹³C-NMR (CDCl₃) δ 187.26 (C), 158.99 (C), 136.71 (CH), 131.15 (CH), 128.81 (CH), 124.37 (CH), 113.77 (CH), 102.13 (C), 98.35 (C), 78.41 (C), 70.86 (CH), 68.13 (CH₂), 63.50 (CH₂), 55.27 (CH₃), 47.10 (CH₂), 39.48 (CH), 38.43 (CH₂), 25.94 (CH₃), 18.51 (CH₃), 18.35 (C), 16.70 (CH₃), 0.80 (CH₃), -5.31 (CH₃), -5.33 (CH₃). HRMS (ESI): [M+Na]⁺ *m/z* calcd for C₃₀H₅₀O₅Si₂Na 569.3094; found 569.3091. IR (film): 2956, 1674, 1514, 1463, 1250, 1086, 844, 776. [α]_D = -3.8° (10 mg/mL, CHCl₃).

Analytical data for the desired isomer (**151**, eluting second):

¹H-NMR (CDCl₃) δ 7.24 (2H, d, *J* = 8.6 Hz), 6.87 (2H, d, *J* = 8.6 Hz), 5.49 (2H, m), 4.47 (1H, d, *J* = 10.6 Hz), 4.41 (1H, d, *J* = 10.7 Hz), 4.23 (1H, m), 3.80 (3H, s), 3.49 (1H, dd, *J* = 9.7, 6.0 Hz), 3.38 (1H, dd, *J* = 9.7, 7.0 Hz), 2.78 (2H, pd, *J* = 6.1 Hz), 2.60 (1H, d, *J* = 5.2 Hz), 2.46 (1H, dd, *J* = 14.4, 6.6 Hz), 2.33 (2H, m), 1.55 (3H, s), 1.26 (1H, s), 1.21 (3H, s), 0.99 (3H, d, *J* = 6.8 Hz), 0.89 (9H, s), 0.24 (9H, s), 0.03 (6H, s). ¹³C-NMR (CDCl₃) δ 186.40 (C), 159.04 (C), 136.90 (CH), 131.05 (C), 128.86 (CH),

124.26 (CH), 113.80 (CH), 102.11 (C), 98.36 (C), 78.78 (C), 71.64 (CH), 68.04 (CH₂), 63.73 (CH₂), 55.27 (CH₃), 47.32 (CH₂), 39.46 (CH), 38.04 (CH₂), 25.93 (CH₃), 19.36 (CH₃), 18.34 (C), 16.70 (CH₃), 0.79 (CH₃), -5.32 (CH₃), -5.34 (CH₃). HRMS (ESI): [M+Na]⁺ m/z calcd for C₃₀H₅₀O₅Si₂Na 569.3094; found 569.3090. IR (film): 2956, 2361, 1677, 1514, 1464, 1251, 1083, 1038, 845, 764, 669 cm⁻¹. [α]_D = +1.0° (10 mg/mL, CHCl₃).

5.15. (5*R*,6*R*,10*R*,*E*)-11-((*tert*-butyldimethylsilyl)oxy)-6-((4-methoxybenzyl)oxy)-5-(methoxymethoxy)-6,10-dimethyl-1-(trimethylsilyl)undec-8-en-1-yn-3-one (105)

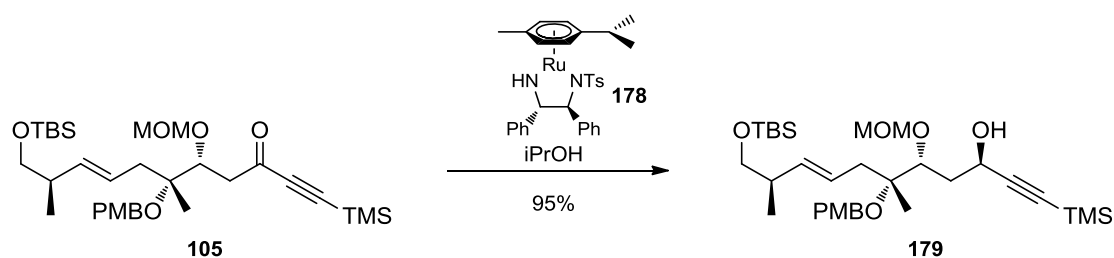


A suspension of **151** (562 mg, 1.028 mmol) in a minimum amount of dichloromethane was cooled to 0°C and *N,N*-diisopropylethylamine (2.15 mL, 12.3 mmol) and methoxymethyl bromide (839 μL, 10.28 mmol) were added. The mixture was slowly warmed to room temperature. After 1 h, before complete consumption of the starting material, the reaction was quenched by addition of NH₄Cl aq. sat. (10 mL). Prolonged reaction times led to lower yields due to decomposition. The phases were separated, and the aqueous layer was extracted with diethylether three times. The combined organic phases were dried over sodium sulfate, filtered, and the solvents were removed. The crude product was purified using column chromatography (hexanes:EtOAc 9:1) at -25°C to give **105** (249 mg, 41%) along with unreacted **151** (167.8 mg, 30%).

¹H-NMR (CDCl₃) δ 7.23 (2H, d, *J* = 8.6 Hz), 6.86 (2H, d, *J* = 8.6 Hz), 5.54 (1H, m), 5.43 (1H, dd, *J* = 15.5, 6.9 Hz), 4.70 (1H, d, *J* = 6.5 Hz), 4.64 (1H, d, *J* = 6.5 Hz), 4.47 (1H, d, *J* = 10.8 Hz), 4.40 (1H, d, *J* = 10.8 Hz), 4.27 (1H, dd, *J* = 7.8, 2.7 Hz), 3.79 (3H, s), 3.50 (1H, dd, *J* = 9.7, 5.9 Hz), 3.38 (1H, dd, *J* = 9.5, 2.2 Hz), 3.34 (3H, s), 3.03 (1H, dd, *J* = 16.9, 2.8 Hz), 2.83 (1H, dd, *J* = 16.9, 7.8 Hz), 2.32 (3H, m), 1.24 (3H, s), 0.99 (3H, d, *J* = 6.8 Hz), 0.89 (9H, s), 0.23 (9H, s), 0.03 (6H, s). ¹³C-NMR (CDCl₃) δ 185.86 (C), 158.89 (C), 136.19 (CH), 131.41 (C), 128.73 (CH), 124.82 (CH), 113.71 (CH), 102.29 (C), 98.08 (C), 97.74 (CH₂), 78.96 (CH), 78.72 (C), 68.16 (CH₂), 64.07 (CH₂), 55.92 (CH₃), 55.26 (CH₃), 47.34 (CH₂), 39.48 (CH), 38.08 (CH₂), 25.94 (CH₃), 20.87 (CH₃), 18.35 (C), 16.78 (CH₃), 0.78 (CH₃), -5.30 (CH₃), -5.33 (CH₃). HRMS (ESI):

$[M+Na]^+$ m/z calcd for $C_{32}H_{54}O_6Si_2Na$ 613.3357; found 613.3360. IR (film): 2928, 1678, 1514, 1466, 1251, 1147, 1037, 845, 776 cm^{-1} . $[\alpha]_D = +13.9^\circ$ (10 mg/mL, $CHCl_3$).

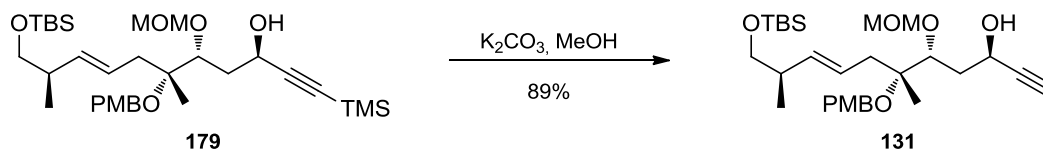
5.16. (3*R*,5*R*,6*R*,10*R*,*E*)-11-((*tert*-butyldimethylsilyl)oxy)-6-((4-methoxybenzyl)oxy)-5-(methoxymethoxy)-6,10-dimethyl-1-(trimethylsilyl)undec-8-en-1-yn-3-ol (179)



Ketone **105** (432 mg, 0.716 mmol) was dissolved in absolute, degassed isopropanol (5.2 mL) under argon, then catalyst **178** (25 mg, 0.043 mmol) was added at once and the mixture was warmed to 40°C overnight. The solvents were removed and the crude mixture was purified by column chromatography (hexanes:EtOAc 19:1 to 9:1) to give **179** (403 mg, 95%) as a viscous, colorless oil. No traces of a second isomer were detected.

1H -NMR ($CDCl_3$) δ 7.23 (2H, d, $J = 8.7$ Hz), 6.86 (2H, d, $J = 8.7$ Hz), 5.48 (2H, m), 4.78 (1H, d, $J = 6.3$ Hz), 4.69 (1H, d, $J = 6.3$ Hz), 4.62 (1H, m), 4.45 (1H, d, $J = 10.8$ Hz), 4.41 (1H, d, $J = 10.7$ Hz), 3.85 (1H, dd, $J = 10.4, 2.8$ Hz), 3.80 (3H, s), 3.50 (2H, m), 3.41 (3H, s), 3.37 (1H, dd, $J = 9.8, 7.1$ Hz), 2.33 (3H, m), 1.99 (1H, ddd, $J = 14.4, 9.7, 2.8$ Hz), 1.85 (1H, ddd, $J = 14.4, 10.5, 3.0$ Hz), 1.22 (3H, s), 0.98 (3H, d, $J = 6.8$ Hz), 0.89 (9H, s), 0.17 (9H, s), 0.04 (6H, s). ^{13}C -NMR ($CDCl_3$) δ 158.85 (C), 136.41 (CH), 131.51 (C), 128.66 (CH), 124.30 (CH), 113.70 (CH), 106.88 (C), 99.20 (CH_2), 88.66 (C), 80.82 (CH), 79.80 (C), 68.15 (CH_2), 63.69 (CH_2), 59.61 (CH), 56.27 (CH_3), 55.26 (CH_3), 39.51 (CH), 38.45 (CH_2), 38.16 (CH_2), 25.95 (CH_3), 19.35 (CH_3), 18.36 (C), 16.76 (CH_3), 0.08 (CH_3), -5.31 (CH_3). HRMS (ESI): $[M+Na]^+$ m/z calcd for $C_{32}H_{56}O_6Si_2Na$ 615.3513; found 615.3528. IR (film): 2956, 2360, 1514, 1249, 1036, 841, 775 cm^{-1} . $[\alpha]_D = +45.4^\circ$ (10 mg/mL, $CHCl_3$).

5.17. (3*R*,5*R*,6*R*,10*R*,*E*)-11-((*tert*-butyldimethylsilyl)oxy)-6-((4-methoxybenzyl)oxy)-5-(methoxymethoxy)-6,10-dimethylundec-8-en-1-yn-3-ol (131)

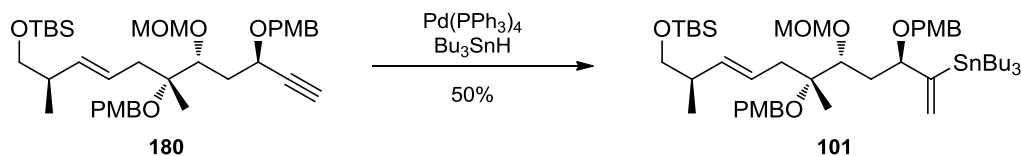


To **179** (166 mg, 0.281 mmol) in absolute methanol (1.4 mL) was added powdered potassium carbonate (19.4 mg, 0.140 mmol) at 0°C. The mixture was stirred at 0°C, then left to warm to room temperature overnight. The reaction was diluted with diethylether (10 mL), quenched with NH₄Cl aq. sat. (10 mL). The phases were separated and the aqueous layer was extracted with diethylether three times. The combined organic phases were dried over Na₂SO₄, and the solvents were removed under reduced pressure. The crude product was purified by column chromatography (hexanes:EtOAc 5:1) to yield **131** (130 mg, 89%) as a colorless oil.

¹H-NMR (CDCl₃) δ 7.23 (2H, d, *J* = 8.6 Hz), 6.86 (2H, d, *J* = 8.6 Hz), 5.48 (2H, m), 4.79 (1H, d, *J* = 6.2 Hz), 4.70 (1H, d, *J* = 6.2 Hz), 4.63 (1H, m), 4.45 (1H, d, *J* = 10.7 Hz), 4.40 (1H, d, *J* = 10.7 Hz), 3.86 (1H, dd, *J* = 10.4, 2.7 Hz), 3.80 (3H, s), 3.60 (1H, d, *J* = 6.4 Hz), 3.50 (1H, dd, *J* = 9.7, 5.9 Hz), 3.41 (3H, s), 3.37 (1H, dd, *J* = 9.7, 7.2 Hz), 2.44 (1H, d, *J* = 2.2 Hz), 2.32 (3H, m), 2.01 (1H, ddd, *J* = 14.4, 9.5, 2.8 Hz), 1.87 (1H, ddd, *J* = 14.3, 10.5, 3.0 Hz), 1.22 (3H, s), 0.98 (3H, d, *J* = 6.7 Hz), 0.89 (9H, s), 0.04 (6H, s). ¹³C-NMR (CDCl₃) δ 158.86 (C), 136.44 (CH), 131.45 (C), 128.66 (CH), 124.19 (CH), 113.71 (CH), 99.25 (CH₂), 85.05 (C), 80.82 (CH), 79.82 (C), 72.30 (CH), 68.13 (CH₂), 63.66 (CH₂), 59.10 (CH), 56.25 (CH₃), 55.26 (CH₃), 39.52 (CH), 38.30 (CH₂), 38.12 (CH₂), 25.95 (CH₃), 19.21 (CH₃), 18.36 (C), 16.74 (CH₃), -5.31 (CH₃). HRMS (ESI): [M+Na]⁺ *m/z* calcd for C₂₉H₄₈O₆SiNa 543.3118; found 543.3125. IR (film): 2955, 2360, 1514, 1463, 1249, 1147, 1035, 836, 775, 669 cm⁻¹. [α]_D = +45.0° (10 mg/mL, CHCl₃).

¹H-NMR (CDCl₃) δ 7.28 (2H, d, *J* = 8.7 Hz), 7.22 (2H, d, *J* = 8.7 Hz), 6.86 (2H, d, *J* = 8.8 Hz), 6.84 (2H, d, *J* = 8.7 Hz), 5.52 (1H, m), 5.41 (1H, dd, *J* = 15.5, 6.9 Hz), 4.74 (1H, d, *J* = 10.9 Hz), 4.64 (1H, d, *J* = 6.3 Hz), 4.57 (1H, d, *J* = 6.4 Hz), 4.40 (4H, m), 3.79 (7H, m), 3.48 (1H, dd, *J* = 9.7, 5.8 Hz), 3.33 (1H, dd, *J* = 9.6, 7.4 Hz), 3.32 (3H, s), 2.47 (1H, d, *J* = 2.0 Hz), 2.25 (4H, m), 1.85 (1H, ddd, *J* = 14.6, 9.7, 2.9 Hz), 1.20 (3H, s), 0.96 (3H, d, *J* = 6.7 Hz), 0.88 (9H, s), 0.02 (6H, s). ¹³C-NMR (CDCl₃) δ 159.22 (C), 158.77 (C), 135.98 (CH), 131.73 (C), 130.16 (C), 129.65 (CH), 128.75 (CH), 124.75 (CH), 113.71 (CH), 113.63 (CH), 98.62 (CH₂), 83.54 (C), 80.26 (CH), 79.37 (C), 73.51 (CH), 70.38 (CH₂), 68.17 (CH₂), 65.46 (CH), 63.70 (CH₂), 56.00 (CH₃), 55.26 (CH₃), 39.41 (CH), 38.19 (CH₂), 37.84 (CH₂), 25.94 (CH₃), 19.97 (CH₃), 18.34 (C), 16.69 (CH₃), -5.30 (CH₃), -5.33 (CH₃). HRMS (ESI): [M+Na]⁺ *m/z* calcd for C₃₇H₅₆O₇SiNa 663.3693; found 663.3715. IR (film): 2953, 2360, 1514, 1464, 1248, 1083, 1036, 835, 775, 669 cm⁻¹. [α]_D = +51.0° (10 mg/mL, CHCl₃).

5.19. (5*R*,6*R*,10*R*,*E*)-6-((4-methoxybenzyl)oxy)-5-((*R*)-2-((4-methoxybenzyl)oxy)-3-(tributylstannyl)but-3-en-1-yl)-6,10,13,13,14,14-hexamethyl-2,4,12-trioxa-13-silapentadec-8-ene (101)

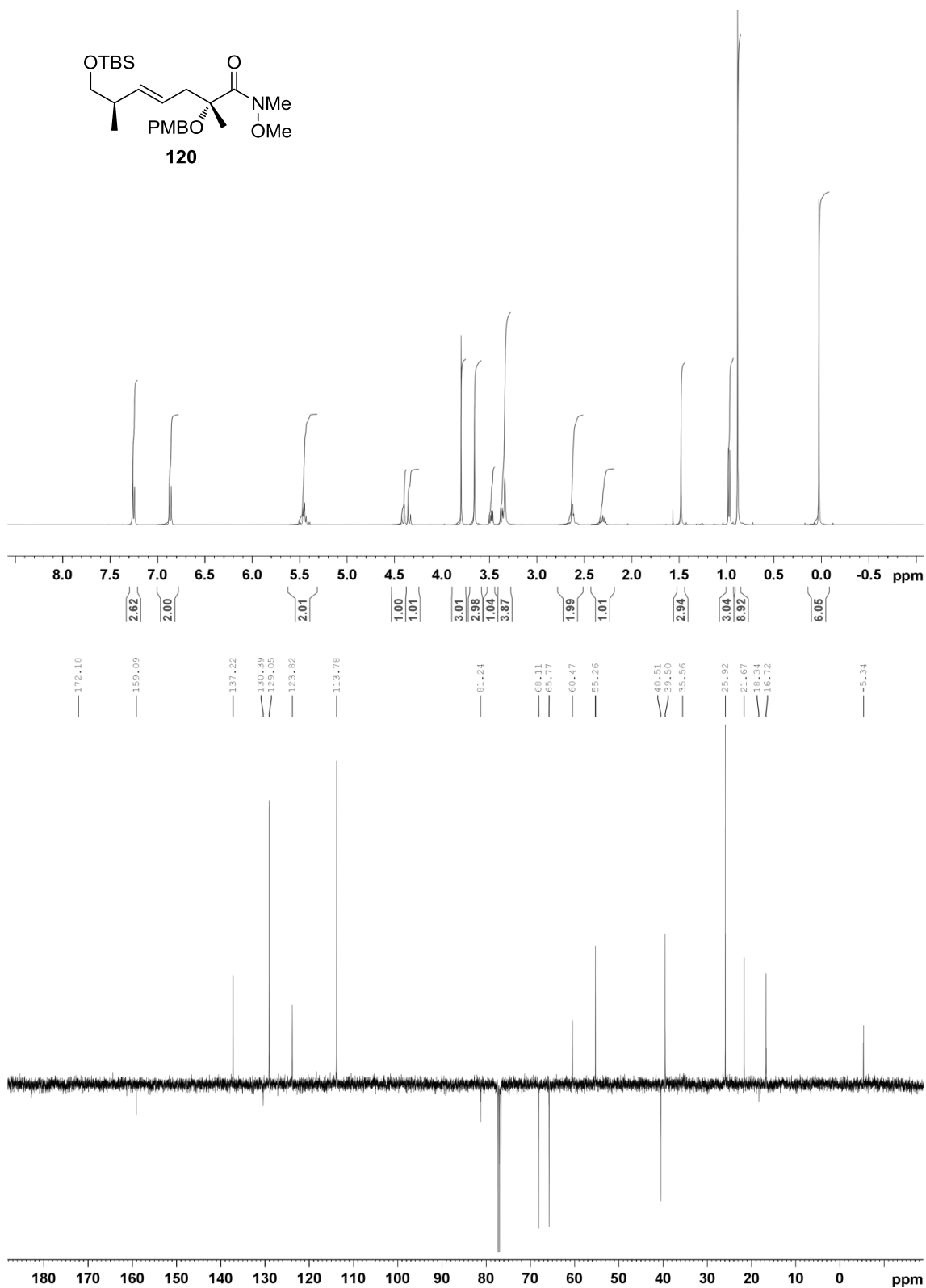
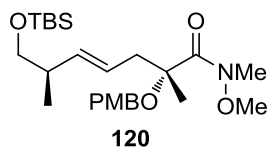


$\text{Pd(PPh}_3)_4$ (7.2 mg, 6.24 μmol) and **180** (200 mg, 0.310 mmol) were dissolved in THF (3.1 mL) and cooled to -40°C , then tributylstannane (168 μL , 0.625 mmol) was added. The mixture was stirred at -40°C until completion (roughly 30 min). The solution was diluted with diethylether and quenched with NH_4Cl aq. sat. (10 mL). The phases were separated, and the aqueous layer was extracted with diethylether three times. The combined organic phases were washed with brine, dried over sodium sulfate, filtered, and the solvents were removed. The crude product was purified using column chromatography (hexanes:EtOAc 19:1) to give **101** (144 mg, 50%) as a colorless oil, along with the undesired linear isomer (112 mg, 38%) and a reduction product (15 mg, 8%).

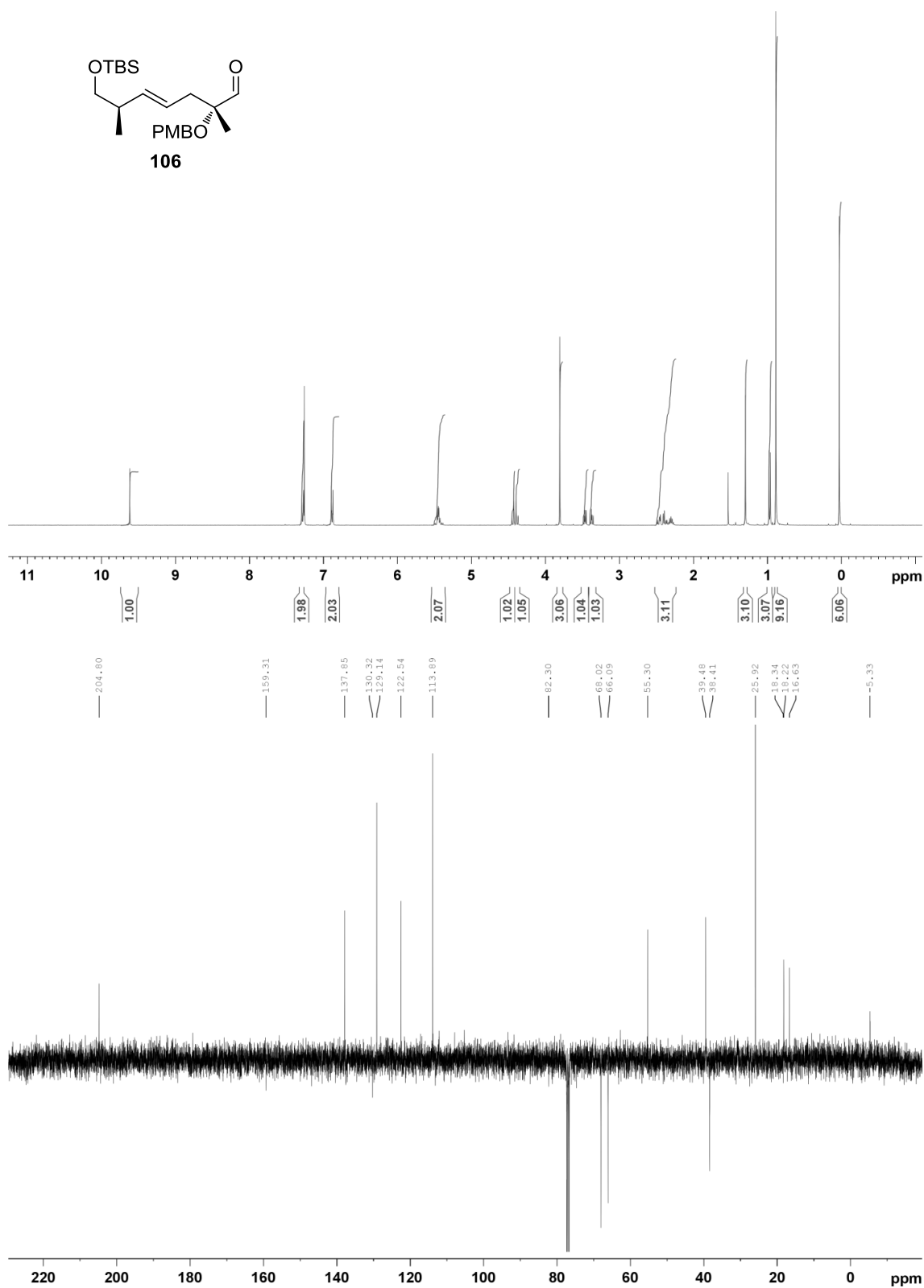
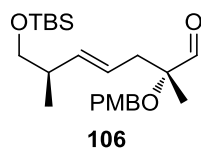
$^1\text{H-NMR}$ (CDCl_3) δ 7.22 (4H, pt, $J = 8.5$ Hz), 6.83 (4H, pt, $J = 8.3$ Hz), 5.91 (1H, d, $J = 2.0$ Hz), 5.55 (1H, m), 5.40 (1H, dd, $J = 15.5, 7.0$ Hz), 5.32 (1H, d, $J = 2.5$ Hz), 4.61 (1H, d, $J = 6.3$ Hz), 4.58 (1H, d, $J = 6.3$ Hz), 4.42 (3H, m), 4.20 (1H, d, $J = 11.4$ Hz), 4.11 (1H, d, $J = 10.5$ Hz), 3.85 (1H, d, $J = 8.8$ Hz), 3.79 (3H, s), 3.78 (3H, s), 3.49 (1H, dd, $J = 9.7, 5.7$ Hz), 3.34 (3H, s), 3.32 (1H, dd, $J = 9.5, 7.3$ Hz), 2.29 (4H, m), 1.89 (1H, dd, $J = 13.2, 11.2$ Hz), 1.46 (6H, m), 1.26 (6H, m), 1.18 (3H, s), 0.97 (3H, d, $J = 6.7$ Hz), 0.91 (6H, m), 0.88 (9H, s), 0.85 (9H, t, $J = 7.3$ Hz), 0.02 (6H, s). $^{13}\text{C-NMR}$ (CDCl_3) δ 158.85 (C), 158.67 (C), 157.49 (C), 135.77 (CH), 131.99 (C), 131.32 (C), 128.98 (CH), 128.64 (CH), 126.18 (CH_2), 125.01 (CH), 113.58 (CH), 113.55 (CH), 98.71 (CH_2), 83.90 (CH), 80.67 (CH), 79.46 (C), 69.86 (CH_2), 68.25 (CH_2), 63.55 (CH_2), 55.93 (CH_3), 55.27 (CH_3), 55.25 (CH_3), 39.44 (CH), 38.97 (CH_2), 38.35 (CH_2), 29.10 (CH_2), 27.39 (CH_2), 25.94 (CH_3), 19.97 (CH_3), 18.35 (C), 16.72 (CH_3), 13.66 (CH_3), 10.10 (CH_2), -5.31 (CH_3), -5.34 (CH_3). HRMS (ESI): $[\text{M}+\text{Na}]^+$ m/z calcd for $\text{C}_{49}\text{H}_{84}\text{O}_7\text{SiSnNa}$ 955.4906; found 955.4924. IR (film): 2927, 2855, 1514, 1463, 1248, 1171, 1084, 1038, 836, 776 cm^{-1} . $[\alpha]_{\text{D}} = +42.7^\circ$ (10 mg/mL, CHCl_3).

6. Spectral data

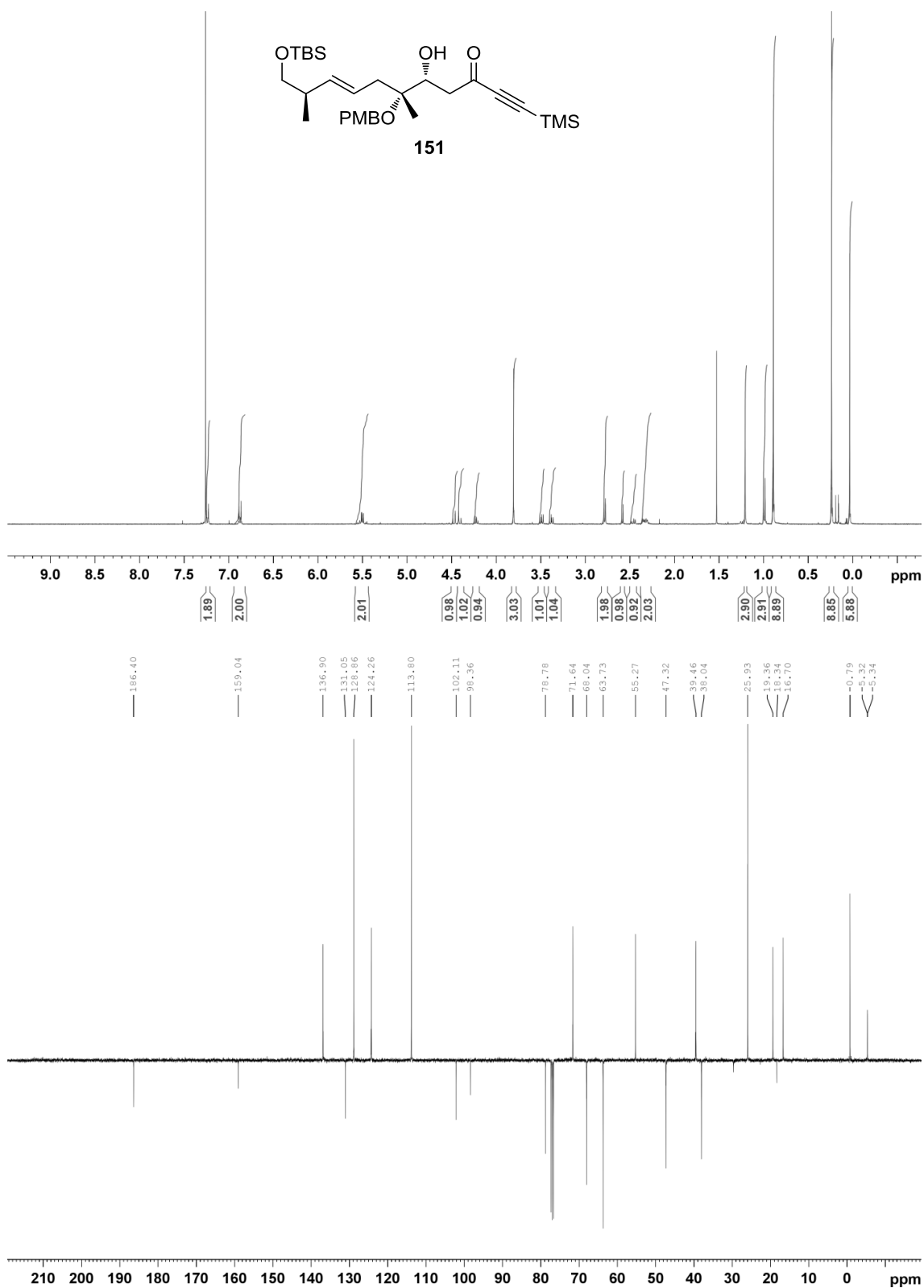
6.1. (2*R*,6*R*,*E*)-7-(*tert*-butyldimethylsilyloxy)-*N*-methoxy-2-(4-methoxybenzyloxy)-*N*,2,6-trimethylhept-4-enamide (120)



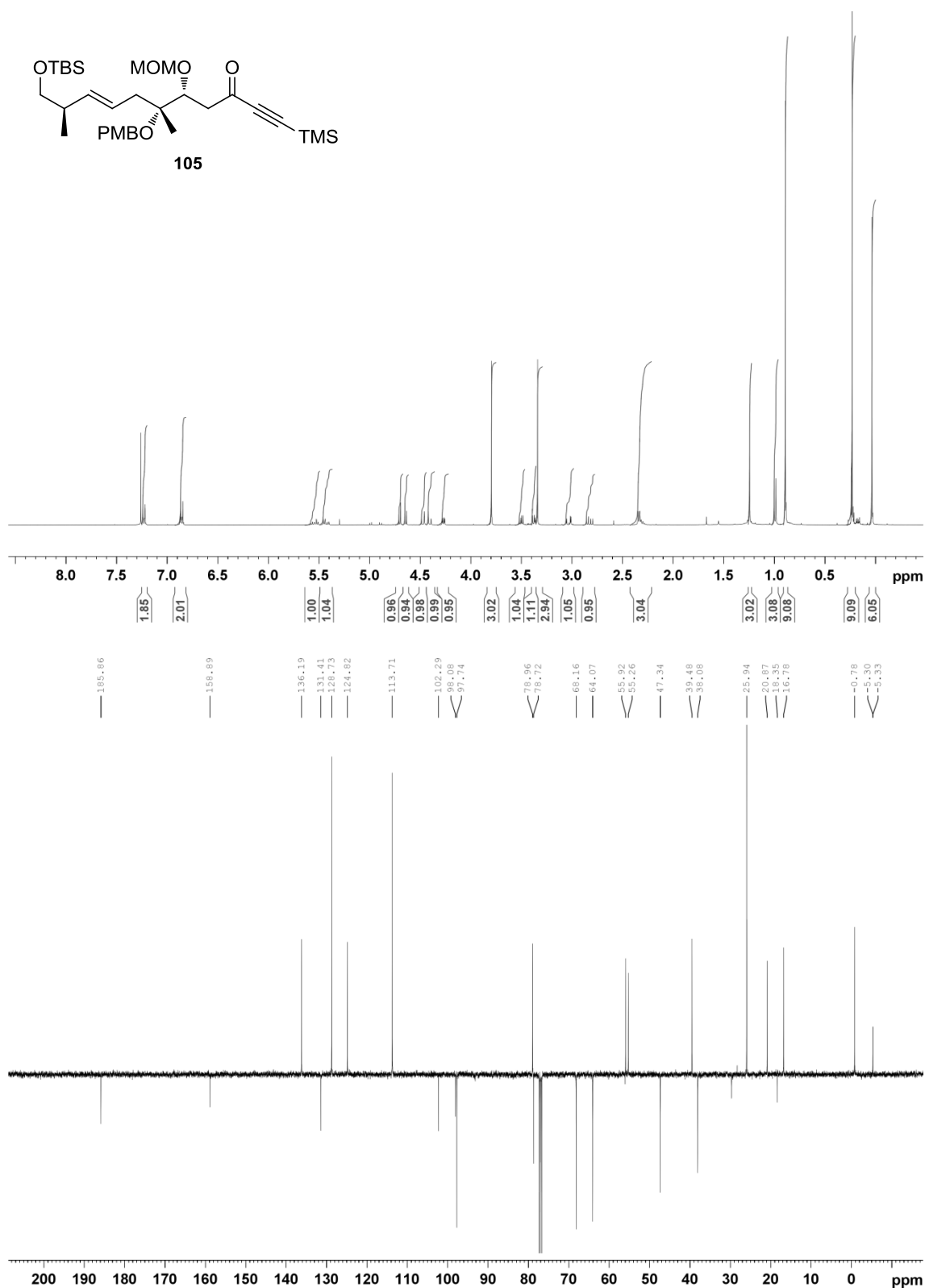
6.2. (2R,6R,E)-7-(tert-butyldimethylsilyloxy)-2-(4-methoxybenzyloxy)-2,6-dimethylhept-4-enal (106)



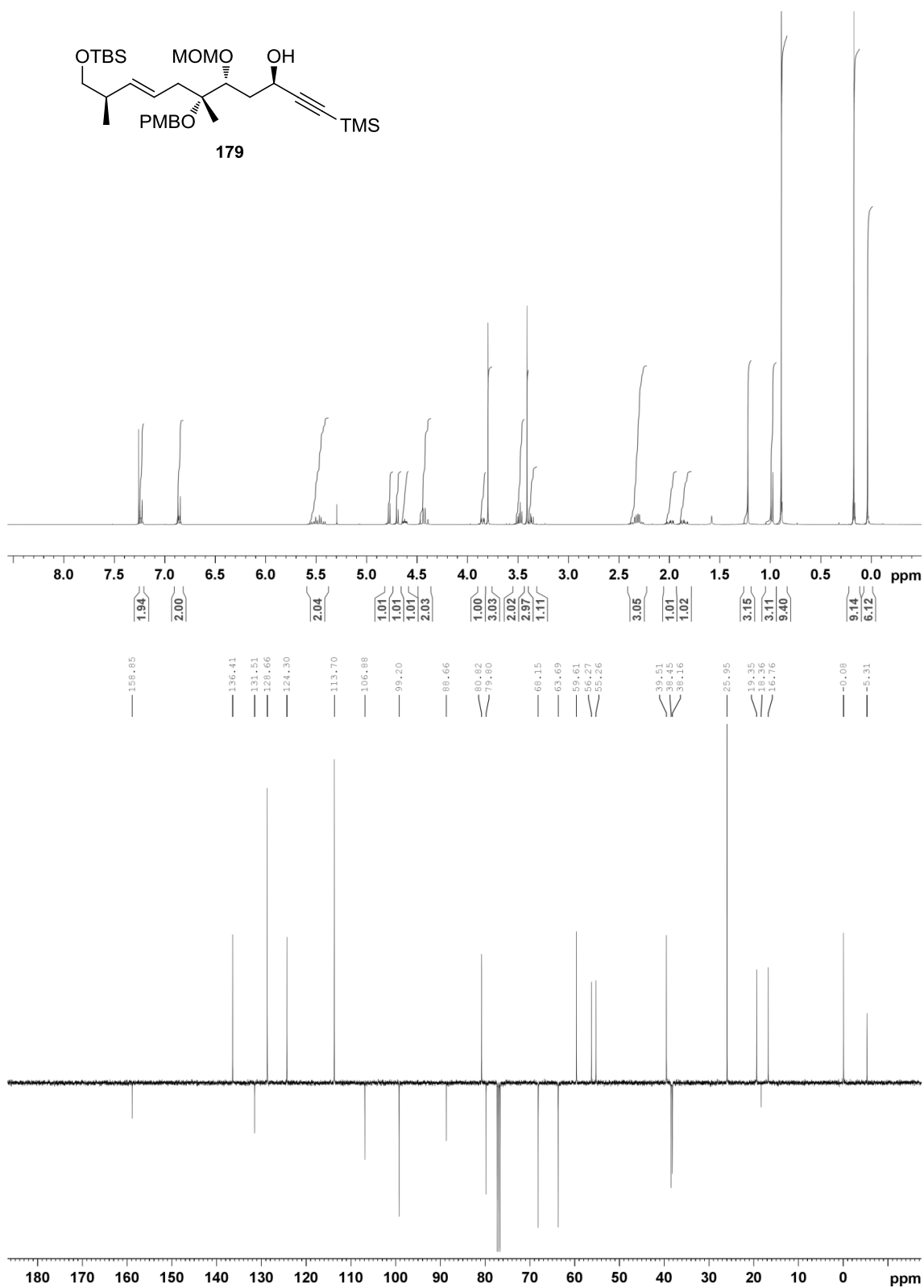
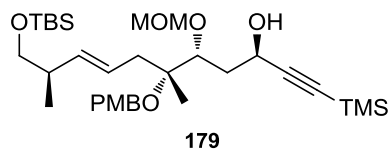
6.3. (5*R*,6*R*,10*R*,*E*)-11-((*tert*-butyldimethylsilyl)oxy)-5-hydroxy-6-((4-methoxybenzyl)oxy)-6,10-dimethyl-1-(trimethylsilyl)undec-8-en-1-yn-3-one (151)



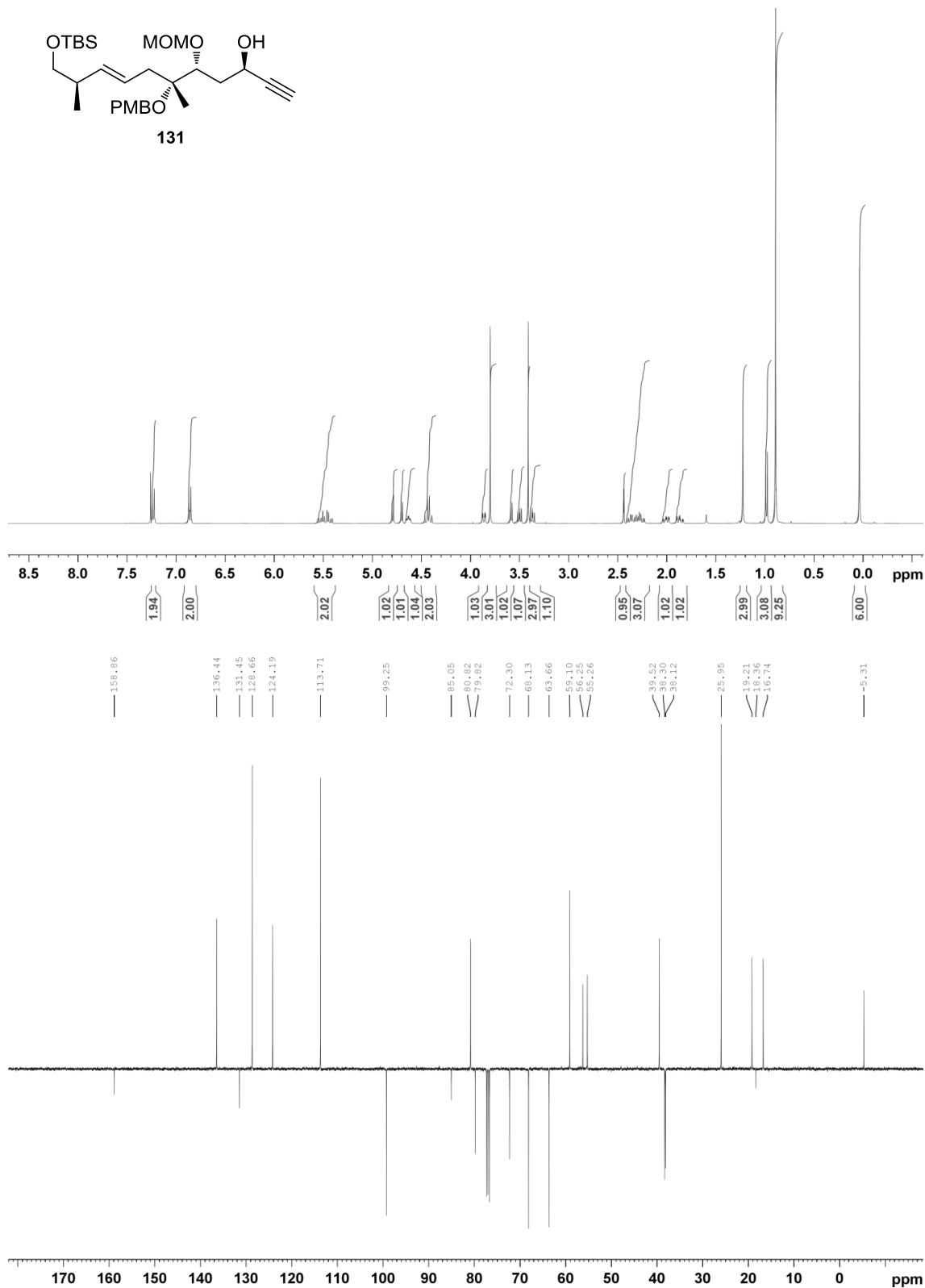
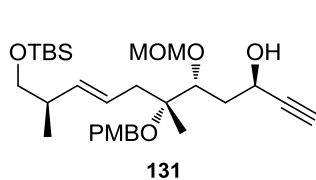
6.4. (5R,6R,10R,E)-11-((tert-butyldimethylsilyl)oxy)-6-((4-methoxybenzyl)oxy)-5-(methoxymethoxy)-6,10-dimethyl-1-(trimethylsilyl)undec-8-en-1-yn-3-one (105)



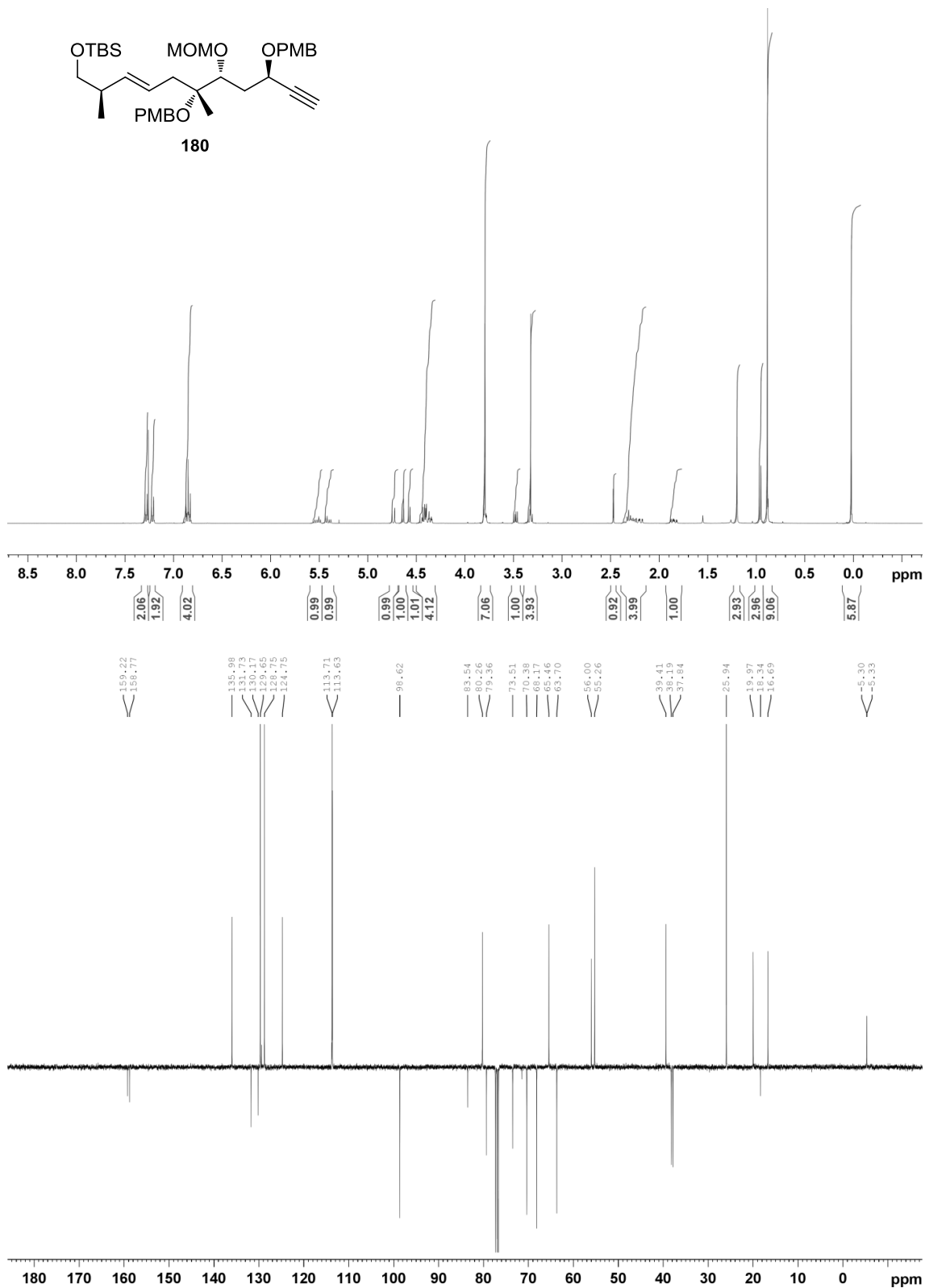
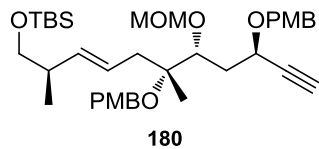
6.5. (3R,5R,6R,10R,E)-11-((tert-butyldimethylsilyl)oxy)-6-((4-methoxybenzyl)oxy)-5-(methoxymethoxy)-6,10-dimethyl-1-(trimethylsilyl)undec-8-en-1-yn-3-ol (179)



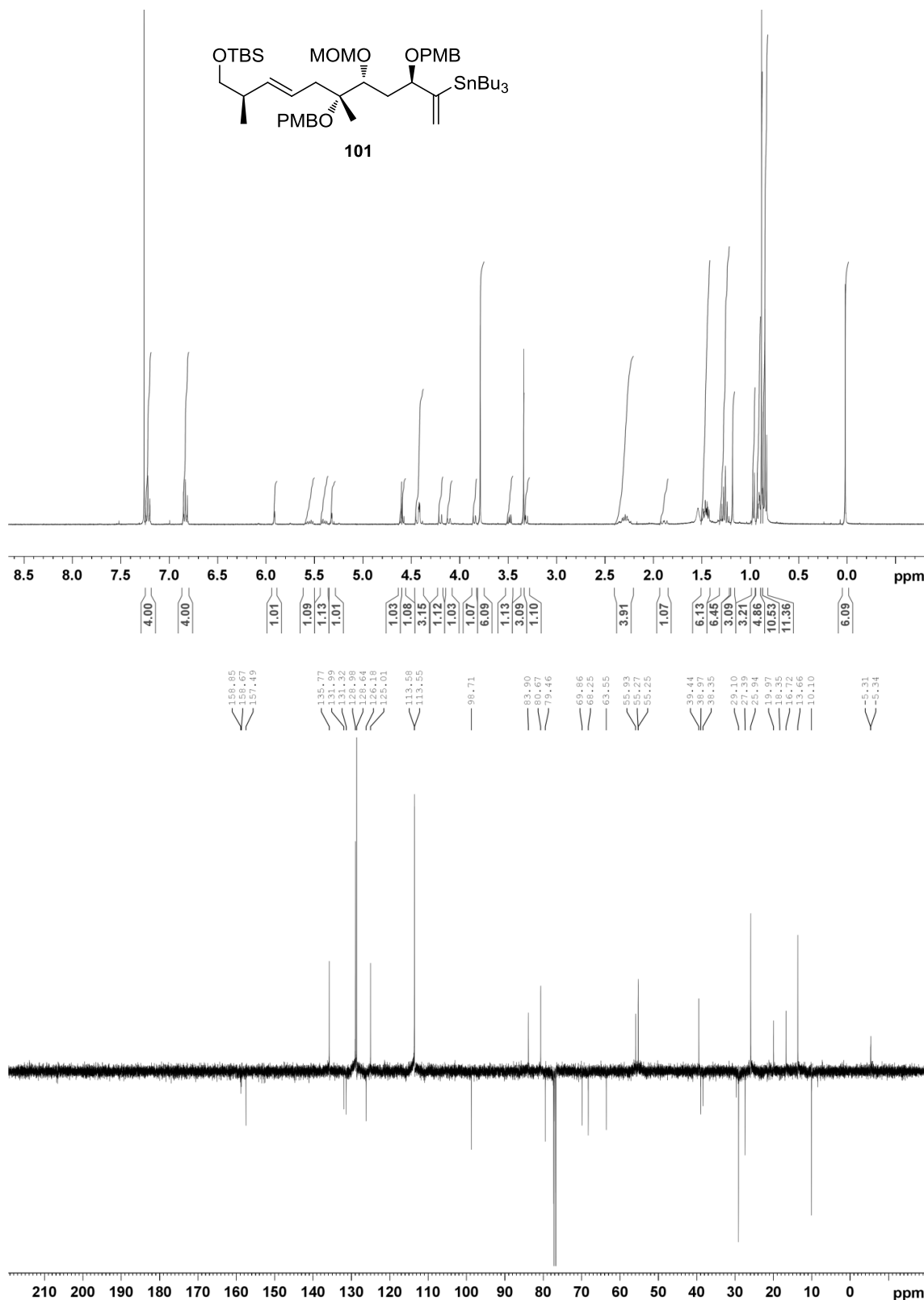
6.6. (3*R*,5*R*,6*R*,10*R*,*E*)-11-((*tert*-butyldimethylsilyl)oxy)-6-((4-methoxybenzyl)oxy)-5-(methoxymethoxy)-6,10-dimethylundec-8-en-1-yn-3-ol (131)



6.7. (5R,6R,10R,E)-6-((4-methoxybenzyl)oxy)-5-((R)-2-((4-methoxybenzyl)oxy)but-3-yn-1-yl)-6,10,13,13,14,14-hexamethyl-2,4,12-trioxa-13-silapentadec-8-ene (180)



6.8. (5*R*,6*R*,10*R*,*E*)-6-((4-methoxybenzyl)oxy)-5-((*R*)-2-((4-methoxybenzyl)oxy)-3-(tributylstannyl)but-3-en-1-yl)-6,10,13,13,14,14-hexamethyl-2,4,12-trioxa-13-silapentadec-8-ene (101)



7. Appendix

7.1. Copyright of figures and schemes

All figures and schemes were created by myself, without using content created by anyone else, except for the cases noted here:

- Figure 2 is a composite image of two photographs. The left one was helpfully provided by Dr József Hamar of “The Carpathian Basin Digital Collection of Species”. The right one was taken by Alexander Mrkvicka. Both photographers kindly gave their permission to use the images in this thesis.
- Figure 6 is a work in the public domain, created by the National Institutes of Health of the United States of America. It was retrieved from:
[en.wikipedia.org/wiki/File:Cancer_smoking_lung_cancer_correlation_from NIH.svg](http://en.wikipedia.org/wiki/File:Cancer_smoking_lung_cancer_correlation_from_NIH.svg)
- Figure 8 is based on a public domain work of Wikimedia user Boghog2, which itself is derived from RCSB Protein Data Bank entry 3g5u. The crystal structure was published as part of Aller, et al., *Science* **2009**, 323, 1718–1722. The image was retrieved from:
en.wikipedia.org/wiki/File:MDR3_3g5u.png
- Figure 9: Taken from Aller, et al., *Science* **2009**, 323, 1718–1722. Reprinted with permission from AAAS.
- Figure 10 is a custom modification of an image in the public domain, created by Wikimedia user LadyofHats. The original image was retrieved from:
en.wikipedia.org/wiki/File:Phospholipids_aqueous_solution_structures.svg

7.2. References

- (1) Hohmann, J.; Evanics, F.; Dombi, G.; Molnár, J.; Szabó, P. *Tetrahedron* **2001**, 57 (1), 211–215.
- (2) .
- (3) Shi, Q.-W.; Su, X.-H.; Kiyota, H. *Chem. Rev.* **2008**, 108 (10), 4295–4327.
- (4) Scott, I. U.; Karp, C. L. *Br. J. Ophthalmol.* **1996**, 80 (9), 823–826.
- (5) spurge - Merriam Webster Dictionary <http://www.merriam-webster.com/dictionary/spurge> (accessed Nov 5, 2014).
- (6) Graham, J. G.; Quinn, M. L.; Fabricant, D. S.; Farnsworth, N. R. *J. Ethnopharmacol.* **2000**, 73 (3), 347–377.
- (7) Breitmaier, E. In *Terpene*; WILEY-VCH Verlag GmbH & Co. KGaA, 2008; pp 1–9.

- (8) Mau, C. J.; West, C. A. *Proc. Natl. Acad. Sci.* **1994**, *91* (18), 8497–8501.
- (9) MacMillan, J.; Beale, M. H. In *Comprehensive Natural Products Chemistry*; Barton, S. D., Nakanishi, K., Meth-Cohn, O., Eds.; Pergamon: Oxford, 1999; pp 217–243.
- (10) Adolf, W. *Isr. J. Chem.* **1977**, *16* (1), 75–83.
- (11) Breitmaier, E. In *Terpene*; WILEY-VCH Verlag GmbH & Co. KGaA, 2008; pp 51–80.
- (12) Wender, P. A.; Jesudason, C. D.; Nakahira, H.; Tamura, N.; Tebbe, A. L.; Ueno, Y. *J. Am. Chem. Soc.* **1997**, *119* (52), 12976–12977.
- (13) Blumberg, P. M. *Cancer Res.* **1988**, *48* (1), 1–8.
- (14) Kupchan, S. M.; Sigel, C. W.; Matz, M. J.; Saenz Renauld, J. A.; Haltiwanger, R. C.; Bryan, R. F. *J. Am. Chem. Soc.* **1970**, *92* (14), 4476–4477.
- (15) Mucsi, I.; Molnár, J.; Hohmann, J.; Rédei, D. *Planta Med.* **2001**, *67* (7), 672–674.
- (16) Chayavichitsilp, P.; Buckwalter, J. V.; Krakowski, A. C.; Friedlander, S. F. *Pediatr. Rev.* **2009**, *30* (4), 119–130.
- (17) Vasas, A.; Sulyok, E.; Rédei, D.; Forgo, P.; Szabó, P.; Zupkó, I.; Berényi, A.; Molnár, J.; Hohmann, J. *J. Nat. Prod.* **2011**, *74* (6), 1453–1461.
- (18) STATISTIK AUSTRIA - Todesursachen im Überblick
http://www.statistik.at/web_de/statistiken/gesundheit/todesursachen/todesursachen_im_ueberblick/ (accessed Nov 9, 2014).
- (19) Croce, C. M. *N. Engl. J. Med.* **2008**, *358* (5), 502–511.
- (20) Greenman, C.; Stephens, P.; Smith, R.; Dalgliesh, G. L.; Hunter, C.; Bignell, G.; Davies, H.; Teague, J.; Butler, A.; Stevens, C.; Edkins, S.; O'Meara, S.; Vastrik, I.; Schmidt, E. E.; Avis, T.; Barthorpe, S.; Bhamra, G.; Buck, G.; Choudhury, B.; Clements, J.; Cole, J.; Dicks, E.; Forbes, S.; Gray, K.; Halliday, K.; Harrison, R.; Hills, K.; Hinton, J.; Jenkinson, A.; Jones, D.; Menzies, A.; Mironenko, T.; Perry, J.; Raine, K.; Richardson, D.; Shepherd, R.; Small, A.; Tofts, C.; Varian, J.; Webb, T.; West, S.; Widaa, S.; Yates, A.; Cahill, D. P.; Louis, D. N.; Goldstraw, P.; Nicholson, A. G.; Brasseur, F.; Looijenga, L.; Weber, B. L.; Chiew, Y.-E.; deFazio, A.; Greaves, M. F.; Green, A. R.; Campbell, P.; Birney, E.; Easton, D. F.; Chenevix-Trench, G.; Tan, M.-H.; Khoo, S. K.; Teh, B. T.; Yuen, S. T.; Leung, S. Y.; Wooster, R.; Futreal, P. A.; Stratton, M. R. *Nature* **2007**, *446* (7132), 153–158.
- (21) Understanding Cancer - Lag Time - NIH.gov
<https://web.archive.org/web/20050122204625/http://press2.nci.nih.gov/sciencebehind/cancer/cancer31.htm> (accessed Jan 7, 2015).
- (22) Devi, U. P. *Health Administrator* **2005**, *17* (1), 16–24.
- (23) Hong, W. K.; Jr, R. C. B.; Hait, W. N.; Kufe, D. W.; Pollock, R. E.; Weichselbaum, R. R.; Holland, J. F.; III, E. F. *Holland-Frei Cancer Medicine*, 8/e, 8 Hardcover/Online edition.; pmph usa: Shelton, Conn, 2009.
- (24) Fearon, E. R.; Vogelstein, B. *Cell* **1990**, *61* (5), 759–767.
- (25) Hanahan, D.; Weinberg, R. A. *Cell* **2011**, *144* (5), 646–674.
- (26) Bucci, M. K.; Bevan, A.; Roach, M. CA. *Cancer J. Clin.* **2005**, *55* (2), 117–134.
- (27) Immunotherapy: Using the Immune System to Treat Cancer
<http://www.cancer.gov/researchandfunding/progress/immunotherapy-using-immune-system-to-treat-cancer> (accessed Jan 11, 2015).
- (28) Finn, O. J. *N. Engl. J. Med.* **2008**, *358* (25), 2704–2715.
- (29) Science - Breakthrough of the Year 2013
<http://news.sciencemag.org/breakthrough-of-the-year-2013> (accessed Jan 11, 2015).
- (30) Zhukov, N. V.; Tjulandin, S. A. *Biochem. Mosc.* **2008**, *73* (5), 605–618.

- (31) Luqmani, Y. A. *Med. Princ. Pract.* **2005**, *14* (1), 35–48.
- (32) *Nat. Biotechnol.* **2000**, *18*, IT18–IT20.
- (33) Goldman, B. J. *Natl. Cancer Inst.* **2003**, *95* (4), 255.
- (34) Raub, T. J. *Mol. Pharm.* **2006**, *3* (1), 3–25.
- (35) Gombar, V. K.; Polli, J. W.; Humphreys, J. E.; Wring, S. A.; Serabjit-Singh, C. S. *J. Pharm. Sci.* **2004**, *93* (4), 957–968.
- (36) Aller, S. G.; Yu, J.; Ward, A.; Weng, Y.; Chittaboina, S.; Zhuo, R.; Harrell, P. M.; Trinh, Y. T.; Zhang, Q.; Urbatsch, I. L.; Chang, G. *Science* **2009**, *323* (5922), 1718–1722.
- (37) Riahi, S.; Beheshti, A.; Mohammadi, A.; Ganjali, M. R.; Norouzi, P. *J. Chin. Chem. Soc.* **2008**, *55* (2), 345–355.
- (38) Ecker, G.; Chiba, P.; Hitzler, M.; Schmid, D.; Visser, K.; Cordes, H. P.; Csöllei, J.; Seydel, J. K.; Schaper, K.-J. *J. Med. Chem.* **1996**, *39* (24), 4767–4774.
- (39) Ward, A.; Reyes, C. L.; Yu, J.; Roth, C. B.; Chang, G. *Proc. Natl. Acad. Sci.* **2007**, *104* (48), 19005–19010.
- (40) Szakács, G.; Paterson, J. K.; Ludwig, J. A.; Booth-Genthe, C.; Gottesman, M. M. *Nat. Rev. Drug Discov.* **2006**, *5* (3), 219–234.
- (41) Crowley, E.; McDevitt, C. A.; Callaghan, R. In *Multi-Drug Resistance in Cancer*; Zhou, J., Ed.; Methods in Molecular Biology; Humana Press, 2010; pp 405–432.
- (42) Hohmann, J.; Molnár, J.; Rédei, D.; Evanics, F.; Forgo, P.; Kálmán, A.; Argay, G.; Szabó, P. *J. Med. Chem.* **2002**, *45* (12), 2425–2431.
- (43) Corea, G.; Fattorusso, E.; Lanzotti, V.; Taglialatela-Scafati, O.; Appendino, G.; Ballero, M.; Simon, P.-N.; Dumontet, C.; Di Pietro, A. *Bioorg. Med. Chem.* **2003**, *11* (23), 5221–5227.
- (44) Corea, G.; Fattorusso, E.; Lanzotti, V.; Taglialatela-Scafati, O.; Appendino, G.; Ballero, M.; Simon, P.-N.; Dumontet, C.; Di Pietro, A. *J. Med. Chem.* **2003**, *46* (15), 3395–3402.
- (45) Corea, G.; Fattorusso, E.; Lanzotti, V.; Motti, R.; Simon, P.-N.; Dumontet, C.; Di Pietro, A. *J. Med. Chem.* **2004**, *47* (4), 988–992.
- (46) Corea, G.; Pietro, A. D.; Dumontet, C.; Fattorusso, E.; Lanzotti, V. *Phytochem. Rev.* **2009**, *8* (2), 431–447.
- (47) Jadranin, M.; Pešić, M.; Aljančić, I. S.; Milosavljević, S. M.; Todorović, N. M.; Podolski-Renić, A.; Banković, J.; Tanić, N.; Marković, I.; Vajs, V. E.; Tešević, V. V. *Phytochemistry* **2013**, *86*, 208–217.
- (48) Sousa, I. J.; Ferreira, M.-J. U.; Molnár, J.; Fernandes, M. X. *Eur. J. Pharm. Sci.* **2013**, *48* (3), 542–553.
- (49) Smith, A. B.; Guaciaro, M. A.; Schow, S. R.; Wovkulich, P. M.; Toder, B. H.; Hall, T. W. *J. Am. Chem. Soc.* **1981**, *103* (1), 219–222.
- (50) Guaciaro, M. A.; Wovkulich, P. M.; Smith III, A. B. *Tetrahedron Lett.* **1978**, *19* (47), 4661–4664.
- (51) Collins, J. C.; Hess, W. W.; Frank, F. J. *Tetrahedron Lett.* **1968**, *9* (30), 3363–3366.
- (52) Mukaiyama, T.; Hayashi, M. *Chem. Lett.* **1974**, *3* (1), 15–16.
- (53) Castro, C. E.; Stephens, R. D. *J. Am. Chem. Soc.* **1964**, *86* (20), 4358–4363.
- (54) Taylor, M. D.; Smith, A. B.; Furst, G. T.; Gunasekara, S. P.; Bevelle, C. A.; Cordell, G. A.; Farnsworth, N. R.; Kupchan, S. M.; Uchida, H. *J. Am. Chem. Soc.* **1983**, *105* (10), 3177–3183.
- (55) Smith, A. B.; Lupo, A. T.; Ohba, M.; Chen, K. *J. Am. Chem. Soc.* **1989**, *111* (17), 6648–6656.

- (56) Smith, A. B.; Dorsey, B. D.; Ohba, M.; Lupo, A. T.; Malamas, M. S. *J. Org. Chem.* **1988**, *53* (18), 4314–4325.
- (57) Davis, F. A.; Abdul-Malik, N. F.; Awad, S. B.; Harakal, M. E. *Tetrahedron Lett.* **1981**, *22* (10), 917–920.
- (58) Davis, F. A.; Harakal, M. E.; Awad, S. B. *J. Am. Chem. Soc.* **1983**, *105* (10), 3123–3126.
- (59) Davis, F. A.; Vishwakarma, L. C. *Tetrahedron Lett.* **1985**, *26* (30), 3539–3542.
- (60) Gyorkos, A. C.; Stille, J. K.; Hegedus, L. S. *J. Am. Chem. Soc.* **1990**, *112* (23), 8465–8472.
- (61) Crisp, G. T.; Scott, W. J.; Stille, J. K. *J. Am. Chem. Soc.* **1984**, *106* (24), 7500–7506.
- (62) Stille, J. K. *Angew. Chem. Int. Ed. Engl.* **1986**, *25* (6), 508–524.
- (63) Corey, E. J.; Kim, C. U. *J. Am. Chem. Soc.* **1972**, *94* (21), 7586–7587.
- (64) Noyori, R.; Nishida, I.; Sakata, J. *J. Am. Chem. Soc.* **1983**, *105* (6), 1598–1608.
- (65) Han, Q.; Wiemer, D. F. *J. Am. Chem. Soc.* **1992**, *114* (20), 7692–7697.
- (66) Horner, L.; Hoffmann, H.; Wippel, H. G. *Chem. Ber.* **1958**, *91* (1), 61–63.
- (67) Wadsworth, W. S.; Emmons, W. D. *J. Am. Chem. Soc.* **1961**, *83* (7), 1733–1738.
- (68) Becicka, B. T.; Koerwitz, F. L.; Drtina, G. J.; Baenziger, N. C.; Wiemer, D. F. *J. Org. Chem.* **1990**, *55* (21), 5613–5619.
- (69) Matthews, R. S.; Oliver, J. D.; Ward, J. F.; Eickhoff, D. J.; Strickland, L. C. *J. Chem. Soc. [Perkin 1]* **1987**, No. 0, 1485–1488.
- (70) Kita, Y.; Yasuda, H.; Haruta, J.; Segawa, J.; Tamura, Y. *Synthesis* **1982**, 1982 (12), 1089–1091.
- (71) Omura, K.; Swern, D. *Tetrahedron* **1978**, *34* (11), 1651–1660.
- (72) Helmboldt, H.; Köhler, D.; Hiersemann, M. *Org. Lett.* **2006**, *8* (8), 1573–1576.
- (73) Helmboldt, H.; Hiersemann, M. *J. Org. Chem.* **2009**, *74* (4), 1698–1708.
- (74) Hiersemann, M. *Synlett* **2000**, 2000 (03), 415–417.
- (75) Hiersemann, M. *Eur. J. Org. Chem.* **2001**, 2001 (3), 483–491.
- (76) Hiersemann, M.; Abraham, L.; Pollex, A. *Synlett* **2003**, No. 8, 1088–1095.
- (77) Helmboldt, H.; Rehbein, J.; Hiersemann, M. *Tetrahedron Lett.* **2004**, *45* (2), 289–292.
- (78) Evans, D. A.; Bartroli, J.; Shih, T. L. *J. Am. Chem. Soc.* **1981**, *103* (8), 2127–2129.
- (79) Parikh, J. R.; Doering, W. v. E. *J. Am. Chem. Soc.* **1967**, *89* (21), 5505–5507.
- (80) Blanchette, M. A.; Choy, W.; Davis, J. T.; Essinfeld, A. P.; Masamune, S.; Roush, W. R.; Sakai, T. *Tetrahedron Lett.* **1984**, *25* (21), 2183–2186.
- (81) Dess, D. B.; Martin, J. C. *J. Org. Chem.* **1983**, *48* (22), 4155–4156.
- (82) Dess, D. B.; Martin, J. C. *J. Am. Chem. Soc.* **1991**, *113* (19), 7277–7287.
- (83) Mitsunobu, O.; Yamada, M. *Bull. Chem. Soc. Jpn.* **1967**, *40* (10), 2380–2382.
- (84) Scholl, M.; Ding, S.; Lee, C. W.; Grubbs, R. H. *Org. Lett.* **1999**, *1* (6), 953–956.
- (85) Schnabel, C.; Hiersemann, M. *Org. Lett.* **2009**, *11* (12), 2555–2558.
- (86) Schnabel, C.; Sterz, K.; Müller, H.; Rehbein, J.; Wiese, M.; Hiersemann, M. *J. Org. Chem.* **2011**, *76* (2), 512–522.
- (87) Shimokawa, K.; Takamura, H.; Uemura, D. *Tetrahedron Lett.* **2007**, *48* (32), 5623–5625.
- (88) Lentsch, C.; Rinner, U. *Org. Lett.* **2009**, *11* (22), 5326–5328.
- (89) Schnabel, C. Synthese von Jatrophane-Diterpenen. Dissertation, TU Dortmund: Germany, 2011.
- (90) Mohan, P. STUDIES DIRECTED TOWARDS THE TOTAL SYNTHESIS OF A JATROPHANE DITERPENE. Dissertation, Texas Tech University: Lubbock, TX, USA, 2011.

- (91) Mohan, P.; Koushik, K.; Fuertes, M. J. *Tetrahedron Lett.* **2012**, 53 (22), 2730–2732.
- (92) Mohan, P.; Fuertes, M. J. *Tetrahedron Lett.* **2013**, 54 (30), 3919–3925.
- (93) Fürst, R.; Lentsch, C.; Rinner, U. *Eur. J. Org. Chem.* **2013**, 2013 (12), 2293–2297.
- (94) Fürst, R.; Rinner, U. *J. Org. Chem.* **2013**, 78 (17), 8748–8758.
- (95) Gilbert, M. W.; Galkina, A.; Mulzer, J. *Synlett* **2004**, 2004 (14), 2558–2562.
- (96) Mulzer, J.; Giester, G.; Gilbert, M. *Helv. Chim. Acta* **2005**, 88 (6), 1560–1579.
- (97) Curran, T. T.; Hay, D. A. *Tetrahedron Asymmetry* **1996**, 7 (10), 2791–2792.
- (98) Wick, A. E.; Felix, D.; Steen, K.; Eschenmoser, A. *Helv. Chim. Acta* **1964**, 47 (8), 2425–2429.
- (99) Ishihara, Y.; Baran, P. *Synlett* **2010**, 2010 (12), 1733–1745.
- (100) Aspinall, H. C.; Greeves, N.; Valla, C. *Org. Lett.* **2005**, 7 (10), 1919–1922.
- (101) Seebach, D. *Angew. Chem. Int. Ed. Engl.* **1979**, 18 (4), 239–258.
- (102) Smith, A. B.; Adams, C. M. *Acc. Chem. Res.* **2004**, 37 (6), 365–377.
- (103) Schlosser, M. *Organometallics in synthesis: a manual*; Wiley: Chichester, West Sussex, England; New York, 1994.
- (104) Fürstner, A. *Chem. Rev.* **1999**, 99 (4), 991–1046.
- (105) Hargaden, G.; Guiry, P. *Adv. Synth. Catal.* **2007**, 349 (16), 2407–2424.
- (106) Schetter, B.; Mahrwald, R. *Angew. Chem. Int. Ed.* **2006**, 45 (45), 7506–7525.
- (107) Morita, Y.; Kashiwagi, A.; Nakasuji, K. *J. Org. Chem.* **1997**, 62 (21), 7464–7468.
- (108) Benaglia, M.; Toyota, S.; Woods, C. R.; Siegel, J. S. *Tetrahedron Lett.* **1997**, 38 (27), 4737–4740.
- (109) Sessler, J. L.; Wang, B.; Harriman, A. *J. Am. Chem. Soc.* **1995**, 117 (2), 704–714.
- (110) Ireland, R. E.; Mueller, R. H. *J. Am. Chem. Soc.* **1972**, 94 (16), 5897–5898.
- (111) Ireland, R. E.; Mueller, R. H.; Willard, A. K. *J. Am. Chem. Soc.* **1976**, 98 (10), 2868–2877.
- (112) Kallmerten, J.; Gould, T. J. *Tetrahedron Lett.* **1983**, 24 (47), 5177–5180.
- (113) Gould, T. J.; Balestra, M.; Wittman, M. D.; Gary, J. A.; Rossano, L. T.; Kallmerten, J. *J. Org. Chem.* **1987**, 52 (17), 3889–3901.
- (114) Evans, D. A.; Takacs, J. M.; McGee, L. R.; Ennis, M. D.; Mathre, D. J.; Bartroli, J. *Pure Appl. Chem.* **1981**, 53 (6), 1109–1127.
- (115) Kim, U. B.; Furkert, D. P.; Brimble, M. A. *Org. Lett.* **2013**, 15 (3), 658–661.
- (116) Li, Q.; Mao, S.; Cui, Y.; Jia, Y. *J. Org. Chem.* **2012**, 77 (8), 4111–4116.
- (117) Gage, J. R.; Evans, D. A. *Org. Synth.* **1990**, 68, 77.
- (118) Neises, B.; Steglich, W. *Angew. Chem. Int. Ed. Engl.* **1978**, 17 (7), 522–524.
- (119) McFarland, C. M.; McIntosh, M. In *The Claisen Rearrangement: Methods and Applications*; Hiersemann, M., Nubbemeyer, U., Eds.; 2007.
- (120) Bartlett, P. A.; Tanzella, D. J.; Barstow, J. F. *J. Org. Chem.* **1982**, 47 (20), 3941–3945.
- (121) Hatakeyama, S.; Sugawara, M.; Kawamura, M.; Takano, S. *J. Chem. Soc. Chem. Commun.* **1992**, No. 17, 1229–1231.
- (122) Kallmerten, J.; Gould, T. J. *J. Org. Chem.* **1986**, 51 (7), 1152–1155.
- (123) Picoul, W.; Urchegui, R.; Haudrechy, A.; Langlois, Y. *Tetrahedron Lett.* **1999**, 40 (26), 4797–4800.
- (124) Romea, P.; Urpí, F. In *Modern Methods in Stereoselective Aldol Reactions*; Mahrwald, R., Ed.; John Wiley & Sons, 2013; p 1.
- (125) Devant, R.; Mahler, U.; Braun, M. *Chem. Ber.* **1988**, 121 (3), 397–406.
- (126) Braun, M.; Gräf, S.; Herzog, S. *Org. Synth.* **1995**, 72, 32.

- (127) Braun, M.; Gräf, S. *Org. Synth.* **1995**, 72, 38.
- (128) Yun, J. M.; Sim, T. B.; Hahm, H. S.; Lee, W. K.; Ha, H.-J. *J. Org. Chem.* **2003**, 68 (20), 7675–7680.
- (129) Bal, B. S.; Childers, W. E.; Pinnick, H. W. *Tetrahedron* **1981**, 37 (11), 2091–2096.
- (130) Satcharoen, V.; McLean, N. J.; Kemp, S. C.; Camp, N. P.; Brown, R. C. D. *Org. Lett.* **2007**, 9 (10), 1867–1869.
- (131) Haack, K.-J.; Hashiguchi, S.; Fujii, A.; Ikariya, T.; Noyori, R. *Angew. Chem.* **1997**, 109 (3), 297–300.
- (132) Matsumura, K.; Hashiguchi, S.; Ikariya, T.; Noyori, R. *J Am Chem Soc* **1997**, 119 (37), 8738–8739.
- (133) Shin, Y.; Fournier, J.-H.; Brückner, A.; Madiraju, C.; Balachandran, R.; Raccor, B. S.; Edler, M. C.; Hamel, E.; Sikorski, R. P.; Vogt, A.; Day, B. W.; Curran, D. P. *Tetrahedron* **2007**, 63 (35), 8537–8562.
- (134) Gabriele, B.; Mancuso, R.; Salerno, G.; Lupinacci, E.; Ruffolo, G.; Costa, M. J. *Org. Chem.* **2008**, 73 (13), 4971–4977.
- (135) Mike, J. F.; Makowski, A. J.; Jeffries-EL, M. *Org. Lett.* **2008**, 10 (21), 4915–4918.
- (136) Mark midland, M.; tramontano, A.; kazubski, A.; graham, R. S.; tsai, D. J. S.; cardin, D. B. *Tetrahedron* **1984**, 40 (8), 1371–1380.
- (137) Graham, R. S.; Midland, M. M. *Org. Synth. Coll Vol* **1990**, 7, 402.
- (138) Corey, E. J.; Bakshi, R. K.; Shibata, S. *J. Am. Chem. Soc.* **1987**, 109 (18), 5551–5553.
- (139) Bialy, L.; Waldmann, H. *Chem. - Eur. J.* **2004**, 10 (11), 2759–2780.
- (140) Zhang, D.; Ready, J. M. *J. Am. Chem. Soc.* **2007**, 129 (40), 12088–12089.
- (141) Hirao, T.; Hayashi, K.; Fujihara, Y.; Ohshiro, Y.; Agawa, T. *J. Org. Chem.* **1985**, 50 (2), 279–281.
- (142) Tsuji, J.; Nagashima, H.; Nemoto, H. *Org. Synth.* **1984**, 62, 9.
- (143) Sun, H.; Roush, W. R. *Org. Synth.* **2011**, 88, 87.
- (144) Duthaler, R. O.; Hafner, A. *Chem. Rev.* **1992**, 92 (5), 807–832.
- (145) Trost, B. M.; Brindle, C. S. *Chem. Soc. Rev.* **2010**, 39 (5), 1600–1632.
- (146) Sakthivel, K.; Notz, W.; Bui, T.; Barbas, C. F. *J. Am. Chem. Soc.* **2001**, 123 (22), 5260–5267.
- (147) List, B.; Pojarliev, P.; Castello, C. *Org. Lett.* **2001**, 3 (4), 573–575.
- (148) Trost, B. M.; Ito, H. *J. Am. Chem. Soc.* **2000**, 122 (48), 12003–12004.
- (149) Trost, B. M.; Shin, S.; Sclafani, J. A. *J. Am. Chem. Soc.* **2005**, 127 (24), 8602–8603.
- (150) Yu, H.; Wan, C.; Han, J.; Li, A. *Acta Chim. Sin.* **2013**, 71 (11), 1488.
- (151) Johnson, C. R.; Adams, J. P.; Braun, M. P.; Senanayake, C. B. W.; Wovkulich, P. M.; Uskoković, M. R. *Tetrahedron Lett.* **1992**, 33 (7), 917–918.
- (152) Stavber, S.; Jereb, M.; Zupan, M. *Synthesis* **2008**, 2008 (10), 1487–1513.
- (153) Krafft, M. E.; Cran, J. W. *Synlett* **2005**, No. 8, 1263–1266.
- (154) Trost, B. M.; Fettes, A.; Shireman, B. T. *J. Am. Chem. Soc.* **2004**, 126 (9), 2660–2661.
- (155) Yamada, Y. M. A.; Yoshikawa, N.; Sasai, H.; Shibasaki, M. *Angew. Chem. Int. Ed. Engl.* **1997**, 36 (17), 1871–1873.
- (156) Yoshikawa, N.; Yamada, Y. M. A.; Das, J.; Sasai, H.; Shibasaki, M. *J. Am. Chem. Soc.* **1999**, 121 (17), 4168–4178.
- (157) Fujii, K.; Maki, K.; Kanai, M.; Shibasaki, M. *Org. Lett.* **2003**, 5 (5), 733–736.

- (158) Denmark, S. E.; Fujimori, S.; Pham, S. M. *J. Org. Chem.* **2005**, 70 (26), 10823–10840.
- (159) Molawi, K.; Delpont, N.; Echavarren, A. M. *Angew. Chem. Int. Ed.* **2010**, 49 (20), 3517–3519.
- (160) Cahnmann, H. J. *Anal. Chem.* **1957**, 29 (9), 1307–1311.
- (161) Wimmer, P.; Widhalm, M. *Phosphorus Sulfur Silicon Relat. Elem.* **1995**, 106 (1–4), 105–114.
- (162) Ito, Y.; Hirao, T.; Saegusa, T. *J. Org. Chem.* **1978**, 43 (5), 1011–1013.
- (163) Zhang, H. X.; Guibe, F.; Balavoine, G. *J. Org. Chem.* **1990**, 55 (6), 1857–1867.
- (164) Mahoney, W. S.; Brestensky, D. M.; Stryker, J. M. *J. Am. Chem. Soc.* **1988**, 110 (1), 291–293.
- (165) Leung, L. T.; Leung, S. K.; Chiu, P. *Org. Lett.* **2005**, 7 (23), 5249–5252.
- (166) Leung, L. T.; Chiu, P. *Pure Appl. Chem.* **2006**, 78 (2), 281–285.
- (167) Evans, D. A.; Chapman, K. T.; Carreira, E. M. *J. Am. Chem. Soc.* **1988**, 110 (11), 3560–3578.
- (168) Evans, D. A.; Hoveyda, A. H. *J. Am. Chem. Soc.* **1990**, 112 (17), 6447–6449.
- (169) Ralston, K.; Hulme, A. *Synthesis* **2012**, 44 (15), 2310–2324.
- (170) Jiang, Y.; Hong, J.; Burke, S. D. *Org. Lett.* **2004**, 6 (9), 1445–1448.
- (171) Aird, J. I.; Hulme, A. N.; White, J. W. *Org. Lett.* **2007**, 9 (4), 631–634.
- (172) Horiuchi, Y.; Gnanadesikan, V.; Ohshima, T.; Masu, H.; Katagiri, K.; Sei, Y.; Yamaguchi, K.; Shibasaki, M. *Chem. - Eur. J.* **2005**, 11 (18), 5195–5204.
- (173) Trost, B. M.; Ball, Z. T. *J Am Chem Soc* **2001**, 123 (50), 12726–12727.
- (174) Gao, F.; Hoveyda, A. H. *J. Am. Chem. Soc.* **2010**, 132 (32), 10961–10963.
- (175) Heathcock, C. H.; Finkelstein, B. L.; Jarvi, E. T.; Radel, P. A.; Hadley, C. R. *J. Org. Chem.* **1988**, 53 (9), 1922–1942.
- (176) Evans, D. A.; Rajapakse, H. A.; Chiu, A.; Stenkamp, D. *Angew. Chem. Int. Ed.* **2002**, 41 (23), 4573–4576.
- (177) Kang, J. A.; Kim, D. H.; Kim, J. H.; Kim, Y. G.; Lee, K. H.; Lee, K. H.; Lee, Y. H.; Song, S. B.; Whang, H. S.; Yoon, Y. H. Cephem derivatives and a method for producing the compounds and an antibacterial composition containing the compounds. WO1999033839 A1, July 8, 1999.
- (178) Rickerby, J.; Vallet, M.; Bernardinelli, G.; Viton, F.; Kündig, E. P. *Chem. – Eur. J.* **2007**, 13 (12), 3354–3368.
- (179) Murphy, J. A.; Scott, K. A.; Sinclair, R. S.; Martin, C. G.; Kennedy, A. R.; Lewis, N. J. *Chem. Soc. [Perkin 1]* **2000**, No. 15, 2395–2408.

7.3. *Abstract in English*

Euphosalicin is a diterpene showing promising biological activity by reversing multi-drug resistance, a major cause of chemotherapy failure. Thus, it could serve as lead structure for drug development efforts directed at battling resistance of cancer cells.

Synthetically, euphosalicin is a challenging target due to its bicyclic structure with a 13-membered macrocycle and its high degree of oxygenation. While previous work produced five-membered ring fragments to access euphosalicin, this work focuses on a complementary fragment for the macrocyclic part of the target molecule.

Several approaches were devised and carried out. They shared the initial steps: an Evans aldol reaction followed by an Ireland-Claisen rearrangement to construct two stereocenters, one of them quaternary. The first approach then used a HYTRA-based aldol reaction for C₂-elongation. Although several more steps were successfully developed, this route was abandoned due to practical difficulties stemming from the low solubility of the aldol products.

The second approach was centered on a planned halocyclopropane/haloenone rearrangement. Despite intensive optimization, this reaction did not produce the desired product, leading to the development of a third approach.

This ultimately successful route used an auxiliary-free, asymmetric aldol reaction to construct the carbon backbone in an expedient and convergent fashion. Although several dead-ends were encountered, these challenges were overcome. The resulting fragment for the euphosalicin macrocycle is orthogonally protected and serves as a useful base for a successful total synthesis.

Thus, this work supports drug development efforts by greatly facilitating the completion of euphosalicin, a promising lead structure for cancer therapy.

7.4. Abstract in German

Euphosalicin ist ein mit den Jatrophanen verwandtes Diterpen, das wegen seiner Fähigkeit, Multiresistenz in Krebszellen – einer der Hauptursachen für das Scheitern von Chemotherapien – entgegenzuwirken von großem biologischem Interesse ist. Es stellt demnach eine nützliche Leitstruktur für die Medikamentenentwicklung dar.

Aufgrund seiner bizyklischen Struktur mit einem 13-gliedrigen Makrozyklus und seinem hohen Oxidationsgrad stellt Euphosalicin eine beachtliche synthetische Herausforderung dar. Während vorhergehende Studien die Synthese eines fünfgliedrigen Ringfragmentes zeigten, beschäftigt sich diese Arbeit mit der Synthese eines ergänzenden Fragments für den Makrozyklus.

Hierzu wurden verschiedene Ansätze herangezogen. Die ersten Stufen blieben dabei stets gleich: mittels einer Evans Aldolreaktion und einer Ireland-Claisen Umlagerung wurden zwei Stereozentren eingeführt, von denen eines quaternär war. In der ersten Syntheseroute folgte darauf eine HYTRA Aldolreaktion. Mehrere Folgereaktionen wurden erfolgreich entwickelt, jedoch wurde diese Strategie aufgrund der geringen Löslichkeit der Aldolprodukte aufgegeben.

Der zweite Syntheszugang basierte auf einer geplanten Halocyclopropan/Halonenon-Umlagerung. Trotz eingehender Optimierung lieferte diese Reaktion nicht das gewünschte Produkt, woraufhin eine dritte Synthesestrategie entwickelt wurde.

Diese letztlich erfolgreiche Route nutzte eine asymmetrische, katalytische Aldolreaktion um das Kohlenstoffgerüst rasch und konvergent aufzubauen. Das resultierende Makrozyklus-Fragment ist orthogonal geschützt und dient als Basis für die Fertigstellung der Totalsynthese in der Zukunft.

Damit unterstützt diese Arbeit die medizinische Forschung über die Unterdrückung von Chemotherapie-Resistenzen in Krebszellen.

7.5. *List of publications*

Publications

Widhalm, Michael; Aichinger, Christian; Mereiter, Kurt

“A new route to 2,2',3,3'-tetrasubstituted binaphthyls”

Tetrahedron Letters, **2009**, 50, 2425-2429.

Rinner, Uwe; Lentsch, Christoph; Aichinger, Christian;

”Syntheses of Galbulimima Alkaloids”

Synthesis, **2010**, 22, 3763-3784.

Hudlicky, Tomas; Adams, David; Aichinger, Christian; Rinner, Uwe

“Chemoenzymatic Synthesis of Idesolide from Benzoic Acid”

Synlett, **2011**, 5, 725-729.

Aichinger, Christian; Mulzer, Johann; Rinner, Uwe

“Synthesis of the C6-C14 fragment of Euphosalicin”

In press

Presentations

“Euphosalicin und Idesolid”

Presentation at the Johannes Kepler University, Linz, 7.4.2011

“Euphosalicin und Idesolid”

Presentation at the Technical University Graz, Graz, 13.5.2011

“Progress Toward the Total Synthesis of Euphosalicin”

Presentation at the Vienna Symposium for Organic Chemistry, Vienna, 22.5.2011

Poster

Rinner, Uwe; Lentsch, Christoph; Aichinger, Christian; Mulzer, Johann

“Synthesis of a highly functionalized cyclopentane segment: Toward the total synthesis of jatrophone diterpenes”

Synthesefest, München, Germany; 17.03. – 18.03. 2009

Aichinger, Christian; Lentsch, Christoph; Rinner, Uwe

“Progress in the first total synthesis of Pl-3, a potent multidrug resistance reversal

agent”

10th Tetrahedron Symposium, Paris, France, 23.6. – 26.6.2009

Aichinger, Christian; Lentsch, Christoph; Rinner, Uwe

“Towards the Total Synthesis of Euphosalicin: Preparation of the C6-C14 Fragment”

Österreichische Chemietage 2009, Vienna, 24.8. – 27.8.2009

Aichinger, Christian; Lentsch, Christoph; Rinner, Uwe

„Progress in the Total Synthesis of Euphosalicin“

14th LTOS Symposium, St. Catharines, ON, Canada, 11.8. – 14.8.2009

Aichinger, Christian; Lentsch, Christoph R.; Rinner, Uwe

„Multi-drug resistance reversal agents: Update on the synthesis of euphosalicin“

240th ACS National Meeting, Boston, USA; 17.08. – 21.8.2010

Aichinger, Christian; Rinner, Uwe

“Progress in the Total Synthesis of Euphosalicin”

Österreichische Chemietage 2010, Linz, 26.9. – 29.9.2011

7.6. Curriculum vitae

Personal Data

Citizenship	Austria
Birthday and location:	July 20, 1984 / St. Pölten
Address	Hauptstraße 44A A-3373 Kemmelbach
Telephone	+43 680 2321429
E-mail	christian.aichinger@univie.ac.at

Education

Jun. 2002	Graduation (Matura) from BG/BRG Wieselburg with Honors
Oct. 2002	Started studies in Chemistry at the University of Vienna
Oct. 2004 – Sep. 2005	Studies interrupted for compulsory civilian service
Feb. 2008 – Oct. 2008	Diploma thesis under Prof. Dr. M. Widhalm: „Synthesis of 2,2',3,3'-tetrasubstituted binaphthyl derivatives and novel approaches to enantiopure 2,2'-dibromo-1,1'-binaphthyl“
Oct. 2008	Graduation with Honors
Since Oct. 2008	Ph.D. studies under the supervision of Prof. Dr. J. Mulzer working on the total synthesis of the diterpene euphosalicin

Awards

Oct. 2009	Merit-based scholarship from the University of Vienna
-----------	---

Experience Abroad

Jan. 2007 – Jul. 2007	Semester abroad at „Lunds Universitet“ in Lund, Sweden
Jun. 2010 – Aug. 2010	Guest researcher at „Brock University“ in St. Catharines, ON, Canada

Work Experience

Summer 2004	Lab work at Krems Chemie Chemical Services
Summer 2004	Shift work at Vetropak Österreich
Since Oct. 2008	Teaching assistance in several practical courses at the University of Vienna

Chemistry Skills

Organic synthesis	Planning and execution of organic syntheses Development of new synthetic routes
Analytical chemistry	Experience with NMR, HPLC, mass spectrometry and IR spectroscopy Developments of methods for qualitative or quantitative detection
Software packages	ChemBioDraw CambridgeSoft E-Notebook Research using Scifinder, Reaxys, Science of Synthesis

Language and Computer Skills

Languages	German: Native language
-----------	-------------------------

Computer	English: Excellent French, Swedish: Basic knowledge Development of computer programs: Resolving scientific literature citations directly to web pages: http://homepage.univie.ac.at/christian.aichinger/journal Formatting of NMR data for publications: http://homepage.univie.ac.at/christian.aichinger/nmr Excellent proficiency with Windows, Linux und Office
----------	---

Vienna, June 23, 2015

Christian Aichinger

Hiermit bestätige ich, Christian Aichinger die vorliegende Dissertation selbständig angefertigt und keine anderen als die angegebenen Quellen und Hilfsmittel benutzt sowie die wörtlich oder inhaltlich übernommenen Stellen als solche kenntlich gemacht und die Satzung der Universität Wien zur Sicherung guter wissenschaftlicher Praxis in der jeweils gültigen Fassung beachtet zu haben.

Wien, 23. Juni 2015

Christian Aichinger